

3D ecosystem modeling of aeration and fumigation in Australian grain silos to improve efficacy
against insects

by

Benjamin Mark Plumier

B.S., University of Illinois, 2011

M.S., University of Illinois, 2013

AN ABSTRACT OF A DISSERTATION

submitted in partial fulfillment of the requirements for the degree

DOCTOR OF PHILOSOPHY

Department of Grain Science and Industry
College of Agriculture

KANSAS STATE UNIVERSITY
Manhattan, Kansas

2018

Abstract

With continued population growth, more food production will be required with lower resource inputs. A significant drain on resources is post-harvest loss due to insects, which results in loss of product, quality and market access, and increased grain spoilage. Aeration and fumigation are key tools to control insect growth in stored grains and grain foods. The implementation of aeration strategies in Australia is made difficult by the warm subtropical climate, meanwhile the success of fumigation is being threatened by the spread of insect resistance to the fumigant phosphine. This dissertation project seeks to improve the understanding of aeration and fumigation by modifying the Maier-Lawrence (M-L) 3D ecosystem model by adding insect growth equations and quantifying fumigant loss from sealed bulk grain silos. The improved model was used to examine aeration under Australian conditions, validate its capability to accurately describe fumigant concentrations during silo fumigation, determine the extent to which fumigations are influenced by operational variables and environmental conditions, and validate its capability to describe fumigant concentrations post-fumigation in order to investigate the time needed to clear a grain storage silo of fumigant in order to assure worker safety.

Six aeration strategies were evaluated under Australian conditions. Of these strategies, two were found to be effective in lowering temperatures, i.e., fans were turned on when ambient temperature was less than 20°C, and less than internal grain temperature. The strategy based on temperature differential was the most effective because it cooled the interior of the grain mass with the least amount of energy (using the fewest fan run hours, and reaching 15°C an average of 11 days after than the fastest strategy). Using a 0°C temperature differential was the most effective strategy in terms of reducing insect growth.

The expanded (M-L-P) model was then validated based on experimental fumigant concentrations. The model was effective in reproducing average fumigant concentrations and fumigant trends vertically through the grain mass, but was not able to reproduce lateral fumigant variations. Verifications of the model with two different periods of phosphine release (i.e., 24h and 30h) were tested. Based on a 24h phosphine release period the predicted Ct-product differed from the experimental value by 0.9%. A 30h release period predicted a Ct-product that differed by 4.3% from the experimental value but it was more accurate during the times of highest concentration. Increases in leakage reduced fumigant concentrations, but the size of the effect decreased as leakage grew. Increasing temperature and wind speed in the model led to decreased phosphine concentrations, with temperature changes having a more significant impact overall than wind speed changes for the conditions investigated. Decreasing silo surface area to volume ratio dampened the impact of changing weather conditions on phosphine concentrations.

A fumigant venting experiment was conducted in a silo at Lake Grace, Australia, to investigate full scale desorption. Two equations estimating fumigant desorption were tested, with an average of 65.5% and -86.3% error. The length of venting periods was simulated to quantify hours needed to mitigate hazardous conditions. For the scenarios investigated 10 to 24 h of venting were needed to reduce residual fumigant concentration below 0.3 ppm depending on simulation assumptions.

3D ecosystem modeling of aeration and fumigation in Australian grain silos to improve efficacy
against insects

by

Benjamin Mark Plumier

B.S., University of Illinois, 2011

M.S., University of Illinois, 2013

A DISSERTATION

submitted in partial fulfillment of the requirements for the degree

DOCTOR OF PHILOSOPHY

Department of Grain Science and Industry
College of Agriculture

KANSAS STATE UNIVERSITY
Manhattan, Kansas

2018

Approved by:
Major Professor
Dirk E. Maier

Copyright

© Benjamin Plumier 2018.

Abstract

With continued population growth, more food production will be required with lower resource inputs. A significant drain on resources is post-harvest loss due to insects, which results in loss of product, quality and market access, and increased grain spoilage. Aeration and fumigation are key tools to control insect growth in stored grains and grain foods. The implementation of aeration strategies in Australia is made difficult by the warm subtropical climate, meanwhile the success of fumigation is being threatened by the spread of insect resistance to the fumigant phosphine. This dissertation project seeks to improve the understanding of aeration and fumigation by modifying the Maier-Lawrence (M-L) 3D ecosystem model by adding insect growth equations and quantifying fumigant loss from sealed bulk grain silos. The improved model was used to examine aeration under Australian conditions, validate its capability to accurately describe fumigant concentrations during silo fumigation, determine the extent to which fumigations are influenced by operational variables and environmental conditions, and validate its capability to describe fumigant concentrations post-fumigation in order to investigate the time needed to clear a grain storage silo of fumigant in order to assure worker safety.

Six aeration strategies were evaluated under Australian conditions. Of these strategies, two were found to be effective in lowering temperatures, i.e. fans were turned on when ambient temperature was less than 20°C, and less than internal grain temperature. The strategy based on temperature differential was the most effective because it cooled the interior of the grain mass with the least amount of energy (using the fewest fan run hours, and reaching 15°C an average of 11 days after than the fastest strategy). Using a 0°C temperature differential was the most effective strategy in terms of reducing insect growth.

The expanded (M-L-P) model was then validated based on experimental fumigant concentrations. The model was effective in reproducing average fumigant concentrations and fumigant trends, but was not able to reproduce lateral variations. Verifications of the model with two different periods of phosphine release were tested, 24h and 30h. Based on a 24h phosphine release model the predicted Ct-product differed from the experimental value by 0.9%. A 30h release model predicted a Ct-product that differed by 4.3% from the experimental value but was more accurate during the times of highest concentration. Increases in leakage reduced fumigant concentrations, but the size of the effect decreased as leakage grew. Increasing temperature and wind speed in the model led to decreased phosphine concentrations, with temperature changes having a more significant impact overall than wind speed changes. Decreasing silo surface to volume ratio dampened the impact of changing weather conditions on phosphine concentrations.

A fumigant venting experiment was conducted in a silo at Lake Grace, Australia, investigated full scale desorption. Two equations estimating fumigant desorption were tested, with an average of 65.5% and -86.3% error. The length of venting periods was simulated to quantify hours needed to mitigate hazardous conditions. For the scenarios investigated, 10 to 24 h of venting were needed depending on simulation assumptions.

Table of Contents

List of Figures	xii
List of Tables	xviii
Acknowledgements	xxi
Chapter 1 - Introduction	1
Approach	4
Chapter 2 - Objectives	7
1. To model aeration under Australian weather conditions to preserve stored grain quality and minimize insect activity	7
2. To develop and validate a fumigant movement and loss model for bulk stored grain to predict phosphine concentrations with fumigant leakage and sorption.	7
3. To conduct a sensitivity analysis of a fumigant movement and loss model for bulk stored grain in order to predict effects of ecosystem conditions and operational procedures on fumigation efficacy.	8
4. To Model post-fumigation desorption of phosphine in bulk stored grain	9
Chapter 3 - Aeration Modeling Under Australian Conditions to Preserve Stored Grain Quality and Minimize Insect Activity	10
Introduction.....	10
Materials and Methods	14
Results and Discussion.....	17
1. Overview of aeration strategy results	17
2. Optimizing the temperature differential to choose the best strategy	25
3. Effect of changing initial grain temperature	28
4. Effect of aeration strategies on insect development	30
Conclusions.....	40
Chapter 4 - Developing and Validating a Fumigant Loss Model for Bulk Stored Grain to Predict Phosphine Concentrations with Fumigant Leakage and Sorption	43
Introduction.....	43
Materials and Methods	50
1. Effect of Sorption	50

2. Effect of Silo Leakage	54
2a. Effect of Wind Speed	54
2b. Effect of Temperature	55
2c. Effect of Concentration Differential	56
3. Model Verification	59
Results and Discussion	61
1. Verification Results for 24 h Phosphine Release	61
1a. Simulation Trends	61
1b. Simulation Accuracy of Ct-Product.....	66
1c. Horizontal Differences in Simulation	70
1d. Scale of Sorption and Leakage	75
2. Verification Results for 30 h Phosphine release	76
Conclusions.....	80
Chapter 5 - Sensitivity Analysis of a Fumigant Movement and Loss Model for Bulk Stored Grain to Predict Effects of Environmental Conditions and Operational Variables on Fumigation Efficacy.....	82
Introduction.....	82
Materials and Methods	83
Results and Discussion	86
1. Effect of Operational Variables.....	86
1a. Effect of Changing Leakage Rate	86
1b. Recirculation Rate	91
1c. Sulfuryl-Fluoride	98
2. Effect of Environmental Conditions.....	102
2a. Temperature of Ambient Air	102
2b. Relative Humidity of Ambient Air	106
2c. Wind Speed	106
2d. Impact of Environmental Conditions on Silos of Different Dimensions.....	110
Conclusions.....	114
Chapter 6 - Modeling Post-Fumigation Desorption of Phosphine in Bulk Stored Grain	116
Introduction.....	116

Materials and Methods	121
1. Changes to Sorption Model.....	121
2. Desorption Modeling Strategies	123
3. Model Verification	124
Results and Discussion.....	125
1. Experimental Results	125
2. Validation Results	128
3. Improving Case 1 Desorption Equation.....	132
4. Fumigation Safety Simulations	135
Conclusions.....	141
Chapter 7 - Contributions and Model Improvements	143
Introduction.....	143
Numerical Solver Improvements	143
Insect Modeling	145
Grain Chiller Modeling	146
Fumigation Modeling	147
Fumigant Desorption Modeling	148
CO ₂ Production Modeling	149
Future Modeling Opportunities	149
Chapter 8 - Conclusions	152
Aeration Modeling Under Australian Conditions to Preserve Stored Grain Quality and Minimize Insect Activity.....	152
Developing and Validating a Fumigant Loss Model for Bulk Stored Grain to Predict Phosphine Concentrations with Fumigant Leakage and Sorption	154
Sensitivity Analysis of a Fumigant Movement and Loss Model for Bulk Stored Grain to Predict Effects of Environmental Conditions and Operational Variables on Fumigation Efficacy.....	155
Modeling Post-Fumigation Desorption of Phosphine in Bulk Stored Grain.....	156
Chapter 9 - Future Work	159
Chapter 10 - Bibliography	160
Chapter 11 - Chapter 4 Appendices	176

Appendix 4.1:.....	176
Appendix 4.2:.....	176
Appendix 4.3:.....	176
Appendix 4.4:.....	177
Appendix 4.5.....	177
Appendix 4.6:.....	181
Appendix 4.7:.....	185

List of Figures

Figure 3:1 Grain temperature averaged across three storage seasons (2010-2013) in a 1500 MT wheat silo for three airflow rates (0.105 m ³ /min ton, 0.21 m ³ /min ton, 0.42 m ³ /min ton) with the aeration fan on whenever ambient air temperature was under 20°C (Strategy 3).....	22
Figure 3:2 Grain temperature averaged across three storage seasons (2010-2013) in a 1500 MT wheat silo for three airflow rates (0.105 m ³ /min ton, 0.21 m ³ /min ton, 0.42 m ³ /min ton) with the aeration fan on whenever ambient air was cooler than air in the center of the grain mass (Strategy 5).....	24
Figure 3:3 Average grain temperature across three storage seasons (2010-2013) in a 1500 MT wheat silo for three airflow rates (0.105 m ³ /min ton, 0.21 m ³ /min ton, 0.42 m ³ /min ton) with the aeration fan on whenever ambient air was at least 3oC cooler than air in the center of the grain mass (Strategy 5 modified).	27
Figure 3:4 Grain temperature averaged for 2010-2011 storage year in a 1500 MT wheat silo at airflow rate of 0.21 m ³ /min ton for five different initial grain temperatures (20°C, 24°C, 25°C, 26°C, and 27°C) with the aeration fan on whenever ambient air was at least 3°C cooler than air in the center of the grain mass (Strategy 5 modified).	30
Figure 3:5 Simulated change (%) in insect number from original infestation in a 1500 MT wheat silo at 20°C initial grain temperature, averaged over 2010-2011 and 2011-2012 storage season with aeration whenever ambient temperature was below 20°C (Strategy 3) for three airflow rates (0.105 m ³ /min ton, 0.21 m ³ /min ton, 0.42 m ³ /min ton).....	31
Figure 3:6 Simulated change (%) in insect number from original infestation in a 1500 MT wheat silo at 20°C initial grain temperature, averaged over 2010-2011 and 2011-2012 storage season with aeration whenever ambient temperature was below internal grain temperature (Strategy 5) for three airflow rates (0.105 m ³ /min ton, 0.21 m ³ /min ton, 0.42 m ³ /min ton). 32	
Figure 3:7 Simulated change (%) in insect number from original infestation in a 1500 MT wheat silo at 20°C initial grain temperature, averaged over 2010-2011 and 2011-2012 storage season with aeration whenever ambient temperature was at least 3°C cooler than air in the center of the grain mass (Strategy 5 modified) three airflow rates (0.105 m ³ /min ton, 0.21 m ³ /min ton, 0.42 m ³ /min ton).....	33

Figure 3:8 Simulated change (%) in insect number from original infestation in a 1500 MT wheat silo at 27°C initial grain temperature, averaged over 2010-2011 and 2011-2012 storage season for low airflow rate (0.105 m ³ /min ton) for each of the top three aeration strategies tested: below 20°C (3), ambient temperature is less than internal temperature (5), and ambient temperature is 3°C less than internal temperature (5 modified).	36
Figure 3:9 Simulated change (%) in insect number from original infestation in a 1500 MT wheat silo at 27°C initial grain temperature, averaged over 2010-2011 and 2011-2012 storage season for medium airflow rate (0.21 m ³ /min ton) for each of the top three aeration strategies tested: below 20°C (3), ambient temperature is less than internal temperature (5), and ambient temperature is 3°C less than internal temperature (5 modified).....	37
Figure 3:10 Simulated change (%) in insect number from original infestation in a 1500 MT wheat silo at 27°C initial grain temperature, averaged over 2010-2011 and 2011-2012 storage season for high airflow rate (0.42 m ³ /min ton) for each of the top three aeration strategies tested: below 20°C (3), ambient temperature is less than internal temperature (5), and ambient temperature is 3°C less than internal temperature (5 modified).....	38
Figure 4:1 Fumigant sampling locations used in the experimental fumigation conducted in a sealed silo containing 45.5 tonnes of corn (Cook, 2016), each represented by a red dot.....	60
Figure 4:2 Average phosphine concentration (ppm) reported from the experimental results of Cook (2016) taken in the sealed silo between August 31 and September 9, 2015.	63
Figure 4:3 Average phosphine concentration (ppm) predicted by the simulation model considering only the same locations from which data were recorded by Cook (2016) between August 31 and September 9, 2015, with a 24h fumigant release.	63
Figure 4:4 Average phosphine concentration (ppm) predicted by the simulation model when considering results from every node in the simulation between August 31 and September 9, 2015, with a 24h fumigant release.....	64
Figure 4:5 Comparison between average experimental and predicted phosphine concentration (ppm) results considering only data at the same locations and times from which data were recorded by Cook (2016) between August 31 and September 9, 2015, with a 24h fumigant release.	66
Figure 4:6 Percent difference (%) in phosphine concentration between simulated and experimental results considering only data at the same locations from which data were	

recorded by Cook (2016) between August 31 and September 9, 2015, with a 24h fumigant release.	67
Figure 4:7 Difference in phosphine concentration (ppm) between simulated and experimental results considering only data at the same locations from which data were recorded by Cook (2016) between August 31 and September 9, 2015, with a 24h fumigant release.	68
Figure 4:8 Vertical averages of experimental phosphine values (ppm) of columns located halfway to the edge of the silo recorded by Cook (2016) between August 31 and September 9, 2015.	72
Figure 4:9 Vertical averages of predicted phosphine values (ppm) of columns located halfway to the edge of the silo considering only the same locations from which data were recorded by Cook (2016) between August 31 and September 9, 2015, with a 24h fumigant release.	72
Figure 4:10 Vertical averages of predicted phosphine values (ppm) of four columns located along the edge of the silo, and one at the center considering only the same locations from which data were recorded by Cook (2016) between August 31 and September 9, 2015, with a 24h fumigant release.	73
Figure 4:11 Comparison between predicted phosphine values (ppm) at specific nodes located 1.9m from the bottom of the grain mass and 0.7, 1.6, 1.9, and 2.2m from center of the silo fumigated between August 31 and September 9, 2015, with a 24h fumigant release.	75
Figure 4:12 Comparison between average experimental and predicted phosphine concentration (ppm) results considering only data at the same locations and times recorded by Cook (2016) between August 31 and September 9, 2015, with a 30h fumigant release.	77
Figure 4:13 Percent difference (%) in phosphine concentration between simulated and experimental results considering only data at the same locations from which data were recorded by Cook (2016) between August 31 and September 9, 2015, with a 30h fumigant release.	78
Figure 4:14 Difference in phosphine (ppm) concentration between simulated and experimental results considering only data at the same locations from which data were recorded by Cook (2016) between August 31 and September 9, 2015, with a 30h fumigant release.	79
Figure 5:1 Overall average phosphine concentration (ppm) for five leakage rates, expressed as a percentage of the leakage rate (100%) used in the verification conducted between August 31 and September 9, 2015.	88

Figure 5:2 Change in overall average phosphine concentration (%) compared for varying leakage rates, expressed as a percentage of the leakage rate (100%) used in the verification conducted between August 31 and September 9, 2015.	89
Figure 5:3 Overall average phosphine concentration (ppm) for five recirculation rates, expressed as a percentage of the recirculation rate (100%) used in the verification conducted between August 31 and September 9, 2015.....	92
Figure 5:4 Change in overall average phosphine concentration (%) for five recirculation rates, expressed as a percentage of the leakage rate (100%) used in the verification conducted between August 31 and September 9, 2015.....	93
Figure 5:5 Overall average phosphine concentration (ppm) for two recirculation rates, the original airflow used in the verification (0.001-0.005 m/s) and fan powered recirculation (0.0062 m/s) in a 1,500 MT wheat silo.....	97
Figure 5:6 Overall average fumigant concentration (kg/m ³) of phosphine and sulfuryl-fluoride fumigations, based on the verification conducted between August 31 and September 9, 2015.	99
Figure 5:7 Change in overall average fumigant concentration (%) of phosphine and sulfuryl-fluoride fumigations, using kg/m ³ , based on the verification conducted between August 31 and September 9, 2015.	100
Figure 5:8 Overall average fumigant concentration (ppm) of phosphine and sulfuryl-fluoride fumigations, based on the verification conducted between Aug 31 and September 9, 2015.	101
Figure 5:9 Overall average phosphine concentration (ppm) for five varying temperature conditions, expressed as a percentage of the temperatures (100%) used in the verification conducted between August 31 and September 9, 2015.	103
Figure 5:10 Change in overall average phosphine concentration (%) for five temperature conditions, expressed as a percentage of the temperatures (100%) used in the verification conducted between August 31 and September 9, 2015.	104
Figure 5:11 Overall average phosphine concentration (ppm) for five wind speeds, expressed as a percentage of the wind speeds (100%) used in the verification conducted between August 31 and September 9, 2015.....	107

Figure 5:12 Change in overall average phosphine concentration (%) for five wind speeds, expressed as a percentage of the wind speeds (100%) used in the verification conducted between August 31 and September 9, 2015.....	108
Figure 5:13 Overall average phosphine concentration (ppm) for five temperature conditions, expressed as a percentage of the temperatures (100%) used in the verification conducted between August 31 and September 9, 2015, for the 1500 MT silo with a surface area to volume ratio of 0.45 m ² /m ³	111
Figure 5:14 Change in overall average phosphine concentration (%) for five temperature conditions, expressed as a percentage of the temperatures (100%) used in the verification conducted between August 31 and September 9, 2015, for the 1500 MT silo with a surface area to volume ratio of 0.45 m ² /m ³	112
Figure 5:15 Overall average phosphine concentration (ppm) for five wind speeds, expressed as a percentage of the wind speeds (100%) used in the verification conducted between August 31 and September 9, 2015, for the 1500 MT silo with a surface area to volume ratio of 0.45 m ² /m ³	112
Figure 5:16 Change in overall average phosphine concentration (%) for five wind speeds, expressed as a percentage of the wind speeds (100%) used in the verification conducted between August 31 and September 9, 2015, for the 1500 MT silo with a surface area to volume ratio of 0.45 m ² /m ³	113
Figure 6:1 Experimental and predicted phosphine concentrations (ppm) for a reversed sorption equation model (Case 1) after conclusion of a fumigation in an 80 ton wheat silo located in Lake Grace, Australia, April 20-21, 2016.	129
Figure 6:2 Experimental and predicted phosphine concentrations (ppm) for an equilibrium differential equations sorption model (Case 2) after conclusion of a fumigation in an 80 ton wheat silo located in Lake Grace, Australia, April 20-21, 2016.....	130
Figure 6:3 Experimental and predicted phosphine values (ppm) for Case 1 and Case 2, 2h after conclusion of a fumigation in an 80 ton wheat silo located in Lake Grace, Australia, April 20-21, 2016. Periods without venting are shaded.	131
Figure 6:4 Experimental and predicted phosphine concentrations (ppm) for a reversed sorption equation model with a 10x multiplier for desorption rate (Modified Case 1) after conclusion	

of a fumigation in an 80 ton wheat silo located in Lake Grace, Australia, April 20-21, 2016.	133
Figure 6:5 Experimental and predicted phosphine values (ppm) for Modified Case 1 and Case 2, 2h after conclusion of a fumigation in an 80 ton wheat silo located in Lake Grace, Australia, April 20-21, 2016. Periods without venting are shaded.	134
Figure 11:1 Phosphine concentrations (ppm) in silo fumigation data provided by the Plant Biosecurity Cooperative Research Center (Darby 2011)	178
Figure 11:2 Phosphine concentrations (ppm) in silo fumigation data provided by Department of Agriculture and Fisheries, Queensland (DAF)	180

List of Tables

Table 3:1 Calendar date and time of day and fan run hours to reach 15°C or below average grain temperature in the grain mass across three storage seasons (2010-2013) in a 1500 MT wheat silo for three airflow rates (low=0.105 m³/min ton, medium=0.21 m³/min ton, high=0.42 m³/min ton) for the six aeration strategies investigated in this study.....19

Table 3:2 Calendar date and time of day for the grain temperature averaged across three storage seasons (2010-2013) to drop below 15°C and 10°C in a 1500 MT wheat silo for three airflow rates (0.105 m³/min ton, 0.21 m³/min ton, 0.42 m³/min ton) with the aeration fan on whenever ambient air temperature was under 20°C (Strategy 3).22

Table 3:3 Yearly electricity consumption (kWh) averaged across three storage seasons (2010-2013) in a 1500 MT wheat silo for three airflow rates (0.105m³/min ton, 0.21 m³/min ton, 0.42 m³/min ton) with the aeration fan on whenever the ambient air temperature was under 20°C (Strategy 3).23

Table 3:4 Yearly electricity consumption (kWh) averaged across three storage seasons (2010-2013) in a 1500 MT wheat silo for three airflow rates (0.105m³/min ton, 0.21 m³/min ton, 0.42 m³/min ton) with the aeration fan on whenever the ambient air temperature was under 20°C until the beginning of June, then adding an EMC requirement of 9% -14% (Strategy 3 modified).....23

Table 3:5 Calendar date and time of day for grain temperature averaged across three storage seasons (2010-2013) to drop below 15°C and 10°C in a 1500 MT wheat silo for three airflow rates (0.105 m³/min ton, 0.21 m³/min ton, 0.42 m³/min ton) with the aeration fan on whenever ambient air was cooler than air in the center of the grain mass (Strategy 5).25

Table 3:6 Yearly electricity consumption (kWh) and average across three storage seasons (2010-2013) in a 1500 MT wheat silo for three airflow rates (0.105 m³/min ton, 0.21 m³/min ton, 0.42 m³/min ton) with the aeration fan on whenever ambient air was cooler than air in the center of the grain mass (Strategy 5).25

Table 3:7 Calendar date and time of day for the average grain temperature across three storage seasons (2010-2013) to drop below 15°C and 10°C in a 1500 MT wheat silo for three airflow rates (0.105 m³/min ton, 0.21 m³/min ton, 0.42 m³/min ton) with the aeration fan on

whenever ambient air was at least 3°C cooler than air in the center of the grain mass (Strategy 5 modified).....	27
Table 3:8 Yearly electricity consumption (kWh) and average across three storage seasons (2010-2013) in a 1500 MT wheat silo for three airflow rates (0.105 m ³ /min ton, 0.21 m ³ /min ton, 0.42 m ³ /min ton) with the aeration fan on whenever ambient air was 3°C cooler than air in the center of the grain mass (Strategy 5 modified).	28
Table 4:1 Cumulative Ct-product, experimental and predicted Ct-products based on four approaches: (1) simulated nodes and reading times are the same as those recorded by Cook (2016), (2) simulated nodes are the same as those recorded by Cook (2016) but reading times are hourly based on the simulation, (3) all nodes in the simulation code are included for hourly calculations, and (4) only the node in the simulation with the least phosphine concentration for hourly calculations.	69
Table 4:2 Cumulative Ct-product predicted at individual nodes along the top outer ring of the grain mass surface of the silo using hourly reading values for fumigation conducted between Aug 31 and September 9, 2015, with a 24h fumigant release.	70
Table 5:1 Cumulative average Ct-products (ppm-h) and the difference from original (%) for five leakage rates, expressed as a percentage of the leakage rate (100%) used in the verification conducted between August 31 and September 9, 2015.	90
Table 5:2 Cumulative average Ct-products (ppm-h) for the whole silo, expressed as a percentage of the recirculation rate (100%) used in the verification conducted between August 31 and September 9, 2015.....	94
Table 5:3 Cumulative Ct-products (ppm-h) for the nodes along the top outer edge of the grain mass by location for nine recirculation rates, expressed as a percentage of the recirculation rate used in the verification (100%) conducted between August 31 and September 9, 2015.	95
Table 5:4 Cumulative average Ct-products (ppm-h) and the difference from original (%) for five ambient temperatures, expressed as a percentage of the ambient temperatures (100%) used in the verification conducted between August 31 and September 9, 2015.....	105
Table 5:5 Cumulative average Ct-products (ppm-h) and the difference from original (%) for wind speeds, expressed as a percentage of the wind speeds (100%) used in the verification conducted between August 31 and September 9, 2015.	109

Table 6:1 Experimental phosphine concentrations (ppm) in the silo headspace and 0.5m, 1.5m, and 3m below the grain surface in the core of the grain and at the North, West, South, and East locations in the grain mass 7m below the grain surface for periods of venting (bolded) and periods of sealed holding (not bolded) after conclusion of a fumigation in Lake Grace, Australia, April 20-21, 2016.	127
Table 6:2 Overall safety analysis with Safe (average phosphine concentration less than 0.3 ppm at conclusion of simulation) and Not Safe (average phosphine concentration more than 0.3 ppm at conclusion of simulation) based on fumigations performed in Lake Grace, Australia, April 12-21, 2016 (Australian Simulation) and Manhattan, Kansas between August 31 and September 9, 2015 (U.S. Simulation) (Cook 2016).	137
Table 6:3 Maximum average phosphine concentrations (ppm) post-venting for fumigations with four pressure half loss times (30 s, 1 min, 3 min, and 5 min) and five venting times (8h, 10h, 12h, 18h, and 24h) under simulation Modified Case 1 (reversed sorption model) based on fumigation performed in Lake Grace, Australia from April 12-21, 2016.	139
Table 6:4 Maximum average phosphine concentrations (ppm) post-venting for fumigations with four pressure half loss times (30 s, 1 min, 3 min, and 5 min) and five venting times (8h, 10h, 12h, 18h, and 24h) under simulation Case 2 (Equations from Darby, 2008) based on fumigation performed in Lake Grace, Australia from April 12-21, 2016.	139
Table 11:1 Comparison between average experimental and predicted phosphine concentration (ppm) considering only data from the same locations and times used in Cook (2016) between Aug 31 and September 9, 2015, with a 24h fumigant release.	181
Table 11:2 Comparison between average experimental and predicted phosphine concentration (ppm) considering only data from the same locations and times used in Cook (2016) between Aug 31 and September 9, 2015, with a 30h fumigant release.	185

Acknowledgements

There were many people whose contributions to this dissertation were essential and without whom I would not have been able to complete this work. Most of all, I would like to thank my major advisor Dr. Dirk Maier for his help and insight in this project. In addition to writing the initial proposal and securing funds, he was exceedingly patient during the time it took me to familiarize myself with the model, despite no previous experience in computer coding. In addition, he used some of his own startup money at Iowa State to provide help for the computer coding portion of the dissertation and to allow me to follow him to Ames. This provided me with the opportunity to work more closely with Dr. Maier, and to begin to execute the plans I had for the model. His help was also instrumental in editing this dissertation and in motivating me to grow as a professional researcher and as a person. I would also like to thank the rest of my graduate committee, for sticking with my research and contributing advice despite a number of administrative difficulties.

I would like to extend a significant acknowledgment to my coworker Sam Cook, whose friendship and advice was one of the few constants throughout my PhD work. In addition, I would like to thank him for providing data and advice related to the fumigations he performed during his Master's thesis at Kansas State. His data set was of the highest quality in thoroughness and completeness, and without it I would not have been able to generate a substantial verification of my model.

It is also important that I extend a sincere thank you to Matt Schramm, without whose knowledge of computer coding and ability to implement improved computational solutions I would have been unable to complete this project. In addition to helping to get the code working,

he made his time available continually to debug and add additional elements to the code well beyond his commitment to do so.

Thanks also to Dr. Johnselvakumar Lawrence, whose dissertation and computer model were the starting point for this dissertation. He graciously hosted me in his own home on several occasions as I needed help in learning and using the code.

I would like to thank the Plant Biosecurity Cooperative Research Center for funding this research and allowing me to grow and develop international contacts in my research, both in Australia and other countries. I would like to thank them as well for providing me with travel funds to attend the science exchange technical conferences hosted in Australia each year, which were highly informative and enjoyable.

I would like to acknowledge the assistance and hospitality that was provided to me by Dr. Yonglin Ren and his laboratory research group at Murdoch University in Perth, Western Australia. Dr. Ren was most gracious in helping provide me with data to understand fumigant desorption, and made my time in Perth thoroughly enjoyable. I would like to especially thank James Newman from Dr. Ren's research group, whose technical abilities, contacts, and hard work allowed for me to complete the silo scale desorption study in Lake Grace, Australia. Also, Mr. and Mrs. Doug and Debby Clarke who allowed us to perform the fumigation and venting trial on their property and allowed us to use one of their silos.

I would like to thank Dr. Manoj Nayak, Dr. Andrew Ridley, Dr. Greg Daghish and all the other members of the Queensland Department of Agriculture and Fisheries who hosted me during my stay in Brisbane. They were very helpful in discussing fumigation and the practical applications that my model could have.

I would like to thank Dr. Casada for providing me with the excel macros that were necessary for me to assemble the large amounts of hourly weather data needed for the aeration analysis.

I would like to acknowledge the Department of Agricultural and Biosystems Engineering at Iowa State University for providing me with an office as a visiting scholar during the last year and a half of my research so that I could continue to work closely with my major professor Dr. Maier.

Chapter 1 - Introduction

The number of food insecure people in the world has been estimated at more than 870 million (FAO et al., 2012). With continued population growth, more food production will be required with lower resource inputs such as labor, fertilizer, water, and land. This is a challenge that cannot be met by focusing exclusively on increasing food production. As a result, reducing post-harvest loss has been recognized as a vital tool for meeting global food and energy needs (FAO, 2014; WorldBank et al., 2011). The most significant sources of post-harvest loss in grain are insect growth and mold spoilage, which result in loss of product, quality and market access, and further increased grain spoilage. In order to minimize these forms of loss, it is important to keep grain conditions cool, dry, and uniform. These conditions are achieved by grain drying and aeration processes. While these are not novel procedures, their success can be influenced by many factors, such as airflow patterns and weather conditions.

Due to the warm subtropical Australian climate, there are a number of grain storage difficulties, one of the largest of which is insect growth. Aeration is a common form of insect growth control throughout the world that relies on cooling the grain mass in order to limit insect growth. Holding grain at a low temperature is an effective insect control strategy, as insect development stops at temperatures between 13°C and 20°C (Fields, 2006). Optimal temperatures for common grain storage insects range from 28°C to 38°C (Burgess and Burrell, 1964). The time needed to lower temperatures is important, however, as delaying cooling fronts by a month can result in insect population increases of 5-25 times the original amount (Hagstrum and Subramanyam, 2006). The warm climate in Australia makes this process more difficult than it is in temperate climates like North America. This does not mean, however, that aeration is not a

feasible technology under Australian conditions. Previous projects have demonstrated success with aeration under Australian conditions, reducing overall temperatures by more than 20°C (Sutherland, 1968). Therefore, the success of aeration strategies in Australia is possible and relies on making the best use of each hour of cool temperature in order to cool the grain. This can be investigated by developing and simulating a range of potential aeration strategies.

Additionally, Australian export regulations beginning in 1963 dictate an export limit of zero live insects. This regulation is highly impactful, as the Australian grain industry relies heavily on exports, with the quantity of exported grain reaching 90% of the harvest in Western Australia (Calderon and Barkai-Golan, 1990). As a consequence, fumigations have become the primary form of pest control. The primary fumigant used in stored grains and grain foods is phosphine (PH₃) because it kills all insect life stages at low cost. However, overuse and misuse is leading to increased insect resistance to phosphine in many parts of the world, including most recently the United States (Opit et al., 2012). The increase and spread of this resistance is a growing threat to commercial bulk handlers in Australia, but also to the global grain storage system. The overuse of phosphine has increased insect resistance to the extent that resistance genes are being found even in places where phosphine is not being used (Kaur et al., 2013). To make matters worse, many grain storage structures and fumigation procedures are not being controlled effectively. Darby (2011) found that the majority of grain storage structures in Australia did not meet gas tightness standards and that weather induced dilution near storage structure boundaries is very difficult to prevent and may stop lethal concentrations being achieved. Insect resistance to phosphine is made worse when insect life stages are exposed to sublethal doses of phosphine in a suboptimal fumigation. In order to extend the usefulness of phosphine as the primary stored grain and grain food fumigant, and reduce the risk of spreading

resistance development among stored product insects, phosphine fumigation efficacy must be improved to ensure 100% mortality of all insect life stages for susceptible populations.

For a fumigation to be effective, it must deliver a sufficient concentration of fumigant to all locations in the grain silo, and hold those concentrations at an optimal temperature long enough to kill insect pests. Environmental factors and operational parameters can significantly impact fumigation success by influencing leakage and fumigant movement (Cryer and Barnekow, 2006). As such, there is a need to better understand grain storage and fumigation conditions and how the fumigant behaves under a range of possible conditions in order to help extend efficacy especially phosphine, and reduce the occurrence of fumigation failures in Australia and around the world.

A significant tool to better understand grain storage environments is three dimensional finite element modeling. The basis for three dimensional modeling of grain storage conditions relies upon differential equations involving conservation of energy, mass, momentum, and species balance. The relevancy of these equations to stored product ecosystem conditions has been previously described (Abe and Basunia, 1996; Beukema et al., 1983; Brooker, 1969; Chourasia and Goswami, 2007; Converse et al., 1969; Jia et al., 2000; Jian et al., 2005; Montross et al., 2002; Rocha and Oliveira, 2013; Singh and Thorpe, 1993; and Thorpe, 1997). A three dimensional finite element model using the Fortran coding language was developed as part of a previous dissertation (Lawrence, 2010), and was used to analyze aeration simulations under U.S. and Indian conditions (Lawrence and Maier, 2011) and insect infestations. This model was adapted from previous two dimensional models developed by Montross et al. (2002), Montross (1999), and Thorpe (1997). The Lawrence code has been adapted for this work to monitor chemical concentrations and their movement and to account for losses of chemicals from the

grain storage structure. With these advances, the goal of this project was to adapt and expand the Maier-Lawrence (M-L) 3D ecosystem finite element model and utilize it to study how fumigation efficacy in Australian grain storage silos can be improved to better control stored product insects.

Approach

In order to extend the usefulness of phosphine, greater control and understanding of fumigant behavior and how it can be affected by various environmental factors needs to be investigated. The M-L 3D ecosystem finite element model for bulk stored grains accurately predicts temperature, moisture and convection currents, and the resulting movement of any gas (phosphine, sulfuryl-fluoride) added to the structure as a fumigant. The model is set up by segmenting the area of the stored grain bulk into discrete elements, and evaluating the governing differential equations of energy, mass, momentum and species balance across each segment, with appropriately realistic boundary conditions.

The model is able to predict grain spoilage as well as monitor conditions such as temperature and moisture content inside the grain mass. To accomplish this, the model uses as inputs the geometric data of a typical grain silo and weather data gathered for that geographical location. The M-L 3D ecosystem model has been used by Lawrence et al. (2010) in examination of aeration under Indian conditions and has been set up to observe fumigant movement as well. It has been adapted for use under Australian conditions by utilizing weather data from an Australian wheat production location in Coreen, NSW, and using the geometry of an Australian grain silo. The fumigation component has been augmented by the addition of equations from the literature that address fumigant loss through sorption and leakage from the silo. Results from the

model were validated by comparison with actual data from a real world fumigation conducted in an Australian grain silo.

In order to enable the model to analyze fumigations, the ability of the model to track specific chemical concentrations was enhanced with the addition of equations governing chemical leakage and sorption. The fumigant movement model is further modified to address the conditions of a closed-loop fumigation model with added fumigant recirculation. The new chemical concentration monitoring capacity was validated using real world fumigation data from a study conducted on an Australian made silo in Manhattan, Kansas (Cook, 2016). The effectiveness of this verification in determining overall fumigation trends and specific values was evaluated.

After the model was validated, the model was used as a basis for analyzing fumigation efficacy under a variety of operational parameters and environmental conditions. These include changes in silo leakage, recirculation rate, type of fumigant, ambient temperature, ambient relative humidity, and wind speed. The effect of changes in silo dimension on the impact of environmental conditions was also analyzed.

The model was then additionally modified to investigate the potential safety risk incurred by workers who handle grain post-fumigation, and what length of time grain would need to be vented in order for fumigant concentrations to be below safe working levels. In order to provide data suitable to validate this model capacity, a fumigation was conducted in Lake Grace, Australia, and was monitored post-fumigation through several silo venting stages. The effectiveness of the model in predicting residual fumigant concentrations post-fumigation is evaluated. This model was then used to draw conclusions about the safety of grain post-

fumigation and evaluate existing regulations and guidelines on their ability to provide for the safety of workers in the grain storage industry.

Chapter 2 - Objectives

The overall goal of this project was achieved by pursuing the following four objectives:

1. To model aeration under Australian weather conditions to preserve stored grain quality and minimize insect activity

The subtropical weather in Australia makes managing stored grain insects with ambient aeration difficult, increasing the reliance upon fumigation, particularly with phosphine. Development of aeration strategies that are effective under Australian weather conditions could lessen the reliance upon fumigation and add aeration as an IPM tool in the effort to suppress and control stored product pests. The focus was on wheat, using the storage location of Coreen, NSW, using four years of weather records, and a silo of height 11m and radius 6.85m. The objectives of this research were to identify potentially useful aeration strategies under Australian weather conditions and evaluate the effectiveness of each with respect to temperature, moisture content, grain uniformity, fan motor electricity costs, and insect population suppression. This objective is presented in chapter 3 of this dissertation.

2. To develop and validate a fumigant movement and loss model for bulk stored grain to predict phosphine concentrations with fumigant leakage and sorption.

In order to improve fumigation effectiveness and address concerns, fumigant movement in a grain storage silo must be fully understood. To achieve this, a mathematically accurate fumigation model was needed. In order to properly represent real world conditions, the fumigation model must be capable of considering fumigant movement, distribution, and loss via sorption into the grain, and fumigant leakage out of the grain silo. The specific objectives of this research were to build a model that is capable of accurately predicting fumigant concentration and movement throughout a grain storage silo that takes into account fumigant loss from leakage and sorption, and to validate this model with real world fumigation data. This objective is presented in chapter 4 of this dissertation.

3. To conduct a sensitivity analysis of a fumigant movement and loss model for bulk stored grain in order to predict effects of ecosystem conditions and operational procedures on fumigation efficacy.

Once a mathematically accurate fumigant movement and loss model has been developed, it can be used to provide bulk grain handlers with an effective prediction tool that can help them understand and manage fumigation events. Factors that may vary between fumigations and change the effectiveness of those fumigations include weather conditions such as wind speed, temperature, solar radiation, and operational variables such as recirculation rate, phosphine generation rate, gas tightness and the amount of phosphine applied. The specific objectives of this research were to use the mathematical model developed and validated in Objective 2 to investigate the effects of environmental conditions (i.e., temperature, relative humidity, and wind speed) and operational variables (i.e., recirculation rate, degree of silo seal, type of fumigant, and

silo dimensions) on fumigation efficacy. This objective is presented in chapter 5 of this dissertation.

4. To Model post-fumigation desorption of phosphine in bulk stored grain

Another issue is extraction of the residual fumigant from the stored grain bulk after completion of the fumigation. The success of lowering the phosphine concentration below the OSHA (Occupational Safety and Health Administration) exposure limit of 0.3 ppm can affect worker safety, market acceptability, and food safety of the treated grain. This is a process that is dependent on fumigant desorption from the grain after fumigation. The specific objectives of this research were to expand the M-L 3D ecosystem finite element model to investigate post-fumigation phosphine desorption, perform a silo scale experiment and use the experimental data to validate the expanded M-L-P model, and then apply the model to predict post-fumigation desorption of phosphine in bulk stored grain. This objective is presented in chapter 6 of this dissertation.

The key contributions of this dissertation research and how they were coded as well as the limits of the application needed to address them were summarized in chapter 7 of this dissertation. Conclusions from all objectives are restated in chapter 8 and future work is summarized in chapter 9 of this dissertation. Derivations of equations and other pertinent data are presented in the appendices.

Chapter 3 - Aeration Modeling Under Australian Conditions to Preserve Stored Grain Quality and Minimize Insect

Activity

Introduction

Stored product insects are an important concern to Australian wheat producers and bulk grain handlers. The warm climate provides optimal conditions for insect growth and makes insect populations difficult to suppress by cooling grain with ambient aeration. As a consequence, fumigation, primarily using phosphine, is the main method of insect control in Australian stored wheat. With an increase in phosphine resistance in Australia, the U.S. and elsewhere (Kaur et al., 2013; Konemann et al., 2014; Opit et al., 2012), it is critical to consider alternative forms of insect suppression for the Australian wheat industry.

Aeration is a proven grain storage management technology used to limit insect growth rates in temperate climates (Armitage and Stables, 1984). Low temperature of stored grain is effective because 20°C is the lower limit at which most insects can complete their development cycle in dry grain (Fields, 2006). Successful implementation of aeration as an insect suppression technique would reduce the reliance on fumigants and insecticides as a strategy in Australia (Arthur and Flynn, 2000; Cuperus et al., 1986; Wilson and Desmarchelier, 1994). When sufficient cooling hours are not available, maintenance aeration can be used to prevent hot spot development; remove heat produced due to respiration of grain, insects and fungi; prevent moisture movement and surface crusting; prevent condensation on the underside of silo roofs; maintain the free-flowing characteristics of grain; and maintain uniform temperature and moisture content of the grain bulk (Lawrence, 2010).

The benefits of aeration are well documented and the technology is widely used as a stored grain quality management practice in temperate climates, particularly in times of the year when there are sufficient cooling hours available. Aeration is used less in subtropical climates or in times of the year with fewer potential cooling hours, as is the situation for Australian wheat storage. Previous studies have considered the efficacy of aeration in Australia at higher ambient temperatures than may be used in the U.S. due to the drier Australian climate.

Wilson and Desmarchelier (1994) investigated using an aeration strategy based on seed wet bulb temperature to estimate insect growth that corresponded to holding various grains and oilseeds at a particular temperature and seed moisture content. This method created a single control parameter that could be used to make aeration decisions that takes both moisture and temperature into account. This approach targets insect damage as the most important form of spoilage but has the advantage of allowing Australian bulk handlers to take into account the grain moisture in determining acceptable aeration hours based on the air wet bulb temperature and the desired seed wet bulb temperature. A suitable number of aeration hours are still necessary, however, in order to achieve the desired seed wet bulb temperature before insect damage is predicted to begin. Another implication of this strategy is that it requires the grain handler to know how long storage is expected to last ahead of time in order to make decisions on what spoilage rates are acceptable. Different insect species have different rates of increase at various seed wet bulb temperatures (Desmarchelier, 1988), so a grain handler would need to understand which insect species may represent the greatest concern in their particular circumstance.

In the U.S., Akdogan and Casada (2006) concluded that useful aeration hours are reduced by higher relative humidity of ambient air, so drier conditions can yield more effective aeration

hours. Arthur and Casada (2005) discussed the feasibility of summer aeration for U.S. wheat and noted that in silos cooled from July through September, temperatures were lowered by 3°C or more and development of insects including the lesser grain borer, rusty grain beetle, and red flour beetle was reduced compared to non-aerated silos. However, the top of the grain mass was still favorable for insect development whether silos were aerated or not. Earlier U.S. studies showed that stored wheat temperature reduction of up to 6°C can be achieved with summer aeration in Dickinson County, Kansas, resulting in reduction of insect population growth of more than 80% (Harner and Hagstrum, 1990). Effective aeration strategies that suppressed insect growth were also developed for wheat stored under subtropical conditions in North India (Lawrence and Maier, 2011). Lawrence and Maier analyzed 15 different possible aeration strategies and selected optimum strategies based on fan run hours, predicted dry matter loss, and predicted insect growth. The strategies considered varied in aeration airflow rate and determined fan run time based on either equilibrium moisture content (EMC), temperature, or time of day. The optimum strategy found was one that ran the aeration fans based on EMC settings of fan operation when the EMC was less than or equal to 12% wet basis during cooler hours in the morning and evening (7-8 am, 8-9 pm).

Sinicio and Muir (1998) studied possible aeration scenarios under Brazilian conditions in eight different geographic locations. They determined that aeration was a useful strategy for each region, based on Allowable Storage Time (AST). This factor is based on a model presented by Fraser and Muir (1981) where AST is the time before seed germination viability drops by 5% or mold appears, based on grain moisture content and temperature. This safe storage time varied between 4 and 12 months for the most successful aeration strategies, which were chosen by calculating the total cost of aeration and spoilage of the different aeration strategies. The most

successful aeration strategies activated the aeration fans when there was a set differential between the outside air temperature and average grain temperature. The optimum temperature varied from 1°C to 5°C, depending on location and fan warming. They concluded that the maximum AST correlated with the number of cooling hours available below 15°C and developed a fit equation where $AST = 3.98 * \Theta_{15}^{0.306}$ where Θ_{15} is the amount of hours that are available in the storage season below 15°C.

While achieving sufficiently low temperatures to suppress insect population growth is the main parameter of interest for aeration conducted in warmer climates, there are other important parameters such as temperature gradients in the grain mass to consider as well. Stored product insects such as rusty grain beetle (*Cryptolestes ferrugineus*) can detect temperature differentials as low as 1°C and will seek out warmer areas of the grain mass if they exist (Flinn and Hagstrum, 1998). Natural convection currents also occur in a non-uniform temperature grain mass, leading to moisture movement and condensation, especially at the grain mass surface (Montross, 1999).

Moisture content is another important consideration in aerating stored grain because it affects the number of offspring, rate of development, longevity and survivorship of insect life stages from egg to adult. For instance, rice weevil (*Sitophilus oryzae*) females were shown to be able to lay only 10 eggs on average at 10.5% moisture content as opposed to 344 eggs at 14% moisture content (Fields, 2006). Monitoring the relative humidity of aeration air is also important because aerating with high humidity air has potentially negative consequences if it causes moisture condensation on cool grain, or results in excessive moisture adsorption in grain near the air inlets (Casada and Alghannam, 1999). Increasing grain moisture could lead to mold growth, as “the ability of storage fungi to germinate, grow and sporulate in stored grain is

dependent on the availability of water in the substrate, temperature and the intergranular gas composition” (Magan and Lacey, 1988)

The number of aeration hours and airflow rates also influence aeration performance. Arthur and Flinn (2000) showed that 120 hours of aeration cooling reduced rusty grain beetle (*Cryptolestes ferrugineus*) populations more substantially than 40 or 60 hours of cooling with 0.11 m³/min/t airflow rate. Lawrence and Maier (2011) showed that higher airflow rates of 0.33 m³/min/t suppressed maize weevil development more effectively due to faster aeration cooling. However, operating aeration fans with higher airflow rates (i.e., larger fan motors) and for longer periods results in higher energy expenditures. Lawrence and Maier (2011) estimated that under the same aeration strategy, increasing aeration air flow rate from 0.11 m³/min/t to 0.67 m³/min/t caused an increase in estimated fan operating expenses from \$920 to \$17,369 over the course of the year. This balance between fan power and energy cost must be considered in order to optimize aeration performance and select the best option among several aeration strategies.

The objectives of this research were to identify potentially useful aeration strategies under Australian weather conditions and evaluate the effectiveness of each with respect to temperature, moisture content, grain uniformity, fan motor electricity costs, and insect populations.

Materials and Methods

The M-L 3D ecosystem model developed by Lawrence and Maier (2011) was used to investigate aeration strategies for rapidly lowering temperature in wheat stored under East Australian weather conditions. The finite element model was programmed in Fortran and

adapted from the two-dimensional PHAST-FEM computer simulation model described by Montross et al. (2002), who also described the relevant governing equations. The model uses weather data inputs (i.e., ambient temperature, relative humidity, wind speed, and solar radiation), operational parameters (airflow rate, type of grain, storage time, initial conditions), and a three dimensional mesh of the grain silo in question. Temperature, moisture content and dry matter loss in the grain mass are predicted using the governing equations (i.e., mass, momentum, energy, and species) and associated parameter values. Dry matter loss is calculated based on ASAE Standard D535 (2005). The initial grain conditions were uniform throughout the silo, at 20°C and 11.3% moisture content dry basis.

For this study, Coreen, New South Wales, Australia was chosen as a representative location of the Eastern Australian wheat growing region, because data was available for wheat stored in silos from a previous study funded by the Plant Biosecurity Cooperative Research Consortium (PBCRC) (Darby, 2011). The silo was a Kotzur Model GP 18-10 silo with a 1500 MT wheat capacity, an eave height of 11.5 m and a diameter of 13.7 m. The silo specifications were used to create a mesh of elements for simulation of the grain storage volume using the program Gambit (Fluent Inc., NH). Ten years of weather data (i.e., solar radiation, temperature, relative humidity, and wind speed) were acquired from the National Climatic Data Center (NCDC) and converted into hourly values by averaging all the data points in each hour. This data was initially analyzed to determine possible aeration strategies based on weather conditions and available fan run hours for cooling stored wheat below 20°C. Aeration strategies were evaluated with the objective to identify which ones would successfully cool the wheat mass without increasing its moisture content. Selection was primarily based on accomplishing cooling as soon as possible after harvest, using the fewest fan run hours, similarly as the approach

described by Lawrence and Maier (2011). Additionally, grain temperature and moisture content uniformity were taken into account in the selection of the best aeration strategy.

Aeration strategies were designed based on levels of temperature, equilibrium moisture content, and time of day, similar to Lawrence and Maier (2011). The parameters of temperature and moisture content were used to provide a minimum of 100 fan run hours in the first three months of storage, based on ten-year average weather data. A total of six aeration strategies were evaluated, including both simple and more complex strategies, i.e., the aeration fan was on: (1) always, (2) whenever the ambient air temperature was under 20°C and equilibrium relative humidity (ERH) of the air was equivalent to the wheat equilibrium moisture content (EMC) between 9 and 14%, (3) whenever ambient air temperature was under 20°C, (4) between 0600-0800 and 1900-2100 hours, (5) whenever ambient air temperature was less than the wheat temperature in the center of the silo, and (6) whenever ambient air temperature was less than the temperature of the wheat in the center of the silo and the ERH of the air was equivalent to the wheat EMC between 9 and 14%. Each simulation run started on November 26 (in order to coincide with the start of a typical Eastern Australian wheat harvest), and ended on October 31 of the following year in order to evaluate long-term storage conditions. Weather data from the three most recent storage seasons at the time of the simulations were used: 2010-2011, 2011-2012, and 2012-2013); each with three different airflow rates: 0.105 m³/min/ton (0.1 cfm/bu), 0.21 m³/min/ton (0.2 cfm/bu), 0.42 m³/min/ton (0.4 cfm/bu). These corresponded to air velocities of 0.0143 m/s, 0.0286 m/s, and 0.0571 m/s, respectively.

To quantify changes in wheat temperature, moisture content and dry matter loss, predicted results were analyzed at five locations in the center of the grain mass, at depths of 0, 2.8, 5.7, 8.3, and 11m above the floor of the silo. Additionally, total fan run hours were

analyzed. The online FANS program from the University of Minnesota (<http://webapps.bbe.umn.edu/fans/>) was used to calculate the power requirements (kW) to deliver the selected airflow rates.

In order to investigate the effect of aeration strategies on the presence of insects, insect growth equations that were derived by Driscoll et al. (2000) were used in the M-L finite element model to calculate the change in insect populations at each node throughout the grain mass. Of the insects modeled by Driscoll et al. (2000), the red flour beetle (*Tribolium Castaneum*) was chosen for the simulations because it is a common pest that has demonstrated phosphine resistance (Opit et al., 2012), has been identified as one of the most important stored grain insect pests in Australia, and the predicted regression values are more accurate for this insect than any of the other insect models produced in Driscoll et al. (2000). The programmed initial value of insects was one insect per node. Tests using different initial insect populations demonstrated no effect on the percentage changes in insect population.

Results and Discussion

1. Overview of aeration strategy results

Table 3.1 summarizes the key results for each of the six aeration strategies and three airflow rates averaged across the 3 years of weather data. Aeration strategy 1 (i.e., aeration fan always on), was not effective because it caused fluctuating temperature and moisture content changes throughout the grain mass as a function of the prevailing weather pattern. Additionally, fan run hours and electricity costs were the highest among all strategies. Also, the grain was initially heated during the Australian summer, causing optimal conditions for insect growth.

The strategies that utilized the air ERH concept (i.e., strategies 2 and 6), as well as strategy 4 (i.e., fan on during specified hours in the morning and evening), were not successful in causing sufficient cooling due to a lack of suitable fan run hours. Even at the highest aeration rate, the average grain temperature for strategies 2 and 6 never reached 15°C. While strategy 4 was able to eventually cool the grain, it was slower than strategies 3 and 5, and had the effect of initially heating the grain during the Australian summer, which is undesirable. The amount of initial heating varied with fan airflow rate, from an average of 0.77°C at the lowest airflow rate of 0.105 m³/min ton, to 2.78°C at the highest airflow rate, 0.42 m³/min ton. When cooling began with this strategy, which had the third fewest fan run hours, it was slow as well, with 15°C average temperature not being reached until May even at the highest airflow rate. Poor performance of strategies 2 and 6 is consistent with previous findings by Reed and Harner (1998) who also determined that adding ambient air relative humidity as a fan control variable to air temperature was generally not cost effective and limited aeration fan operating times.

Table 3:1 Calendar date and time of day and fan run hours to reach 15°C or below average grain temperature in the grain mass across three storage seasons (2010-2013) in a 1500 MT wheat silo for three airflow rates (low=0.105 m³/min ton, medium=0.21 m³/min ton, high=0.42 m³/min ton) for the six aeration strategies investigated in this study.

Strategy	Airflow Rate	Date to reach 15°C	Fan Run Hours
		Average	Used
1	low	5/27/13	8160
	med	4/29/13	8160
	high	N/A	8160
2	low	Never Achieved	655
	med	Never Achieved	655
	high	Never Achieved	655
3	low	4/12/13	5748
	med	4/1/13	5748
	high	2/12/13	5748
4	low	8/25/13	2040
	med	5/26/13	2040
	high	5/6/13	2040
5	low	4/13/13	4445
	med	3/6/13	2934
	high	1/2/13	1980
6	low	Never Achieved	856
	med	Never Achieved	720
	high	Never Achieved	575

Strategies 3, 4 5 successfully cooled the grain mass below 15°C for all three airflow rates. Strategies 3 and 5 achieved that level of cooling by January and February (high airflow rates) and March and April (low airflow rates). Strategy 5 cooled the wheat faster, reaching 15°C three weeks faster at the medium rate, and over a month faster at the high rate. In addition, strategy 5 used 22.8% fewer fan run hours than strategy 3 at the lowest airflow rate of 0.105 m³/min ton, and 65.6% fewer fan run hours than strategy 3 at the highest airflow rate, 0.42 m³/min ton. Where strategy 3 used 5,748 fan run hours over the course of the year, strategy 5 used 4,445, 2,934, and 1,980 hours for the low, medium, and high aeration rates, respectively. Strategy 3 used the same average fan run hours with all airflow rates because it only used weather in decision making, whereas strategy 5 also included the current state of the grain in the decision to turn on aeration fans, and therefore faster cooling resulted in the fan being turned off sooner. However, it is a more complex strategy to implement and requires at least one temperature cable installed in the center of the grain mass.

Strategy 3 caused moisture content increases, particularly in the lowest region of the grain mass. These moisture content increases began slowly, but increased in magnitude around March and April, reaching as high as 18% in the bottom layers of the grain mass when using the highest airflow rate. How much the moisture content increased, and how far into the grain mass it progressed was dependent on time and airflow rate. For the low airflow rate, for example, the increase was confined to the bottom of the grain mass (less than 2.8m) and reached 14% moisture content by the end of the year. For the highest airflow rate tested, moisture content increases were seen throughout the grain mass, with the grain at the bottom of the silo (less than 2.8m) reaching 18% moisture content by the end of the year. The moisture content increase

began slowly, occurring mostly after the grain had already reached a cool temperature. For example, under the highest airflow rate scenario, the grain mass was cooled below 15°C before moisture content increase. There is the potential to limit this effect by lowering fan run hours after sufficient cooling has been reached. Strategy 3 was modified by switching to maintenance aeration at the beginning of June, a date by which sufficient cooling had been achieved. In this mode the air ERH was taken into account by adding the condition that the equilibrium moisture content had to be between 9% and 14% for the fan to be turned on. The modified strategy 3 effectively maintained grain conditions for the rest of each storage season around the temperature and moisture content values obtained by the end of the aeration cooling phase. As a result, the wettest area in the grain mass was consistently 2-3 percentage points drier than it was in the unmodified strategy 3. This change also reduced the fan run hours by 54% from an average of 5,748 for the unmodified strategy 3 to 2,650 for the modified strategy. The combined strategy of aeration when the ambient air temperature is lower than the set temperature threshold and then switching to maintenance aeration after cooling appears to be complete is a reasonably successful aeration strategy. Darby (1999) identified simplicity as a desirable characteristic for aeration control systems in Australia. When comparing the three airflow rates to modified strategy 3, the two higher rates cool the wheat faster but use more energy (8,895 kWh for the low airflow rate, 29,650 kWh for the medium airflow rate, and 138,366 kWh for the high airflow rate) and result in greater DML (0.039% low airflow rate, 0.06% medium airflow rate, 0.125% high airflow rate). However, because the higher aeration rates are capable of reaching grain temperatures below 15°C more rapidly, they were also more effective at suppressing insect development, as will be discussed.

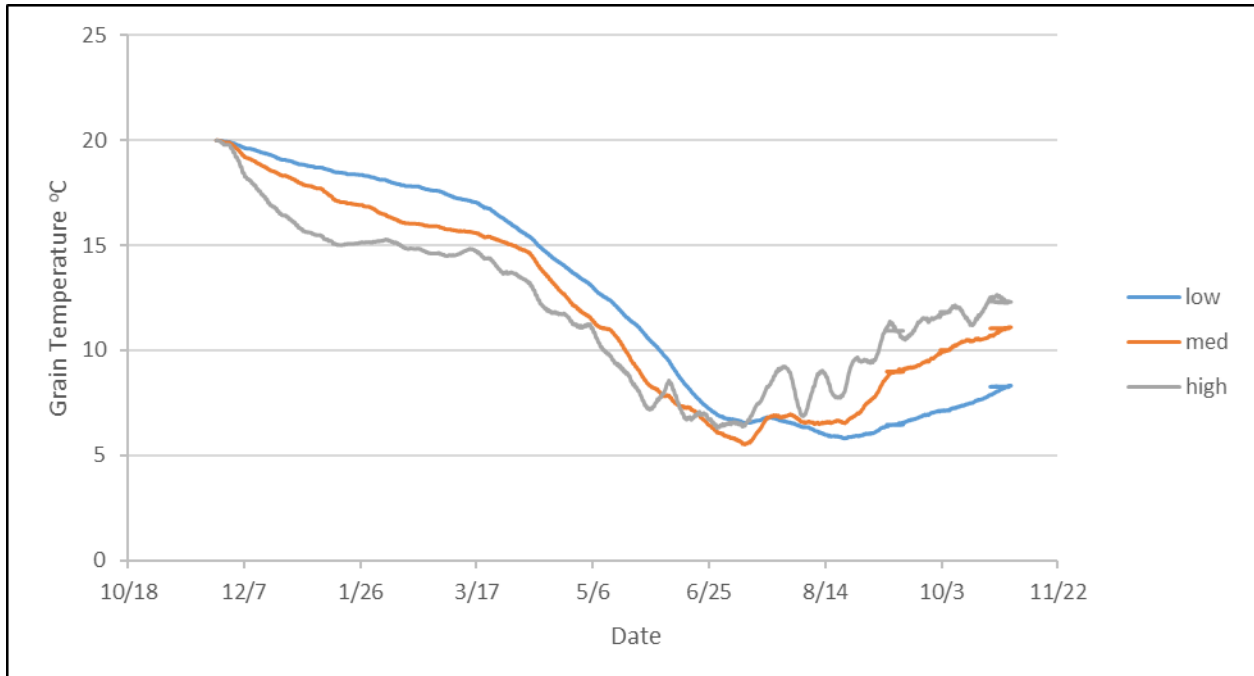


Figure 3:1 Grain temperature averaged across three storage seasons (2010-2013) in a 1500 MT wheat silo for three airflow rates (0.105 m³/min ton, 0.21 m³/min ton, 0.42 m³/min ton) with the aeration fan on whenever ambient air temperature was under 20°C (Strategy 3).

Table 3:2 Calendar date and time of day for the grain temperature averaged across three storage seasons (2010-2013) to drop below 15°C and 10°C in a 1500 MT wheat silo for three airflow rates (0.105 m³/min ton, 0.21 m³/min ton, 0.42 m³/min ton) with the aeration fan on whenever ambient air temperature was under 20°C (Strategy 3).

	under 15°C	under 10°C
low	4/12/13 8:00	6/3/13 23:00
med	4/1/13 8:00	5/20/13 1:00
high	2/12/13 5:00	5/11/13 0:00

Table 3:3 Yearly electricity consumption (kWh) averaged across three storage seasons (2010-2013) in a 1500 MT wheat silo for three airflow rates (0.105m³/min ton, 0.21 m³/min ton, 0.42 m³/min ton) with the aeration fan on whenever the ambient air temperature was under 20°C (Strategy 3).

	2011	2012	2013	average
Low	19,400	19,700	18,800	19,300
Medium	64,800	65,600	62,600	64,300
high	302,100	306,300	292,000	300,200

Table 3:4 Yearly electricity consumption (kWh) averaged across three storage seasons (2010-2013) in a 1500 MT wheat silo for three airflow rates (0.105m³/min ton, 0.21 m³/min ton, 0.42 m³/min ton) with the aeration fan on whenever the ambient air temperature was under 20°C until the beginning of June, then adding an EMC requirement of 9%-14% (Strategy 3 modified).

	2011	2012	2013	average
Low	8,900	9,100	8,700	8,900
Medium	29,900	30,300	29,000	29,700
High	139,300	137,200	135,100	137,200

Compared to strategy 3, strategy 5 cooled the grain faster, reaching below 15°C about 4 weeks faster at medium airflow rate, and 6 wks faster at high airflow rate, although it was one day slower than strategy 3 at low airflow rate. Strategy 5 also caused less of a moisture content increase in the bottom layer of the grain mass. In addition, cooling was achieved with fewer fan run hours (an average of 5700 hours for strategy 3 compared to averages of 4,400, 2,900, and 2,000 at low, medium and high airflow rates, respectively) and therefore fewer kilowatt hours

(19,200, 64,300, and 300,200 for strategy 3, and 14,900, 32,800, and 103,400 for strategy 5).

The number of fan run hours in strategy 5 was heavily influenced by airflow rate. The faster cooling times due to the higher airflow rates lowered the temperatures faster, resulting in fewer total fan run hours. These benefits were partially offset by the increase in energy expenditures due to the larger fans needed for higher airflow. The temperatures in strategy 5 were also more consistent than in strategy 3, because strategy 3 was more influenced by weather variations than strategy 5. This is particularly noticeable in the winter months when the temperature was consistently low and the fan was on most of the time. This meant that every weather pattern that passed through the area was seen in the grain mass, whereas strategy 5 demonstrated a consistent decrease in temperatures.

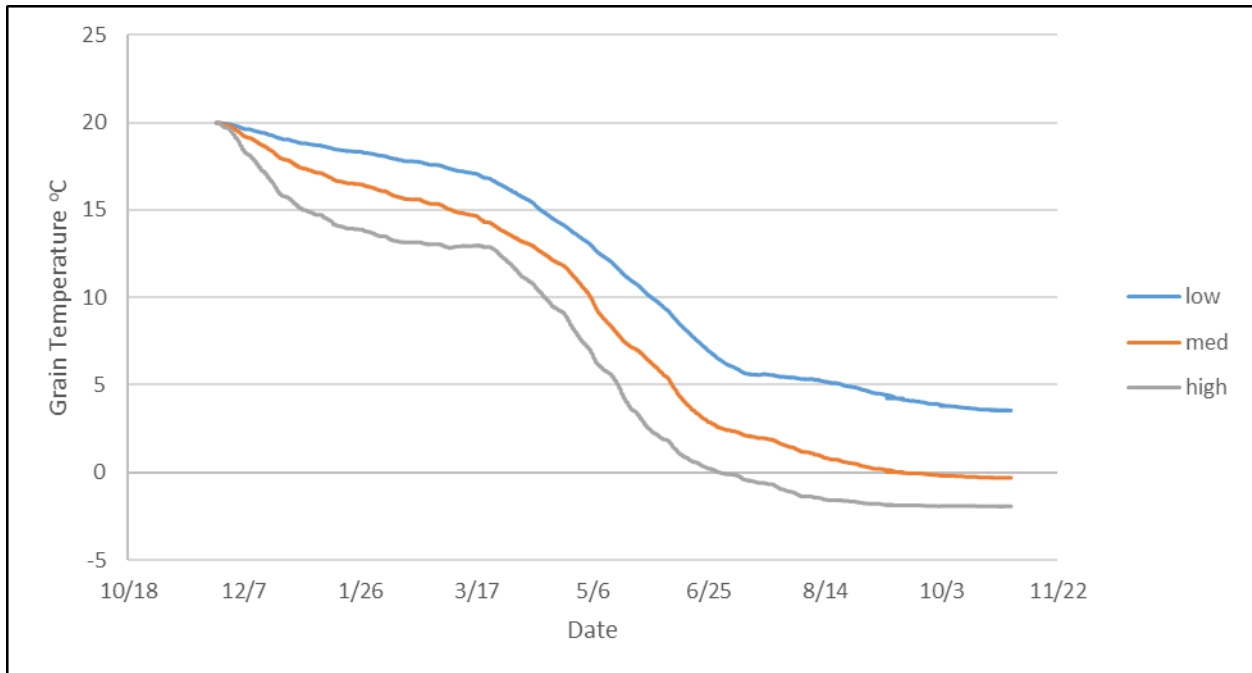


Figure 3:2 Grain temperature averaged across three storage seasons (2010-2013) in a 1500 MT wheat silo for three airflow rates (0.105 m³/min ton, 0.21 m³/min ton, 0.42 m³/min ton) with the aeration fan on whenever ambient air was cooler than air in the center of the grain mass (Strategy 5).

Table 3:5 Calendar date and time of day for grain temperature averaged across three storage seasons (2010-2013) to drop below 15°C and 10°C in a 1500 MT wheat silo for three airflow rates (0.105 m³/min ton, 0.21 m³/min ton, 0.42 m³/min ton) with the aeration fan on whenever ambient air was cooler than air in the center of the grain mass (Strategy 5).

	under 15	under 10
low	4/13/13 20:00	5/31/13 5:00
med	3/6/13 7:00	5/5/13 4:00
high	1/2/13 4:00	4/15/13 5:00

Table 3:6 Yearly electricity consumption (kWh) and average across three storage seasons (2010-2013) in a 1500 MT wheat silo for three airflow rates (0.105 m³/min ton, 0.21 m³/min ton, 0.42 m³/min ton) with the aeration fan on whenever ambient air was cooler than air in the center of the grain mass (Strategy 5).

	2011	2012	2013	average
Low	15,100	15,200	14,500	14,900
Medium	33,900	33,300	31,400	32,800
High	111,100	101,800	97,200	103,400

2. Optimizing the temperature differential to choose the best strategy

Strategy 5 was further investigated in order to optimize the cooling times by adjusting the temperature differential between the center of the grain mass and the ambient temperature.

Adding a temperature differential limits the fan run hours further, making use of only the fan run hours that are the most useful for cooling in an attempt to further reduce fan run hours.

Temperature differentials of 2, 3, 4, and 5°C were compared. To some degree the optimum differential is not immediately clear. Generally, the higher offsets caused delays in reaching an average grain temperature of 15°C or less (February 24 for no offset, March 10 for 2°C, March 18 for 3°C, March 24 for 4°C, all on medium airflow rate) and caused greater differences in temperature between the warmest and coolest points monitored the grain mass. The cooling effects were similar, however, while fewer fan run hours of (2,975, 2,405, 2,169, 1,993, for temperature differences of 2, 3, 4, and 5°C, respectively) were needed for larger temperature offsets. Additionally, while requiring additional time to cool the grain mass to 15°C average, higher offsets were able to reach 10°C earlier (10°C was reached on April 12, April 10, April 12, and April 13 for offsets of 0°C, 2°C, 3°C and 4°C, respectively). Temperature uniformity was an issue with these strategies, as the bottom layers of the grain silo were cooler than the upper layers of the grain silo at most times. This is a reasonable occurrence as the strategy relied on the temperature at the middle of the grain silo in order to make fan decisions, which could result in the aeration front being terminated after cooling reaches the center of the grain mass. At the end of the simulation, the temperature differences between the coolest and warmest area measured were 8°C, 8.9°C, 11°C, and 10.9°C for offsets of 2°C, 3°C, 4°C and 5°C, respectively. A reasonable temperature differential for strategy 5 was the 3°C strategy, as this was a middle ground between reducing fan run hours and reducing aeration quality. The decrease in fan run hours between the 2°C and 3°C fan run hours was larger than between the 3°C and 4°C offsets (570h and 236h, respectively) and the decrease in temperature uniformity was less between the 2°C and 3°C offsets than between the 3°C and 4°C offsets (0.9°C, 2.1°C)

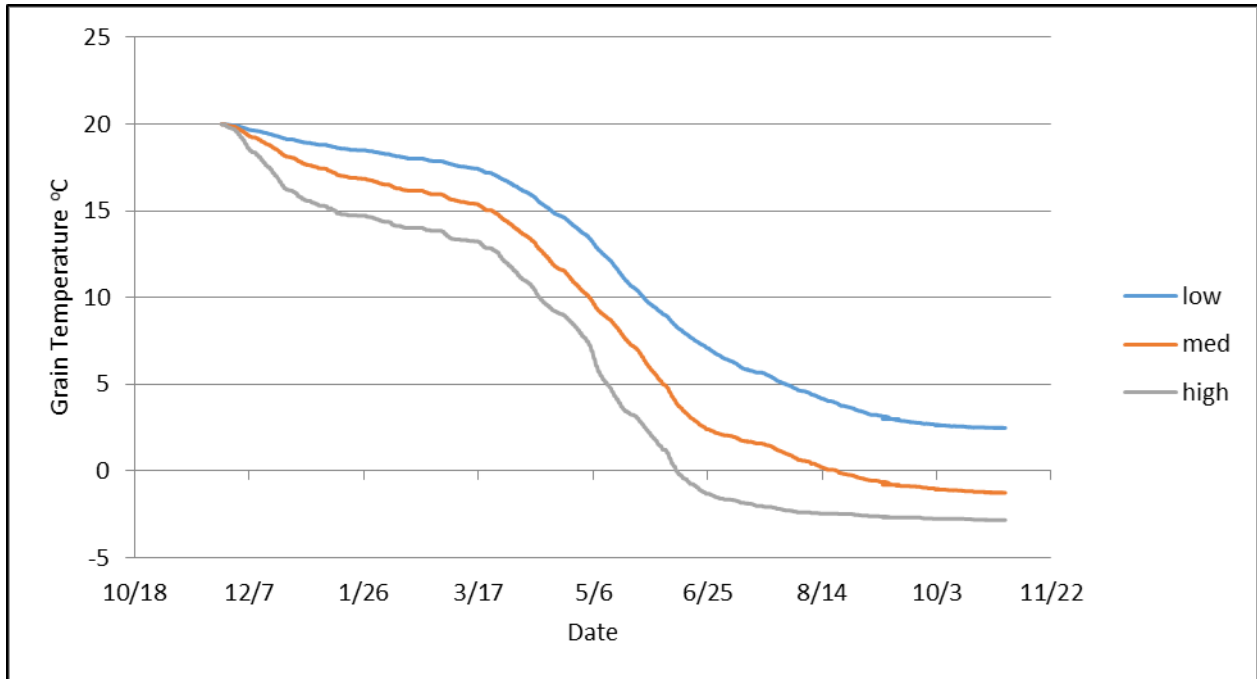


Figure 3:3 Average grain temperature across three storage seasons (2010-2013) in a 1500 MT wheat silo for three airflow rates (0.105 m³/min ton, 0.21 m³/min ton, 0.42 m³/min ton) with the aeration fan on whenever ambient air was at least 3°C cooler than air in the center of the grain mass (Strategy 5 modified).

Table 3:7 Calendar date and time of day for the average grain temperature across three storage seasons (2010-2013) to drop below 15°C and 10°C in a 1500 MT wheat silo for three airflow rates (0.105 m³/min ton, 0.21 m³/min ton, 0.42 m³/min ton) with the aeration fan on whenever ambient air was at least 3°C cooler than air in the center of the grain mass (Strategy 5 modified).

	under 15°C	under 10°C
low	4/18/13 0:00	5/28/13 4:00
med	3/23/13 3:00	5/4/13 8:00
high	1/13/13 20:00	4/12/13 21:00

Table 3:8 Yearly electricity consumption (kWh) and average across three storage seasons (2010-2013) in a 1500 MT wheat silo for three airflow rates (0.105 m³/min ton, 0.21 m³/min ton, 0.42 m³/min ton) with the aeration fan on whenever ambient air was 3°C cooler than air in the center of the grain mass (Strategy 5 modified).

	2011	2012	2013	average
low	10,700	11,000	10,000	10,600
med	24,000	23,400	22,000	23,100
high	66,400	62,300	61,300	63,300

3. Effect of changing initial grain temperature

The effect of high initial grain temperature at the time of harvesting Australian grain on aeration cooling times was further analyzed. Modified strategy 5 with the 3°C temperature offset was evaluated with wheat at initial temperatures of 20, 24, 25, 26, and 27°C. The time required for the average value to reach 15°C or less decreased by one day at the lowest airflow rate and three weeks at the highest rate with an increase in starting temperature from 20°C to 27°C. This was caused by the increase in fan run hours to cool grain at the higher initial grain temperature, because the center of the grain mass cooled slowly. Therefore, the fan stayed on longer for warmer grain. At medium airflow rate, the fan run hours increased by 15.4% as the initial temperature went from 20°C to 27°C (2,214 to 2,555, respectively). For the low airflow rate of 0.105 m³/min ton, wheat reached 15°C average temperature by mid-April for all four initial grain temperatures, compared to mid to late March for the medium airflow rate (0.21 m³/min ton), and late December to late January for the higher airflow rate (0.42 m³/min ton). Temperature uniformity decreased in the grain mass with increasing initial temperatures, with temperature difference between coolest and warmest locations tested at the end of the simulation increasing

from 8.9°C to 11.3°C as initial grain temperature increased from 20°C to 27°C. The temperature uniformity was lower at lower airflow rates, with the difference in temperature between the coolest and warmest locations at the end of the simulation decreasing from 16.4°C at the low airflow rate to 10°C at the high airflow rate for the 27°C grain. As seen in figure 3.7, for all initial grain temperatures tested there was a period of rapid cooling initially after harvest, ending near the end of December, as the air fronts are first applied. Cooling was gradual for the next several months, as there is not much cool weather available for aeration. Towards the end of March, cool weather conditions became available, and rapid cooling began again until the average temperatures level off again in mid-June. The grain with higher initial temperatures eventually became cooler on average than the grain with lower initial temperatures due to the decreased temperature uniformity. The warmer grain in the center top of the silo causes the aeration fans to accept more fan run hours in the silos with warmer initial grain, particularly during the winter. These additional hours are effective at cooling the lower levels of the grain, but the air in the middle of the silo remains warmer in the silos with grain of higher initial temperature.

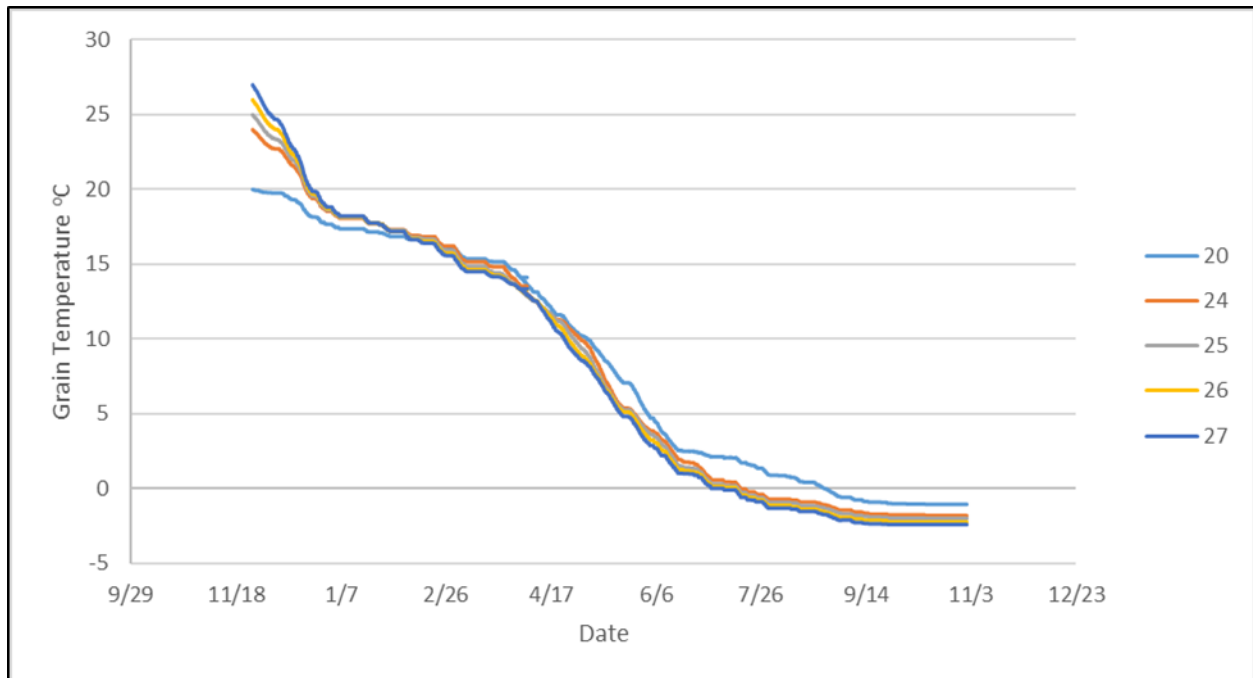


Figure 3:4 Grain temperature averaged for 2010-2011 storage year in a 1500 MT wheat silo at airflow rate of 0.21 m³/min ton for five different initial grain temperatures (20°C, 24°C, 25°C, 26°C, and 27°C) with the aeration fan on whenever ambient air was at least 3°C cooler than air in the center of the grain mass (Strategy 5 modified).

4. Effect of aeration strategies on insect development

Insect development was also simulated for strategy 3 (aeration fans on when the temperature is under 20°C), strategy 5 (aeration fans on when ambient temperature is less than internal temperature), and strategy 5 modified (Aeration fans on when ambient temperature is less than internal temperature by 3°C or more) for storage years 2010-2011 and 2011-2012. The results for a 20°C initial grain temperature are shown in figures 3.5-3.7. In all of the simulations, insect populations began decreasing initially, with higher airflow rates resulting in greater reduction of insects presumably due to the faster cooling of the grain mass. Insect populations then begin to increase in mid-January, reaching a maximum in late March before decreasing

again, presumably due to the influence of the warm weather conditions, particularly along the silo walls. In all simulations, insect populations eventually dropped to low amounts (below 5% of the initial insect population) and remained there for the rest of the simulation. At the lowest airflow rates, simulations reported less than 5% of the initial population by August 1, July 11, July 4 for the 20°C initial grain temperature (strategies 3, 5, and 5 modified, respectively) and August 28, September 11, September 8, for the 27°C initial grain temperature. This means that all strategies were able to cool the grain to a low enough temperature to be inhospitable to insects after the cool winter months.

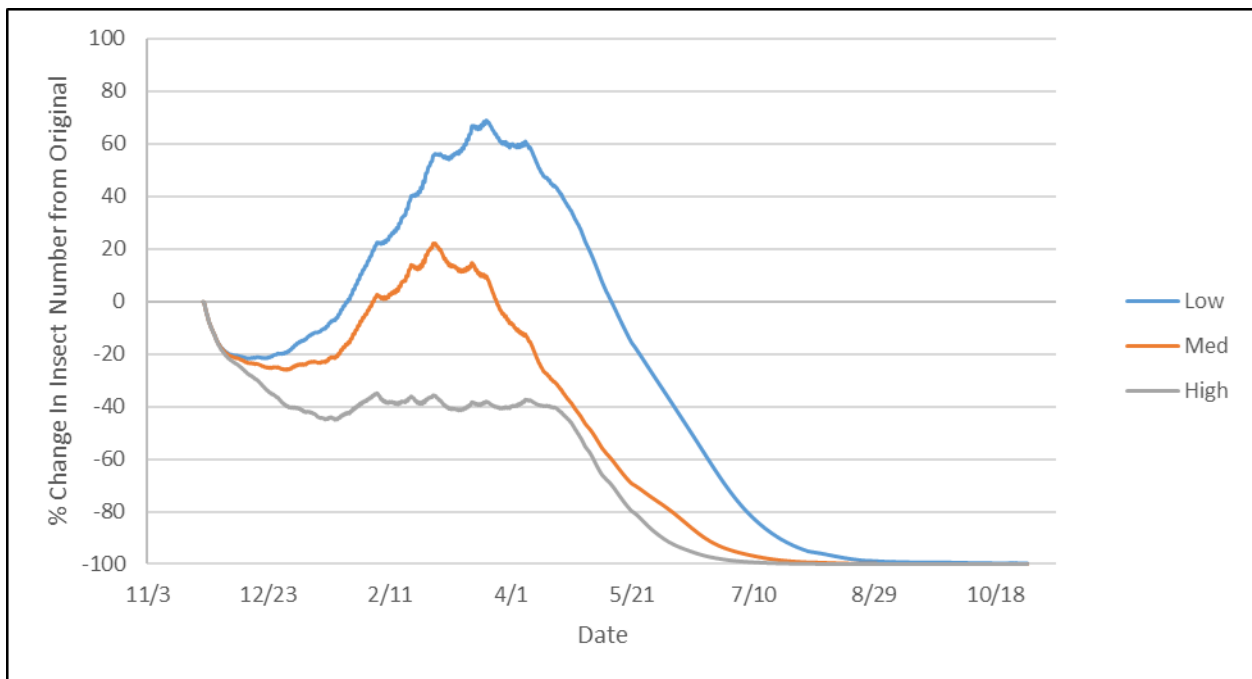


Figure 3:5 Simulated change (%) in insect number from original infestation in a 1500 MT wheat silo at 20°C initial grain temperature, averaged over 2010-2011 and 2011-2012 storage season with aeration whenever ambient temperature was below 20°C (Strategy 3) for three airflow rates (0.105 m³/min ton, 0.21 m³/min ton, 0.42 m³/min ton).

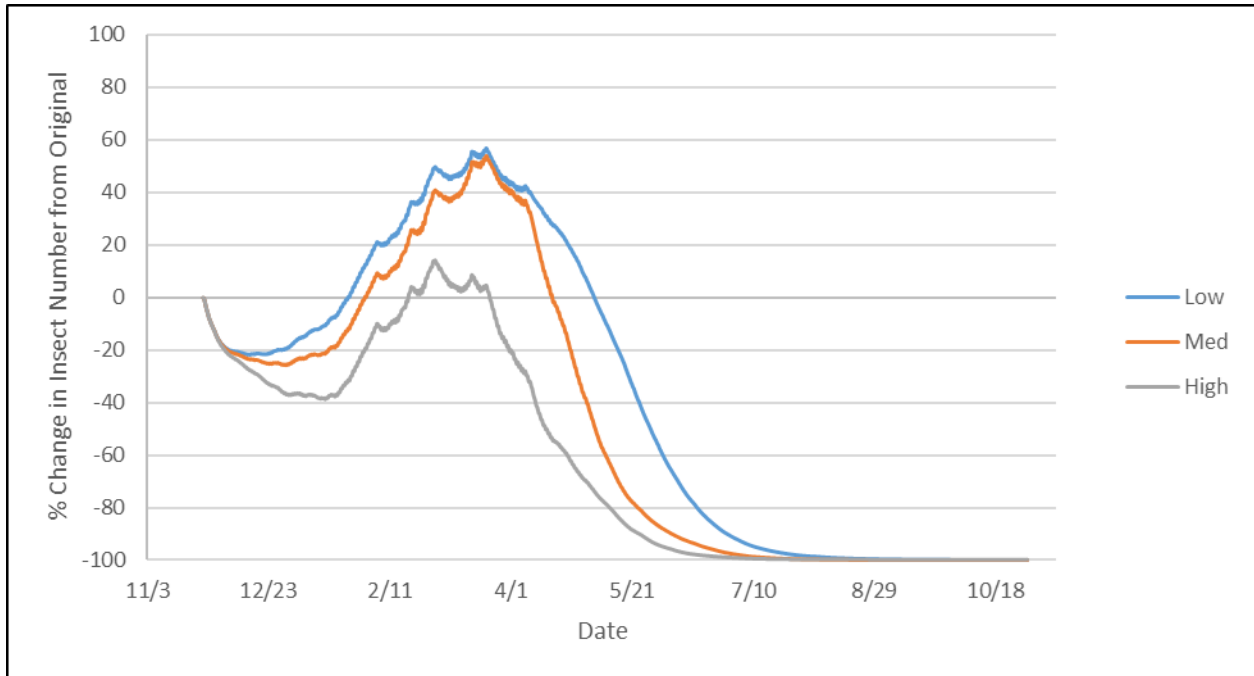


Figure 3:6 Simulated change (%) in insect number from original infestation in a 1500 MT wheat silo at 20°C initial grain temperature, averaged over 2010-2011 and 2011-2012 storage season with aeration whenever ambient temperature was below internal grain temperature (Strategy 5) for three airflow rates (0.105 m³/min ton, 0.21 m³/min ton, 0.42 m³/min ton).

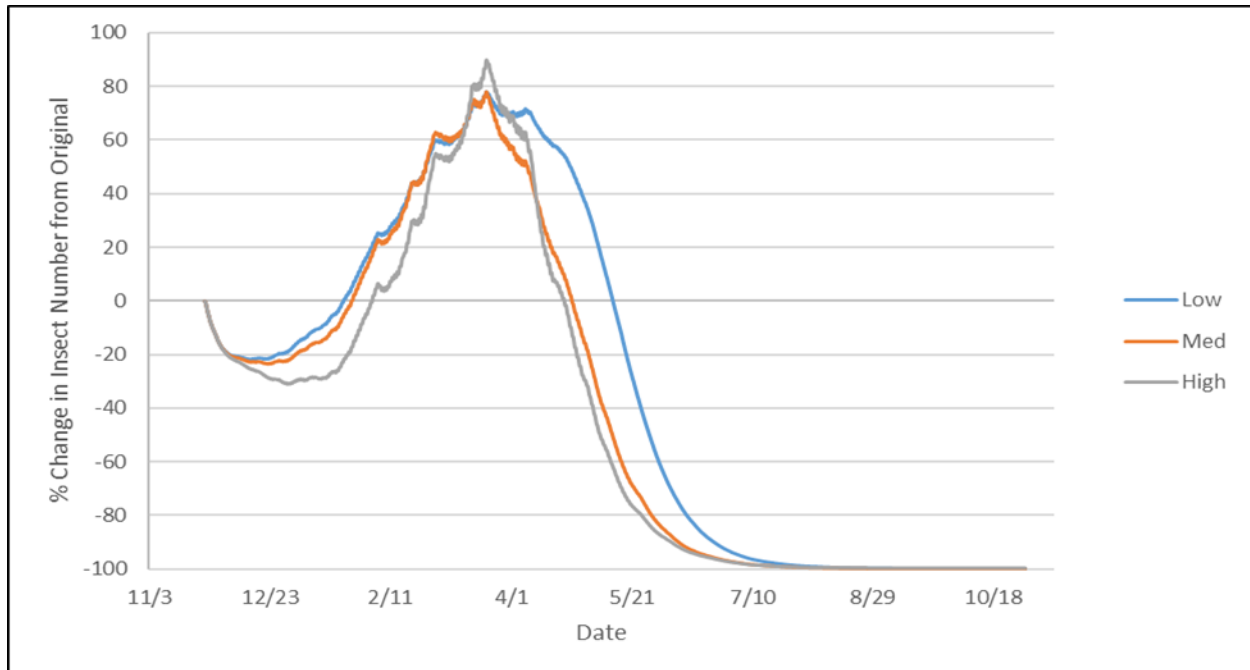


Figure 3:7 Simulated change (%) in insect number from original infestation in a 1500 MT wheat silo at 20°C initial grain temperature, averaged over 2010-2011 and 2011-2012 storage season with aeration whenever ambient temperature was at least 3°C cooler than air in the center of the grain mass (Strategy 5 modified) three airflow rates (0.105 m³/min ton, 0.21 m³/min ton, 0.42 m³/min ton).

For aeration strategy 3, aeration whenever ambient air is below 20°C, there was a clear difference in the effectiveness of the strategy at different airflow rates, as seen in figure 3.5. The low airflow rate (0.105 m³/min ton) resulted in a maximum insect population of 69% higher than the initial population, whereas the medium airflow rate resulted in a maximum population that was 22% higher than the original population. The high airflow rate (0.42 m³/min ton) was able to keep insect populations below the original infestation level for the entire storage cycle. The high airflow rate was able to reduce insect populations to less than 5% of their initial values by June 13, whereas the medium and low airflow rates reached that insect level by July 1 and August 1, respectively.

For strategy 5 (aeration whenever ambient air is less than internal grain temperature) the low and medium airflow rates performed similarly in terms of maximum insect population, with maximum insect populations of 57% and 54% increase, compared to the high airflow rate recording a maximum of a 14% increase. Insect populations of less than 5% of the initial infestations were achieved on July 11, June 19, June 3 for the low, medium, and high airflow rate, respectively. However, the medium airflow rate had lower insect populations before and after the maximum value was obtained. The reason for this is that strategy 5 had few fan run hours during the summer period. Daily temperature increases on the side walls would not affect the internal grain temperature, but would provide a good environment for insects near the side walls and the grain surface. Also, as mentioned earlier, higher airflow rates in strategy 5 decreased temperature uniformity in the grain mass, cooling the lower levels of the grain a greater degree while leaving the upper levels at similar temperatures to those seen in the lower airflow rates. This would allow for similar insect growth in the upper levels during the summer periods with few fan run hours. These effects are also noticed in the modified version of strategy 5, in which the aeration fan was only operated if the ambient temperature was 3°C or more less than internal grain temperature. The resulting maximum insect populations were 78%, 78%, and 90% above initial population for the low, med, and high airflow rate respectively. Insect populations reached below 5% of initial values on July 4, June 21, and June 18 for the low, medium, and high airflow rates, respectively. Despite the increased capacity of the higher airflow rates to reduce insect populations at the beginning and at the end of the simulation, the highest airflow rate performed poorly during the summer where few fan run hours were available. As seen previously, the modified version of strategy 5 operated on fewer fan run hours than strategy 5 and had a lower temperature uniformity, especially at higher airflow rates.

While the reduction in fan run hours saved costs, the fact that these strategies did not utilize the few moderately cool fan run hours that were available in the summer to interrupt insect growth along the edges of the silo caused increases in insect population.

Regardless of the strategy used, each of these strategies was capable of reducing insect numbers immediately after harvest and suppressing insect development starting in May. Each strategy was an improvement over the no aeration case, which demonstrated approximately exponential growth of insects that continued throughout storage and resulted in a population that was 99 times larger than the original population (data not shown).

Figures 3.8-3.10 show the results of using the same three aeration strategies and airflow rates for wheat harvested at a higher initial temperature of 27°C. In this case, each graph compares strategies at the same airflow rate. In each case, insect populations began increasing immediately after harvest. For the first six months of storage, all three strategies demonstrated poor control of total insect numbers, increasing insect values by 3,515%, 4,686%, and 4,260% increases for strategies 3, 5, and 5 modified respectively. For the low airflow rates shown in figure 3.9, little insect growth suppression is achieved until the beginning of March, by which time insect populations had grown beyond 30x their initial populations. From that point, small changes in the rate of insect change had a large impact, resulting in minor peaks. This continued from March through the beginning of May, then sufficiently cold weather was provided to control insect populations. Insect populations below 5% of the original values were reached on Aug 28, Sept 11, and Sept 8, for strategies 3, 5, and 5 modified respectively.

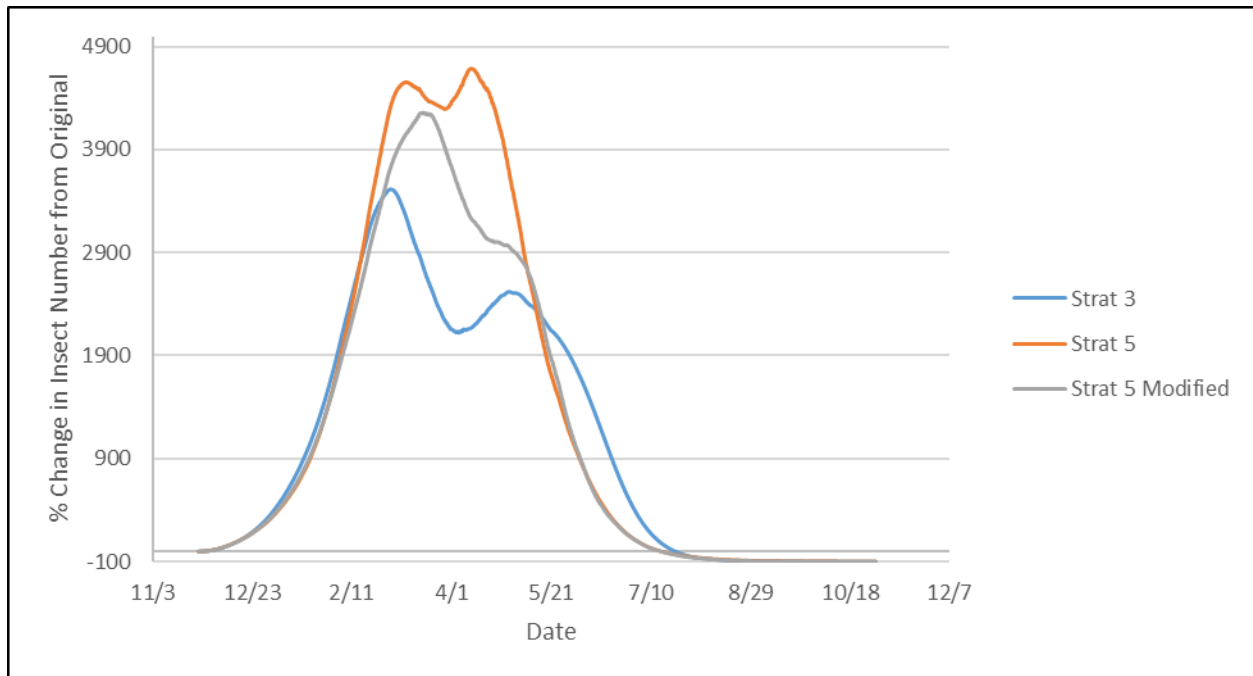


Figure 3:8 Simulated change (%) in insect number from original infestation in a 1500 MT wheat silo at 27°C initial grain temperature, averaged over 2010-2011 and 2011-2012 storage season for low airflow rate (0.105 m³/min ton) for each of the top three aeration strategies tested: below 20°C (3), ambient temperature is less than internal temperature (5), and ambient temperature is 3°C less than internal temperature (5 modified).

For the medium airflow rate, shown in figure 3.9, strategy 5 and strategy 5 modified show continued increase in insect populations from the beginning of the simulation until the maximum values are reached. The maximum insect populations were reached represented 738%, 407%, and 879% population increases for strategies 3, 5 and 5 modified, respectively. Strategy 3 shows a brief decrease in populations in late January before increasing again to the maximum value. Strategy 5 shows a superior ability to control insect populations when compared to both of the other strategies tested, departing from the values of the other two strategies in mid-February, showing slight decreases in insect population over the next two months whereas strategy 2 and strategy 5 modified continue to increase. Insect populations fell

to less than 5% of their original values on July 15, July 17, and July 26 for strategies 3, 5, and 5 modified respectively.

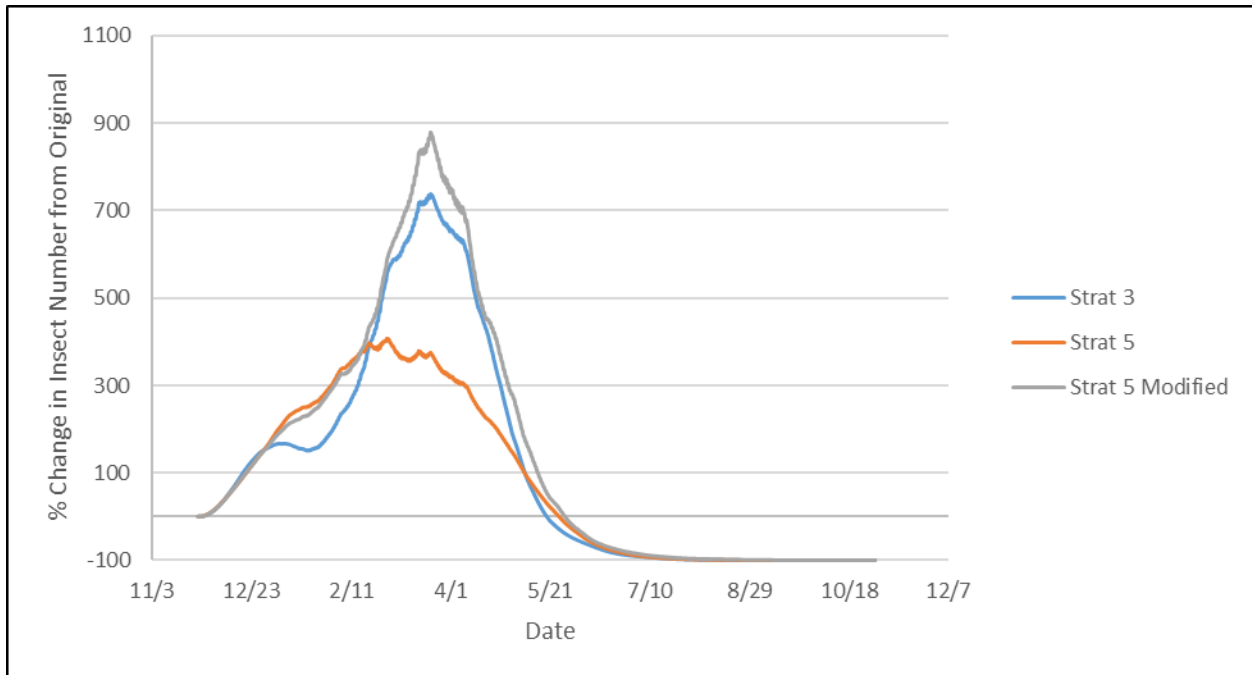


Figure 3:9 Simulated change (5) in insect number from original infestation in a 1500 MT wheat silo at 27°C initial grain temperature, averaged over 2010-2011 and 2011-2012 storage season for medium airflow rate (0.21 m³/min ton) for each of the top three aeration strategies tested: below 20°C (3), ambient temperature is less than internal temperature (5), and ambient temperature is 3°C less than internal temperature (5 modified).

For the high airflow rate at 27°C initial temperature (figure 3.10), each strategy tested showed that the immediate increase in insect population could be stopped by mid to late December. By the middle of January, populations in all three strategies began to rise again, with the insect populations in strategy 3 and strategy 5 leveling out below a 50% increase off of the initial values, and the population in strategy 5 modified reaching a maximum value that represents a more than 150% increase from initial insect values. This is due to the inability of the modified strategy 5 to make use of fan run hours from mid-February to mid-March that

allowed strategy 3 and strategy 5 to maintain insect populations, whereas the modified strategy 5 demonstrated increasing insect populations over that time period. The maximum insect populations reached represented 35%, 36%, and 164% increases off the original population for strategy 3, strategy 5, and modified strategy 5, respectively. Strategies 3 and 5 began downward trends in early March, with strategy 5 modified declining in late March. Insect populations dropped to less than 5% of the initial values on June 2, June 10, and July 2 for strategies 3, 5 and 5 modified respectively.

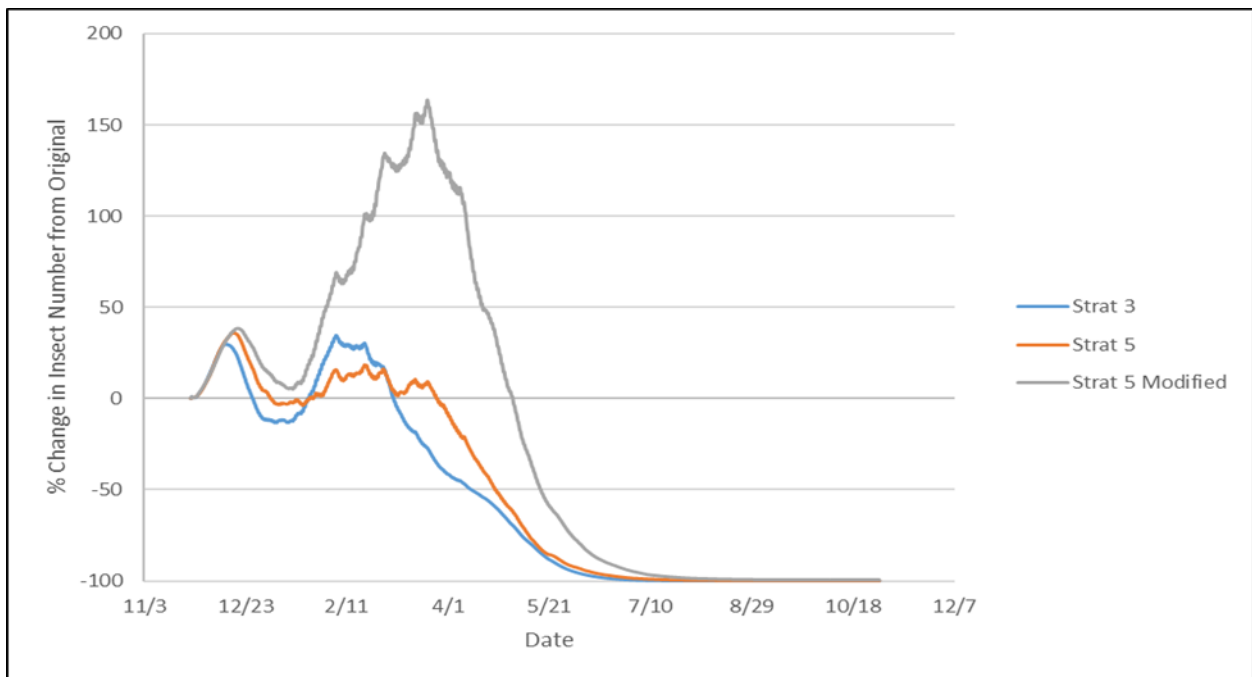


Figure 3:10 Simulated change (%) in insect number from original infestation in a 1500 MT wheat silo at 27°C initial grain temperature, averaged over 2010-2011 and 2011-2012 storage season for high airflow rate (0.42 m³/min ton) for each of the top three aeration strategies tested: below 20°C (3), ambient temperature is less than internal temperature (5), and ambient temperature is 3°C less than internal temperature (5 modified).

These results demonstrate substantial differences in effectiveness between the three airflow rates, with higher airflow rates resulting in better insect suppression regardless of initial temperature or aeration strategy. For the low airflow rate, strategy 3 had the best overall results in terms of insect suppression, whereas strategy 5 had the best results at the medium airflow rate. At the high airflow rate, strategies 3 and 5 performed similarly, with strategy 3 achieving a higher maximum, but also dropping below the initial insect infestation faster than strategy 5. However, these simulations did demonstrate the usefulness of aeration to limit the growth of insects under Australian conditions, as all of these strategies are improvements on the no aeration case. Without aeration, the insects demonstrated exponential growth leading to a final insect population that was 2,800,000,000 times the original.

Based on these results, strategies 3 and 5 are clearly better than the modified strategy 5. Strategy 5 seems to represent the most economical strategy, combining good insect suppression at the medium and high airflow rate with reduced fan run hours and resulting electricity costs. The best comparative situation for strategy 3 over strategy 5 was the low airflow rate under 27°C initial temperature. This was the only situation where the increase in average insect population under strategy 5 (23%) was greater than the fan run hour reduction (22%). Under the other situations where strategy 3 had a better insect performance (low initial temperature under medium and high airflow rate), the percent fan run hour reduction was greater than the percent insect increase. Additionally, while the performance of strategy 5 under the low airflow rate and high initial temperature was poor, all of the strategies at that airflow rate would likely have required fumigant intervention, as all peaked at insect populations more than 30 times the original. With this level of increase, only an initial population of 0.067 insects per kg would

have been required to breach the U.S. Federal Grain Inspection Service limit of 2 live insects per kg to receive the 'infested' label.

While these strategies demonstrated overall success, they have not been fully optimized and several potential changes could be investigated to further improve performance. These approaches could include utilizing maintenance aeration in order to slow the increase in temperatures along the side walls during summer and using average temperatures for aeration decisions instead of a single internal temperature. All of these solutions would involve relaxing the temperature requirements for using the aeration fan during the summer months to prevent continuous temperature increases along the side wall. Further modifications of strategy 5 that used a full silo average temperature for control decisions, and a strategy that utilized increased maintenance aeration during the summer were briefly tested. Both demonstrated slightly worse performance overall when compared to strategy 5.

Conclusions

The effectiveness of six aeration strategies for the cooling of stored wheat under East Australian weather conditions were examined. The strategies were compared on the basis of time required to cool grain to 15°C or less, moisture content and uniformity in the grain mass, fan motor electricity usage, temperature uniformity in the grain mass, and insect populations.

The key results are:

- An effective strategy at airflow rates of 0.105 m³/min/t to 0.42 m³/min/t that does not require complex controls would be to run the aeration fan to cool stored grain whenever

the ambient air temperature is below 20°C (Strategy 3), and switch to maintenance aeration once the targeted grain temperature of 15°C or less is reached.

- A more effective but more complex strategy where the aeration fan is turned on whenever the ambient temperature is less than the grain temperature at the center of the grain mass (Strategy 5) will cool the grain to 15°C one day later, 26 days earlier, and 41 days earlier for 0.105, 0.21, and 0.42 m³/min respectively, and require 23%, 49%, and 66% fewer fan run hours, respectively.
- For the higher airflow rate of 0.42 m³/min when compared to a lower airflow rate of 0.105 m³/min proved to be a tradeoff between faster wheat cooling and higher energy costs (achieved 15°C 101 days earlier with Strategy 5 compared to a 594% increase in kWh)
- Placing wheat into a silo at increased initial temperatures of 20°C-27°C does not substantially increase the cooling time of the grain with the 3°C temperature differential between ambient and internal grain temperature (Strategy 5 modified). However, it does increase fan run hours (from 2,214 to 2,555 at 0.21 m³/min/t, +15.5%) and insect development (an overall average of 52% of original at 20°C to 179% of original at 27°C, +244%).
- The three strategies tested to mitigate insect growth rates all successfully reduced insect numbers to less than 5% of their original value by the end of the simulated storage period. While strategies 3 and 5 were most effective in controlling insect populations in 3 of the 6 tested situations each, strategy 5 had the lowest energy usage in all scenarios.
- While the 3°C temperature differential strategy (modified strategy 5) had the most efficient energy use (using the fewest fan run hours, and reaching 15°C an average of 11

days after the fastest strategy, strategy 5), it performed comparatively poorly on overall insect growth. This was seen most notably at the highest airflow rate of 0.42 m³/min ton, where total average insect numbers increased from strategy 5 levels, where overall average insect levels increased by 28% at 20°C and by 66% at 27°C.

- Overall, the temperature differential strategy based on internal grain temperature (strategy 5) performed the best out of all strategies tested. It was able to cool the grain mass the fastest, used fewer fan run hours than every strategy except strategy 5 modified, and also controlled insect populations as well as any other strategy. This strategy is recommended under East Australian weather conditions in order to preserve stored grain quality and minimize insect activity in commercial silos.

Chapter 4 - Developing and Validating a Fumigant Loss Model for Bulk Stored Grain to Predict Phosphine Concentrations with Fumigant Leakage and Sorption

Introduction

A successful fumigation relies on exposing each insect within a grain mass to a specific concentration of fumigant for a specified amount of time in order to kill all insects present at all life stages. Modeling the behavior of gas fumigants in the interstitial air volume of the stored grain mass is helpful in determining what factors may cause fumigation failures, and how those factors can be affected by environmental conditions. The M-L 3D finite element ecosystem model was previously developed to investigate stored grain environments and has the capacity to monitor chemical concentrations throughout the grain mass (Lawrence, 2010). In order for this model to accurately predict fumigant concentrations the model must be improved with the added capacity to account for fumigant loss. The primary sources of fumigant loss are fumigant leakage from the silo and fumigant sorption into the grain.

Adsorption refers to chemicals that merely adhere to the grain surface, whereas absorption refers to chemicals that are drawn into the grain kernel. Sorption is used as a blanket term to refer to both processes. Many investigations calculate sorption values based on chemicals lost from the headspace above the product due to the relative ease of measuring gaseous concentrations (Daglish and Pavic, 2008; Darby, 2011; Dumas, 1980). Such investigations do not quantify the difference between phosphine adsorbed and absorbed due to the chosen method of measuring the value. For the purposes of this analysis, the primary interest

is in the concentration of fumigant in the interstitial air spaces, and therefore, the general term 'sorption' is used for literature that does not differentiate between adsorbed and absorbed chemicals. Literature that does differentiate between adsorbed and absorbed fumigant will have its values referenced as either adsorbed or absorbed.

Sorption of gas by grain was listed as one of the factors most likely to cause inadequate fumigation conditions in Australia (Darby, 2011). Wheat at higher temperature sorbed a greater amount of phosphine than lower temperature wheat. After 96 hours in a container with initially 1 mg/L phosphine, the fumigant concentration in the interstitial airspace of stored wheat at 35°C was below 0.1 mg/L, whereas in wheat at 15°C it was around 0.5 mg/L (Darby, 2011). That result was supported by Reed and Pan (2000), Sato and Suwanai (1974) and Dumas (1980) who reported phosphine sorption increased with higher grain temperature and moisture content. An increase of temperature also caused faster rates of sorption of phosphine in wheat independently from moisture content. An increase from 24°C to 35°C caused the sorption rate constant to increase from 0.0064 to 0.186 (Banks, 1986; Berck, 1968). In another study, the average phosphine concentration over the course of a fumigation in a silo increased faster for wheat at higher temperature reaching a maximum concentration of 0.8 to 1 mg/L at 30°C and 0.3 to 0.5 mg/L at 20°C. After the maximum concentration was reached, the phosphine concentrations decreased faster in the warmer silos and dropped below detectable levels earlier, i.e., in wheat at 30°C after 4 days, wheat at 25°C after 6 days, and wheat at 20°C after 7 days (Reed and Pan, 2000).

The chemical composition of fumigated grain is also important when considering how much fumigant loss to anticipate from grain sorption. While the study did not include phosphine, Banks (1986) showed that the composition of wheat affected the amount of methyl

bromide fumigant adsorbed. Specifically, increases in fat and/or protein percentages led to increases in fumigant adsorbed. An increase of five percentage points in fat content resulted in a 100 mg/kg increase in adsorption at constant temperature. A similar effect was observed with an eight percentage point increase in protein content. This conclusion might reasonably be extended to phosphine, because oilseeds and tree nuts, which have higher oil and protein percentages than cereal grains, were shown to be more sorptive of phosphine than starchy cereal grains such as wheat and milled rice (Reddy et al., 2007). Reddy et al. showed that the head space above the commodity had generally higher terminal concentrations of unabsorbed phosphine for most cereal grains (578 to 1870 ppm, with paddy rice being the only grain under 1000 ppm) than in oilseeds (112 to 1623 ppm, with soybeans, shelled peanuts, and sesame seeds being the only oilseeds above 1000 ppm).

The amount of phosphine adsorbed by wheat increased linearly with an increase in concentration of phosphine applied (Sato and Suwanai, 1974). This result was reinforced by an additional experiment in which the sorption coefficients for phosphine in wheat were shown to be higher for fumigations conducted with higher concentrations of phosphine (Daglish and Pavic, 2008). Phosphine loss was also shown to increase with an increase in grain moisture content (Reed and Pan, 2000) where the mean phosphine concentration at 25°C was 0.38 mg/l at 10.8 % moisture content and 0.32 mg/l at 13.2%. In another sorption experiment, percent daily loss of phosphine, meaning the amount sorbed, increased with an increase in the percent of the silo that is filled with grain, known as the filling ratio. A container with 1 mg/L phosphine had a daily loss of phosphine increase from 1.5% to 5.5% as the filling ratio increased from 25% to 95% (Daglish and Pavic, 2008) as more grain was available to absorb phosphine. Adsorption of

phosphine to the surface of cereal grains also increased with increasing temperature (Sato and Suwanai, 1974).

For sorption to take place, the airborne chemical must come into contact with the grain. Therefore, a porous medium, such as a grain mass, that allows for more area of contact between the medium and the air will exhibit more sorption than a solid medium or one with less contact between air and substrate. In fact, “gas adsorption measurements are widely used for determining the surface area and pore size distribution of a variety of different solid materials” (Sing, 1982). For this reason, it is not surprising that phosphine adsorption increased with a decreasing particle size (Sato and Suwanai, 1974). Particle size of wheat flour, however, did not influence phosphine sorption (Reddy et al., 2007). With the exception of rice, all grains tested had the same amount of hydrogen phosphine adsorbed per unit area of grain i.e., 27 ng/cm² (Sato and Suwanai, 1974).

Sorption of fumigant into the grain mass includes both diffusion and chemical reactions in the grain. It typically occurs rapidly initially, corresponding to diffusion, and slows to semi logarithmic behavior as it is driven by the chemical reaction in the grain (Banks, 1990). The decline of phosphine during a fumigation due to grain sorption was shown to behave approximately like a first order equation (Daglish and Pavic, 2008). Whole wheat exposed to 2 g/m³ phosphine for 7 days at 25°C adsorbed 19% of the available phosphine (Reddy et al., 2007). The amount of phosphine sorbed in 10 g of wheat in a flask at 25°C was around 5 µg more than in the control, an empty flask. At 85°C that increased to 20-50 µg, depending on duration of fumigation (Dumas, 1980). After 8 days of fumigation with constantly applied phosphine varying from 0.1 to 1.5 mg/L, the fumigant concentrations at the end of the experiment were greater than 90% of the concentration applied (Daglish and Pavic, 2008).

In addition to fumigant sorption, it is also important to understand how much fumigant is being lost from the grain storage structure into the environment. Leakage from a grain silo, either small and dispersed over the whole of the silo, or large and from a specific point, can cause substantial fumigant loss. This in turn can cause areas of the silo to receive a sub lethal dose of the fumigant. This is especially important considering that the majority of grain in Australia is fumigated in silos that do not meet gas tightness standards (Darby 2011). The industry pressure test standards used in Western Australia for airtightness in storage silos is based on a pressure decay of 200 to 100 Pa in 15 minutes (Ripp, 1984).

Leaks are the most important means of phosphine loss from the fumigated structure. Fumigant loss through a leak is composed of both convective and diffusive components. Of these two components, loss due to diffusion is low compared to fumigant loss due to convection (Banks and Annis, 1984; Cryer, 2008). Convection losses from a leak are composed of chimney effect loss and loss due to wind. Additionally, wind speed, average daily temperature, and solar radiation all have a large effect on gas loss from silos (Navarro 1998).

The chimney effect can be caused both by temperature differences between the grain silo and the outside environment, and by differences in concentration between the grain silo and the environment. The chimney effect on fumigant loss is higher for the concentration differences than it is for temperature differences (Banks and Annis, 1984). This is also supported by Noyes and Phillips (2007) who state that higher concentrations will lead to greater amounts of leakage from the storage structure. The amount of fumigant lost is a function of the sealing efficacy for both chimney and wind effect losses. The temperatures and pressures inside the grain silo, however, are not heavily affected by the sealing (Banks and Annis, 1984).

Wind effect is the more important of the two convective fumigant loss factors (Banks, 1990). Fumigant leakage rate was analyzed for methyl bromide and sulfuryl-fluoride fumigations in grain processing building structures (Chayaprasert et al., 2012). They showed that wind speed is the only environmental factor that affected fumigant leakage rate. This finding might be extended to phosphine as wind-driven convection loss of fumigants is not significantly affected by the kind of fumigant used (Cryer, 2008). In a separate experiment, phosphine leakage was reported to increase with an increase in grain temperature and moisture content (Reed and Pan, 2000).

Wind forces can cause air to flow both into and out of a grain silo, with the maximum impact occurring at $\frac{3}{4}$ of the structure's height and at the roof joints (Mulhearn et al., 1976). The area of the silo experiencing the next highest wind effect was the roof wall joint. This was considered the primary location of importance for wind losses, as it is also an area at high risk of leakage. Wind speed and direction can affect the resulting concentrations of fumigant gas in the surrounding environment (Cryer and Barnekow, 2006), and therefore, the rate of leakage from the silo. In another experiment on controlled atmosphere storage, wind displacement effects were able to rapidly increase oxygen concentrations from 2% to 14% mass fraction on the wind affected side of the silo (Bibby and Conyers, 1998). However, they also determined that "wind has little effect at disturbing gas flow" inside the silo.

In a mathematical examination of fumigant loss, the most important environmental factor causing leakage from an enclosure is wind effect, followed by chimney effect, headspace temperature variation, barometric pressure variation, temperature variation in the grain bulk, and diffusion (Banks, 1990). Quantitatively, for a medium sized leak (estimated equivalent area of leak at 650 mm²), wind was calculated to have a fumigant loss rate of 6.3% per day, and

chimney effects of about 4% per day (Banks and Annis, 1984). The maximum acceptable loss of phosphine for a fumigation was estimated at around 10% per day. When comparing the leak-dependent sources (such as wind and chimney effects) to leak-independent sources (such as temperature and pressure effects) in a typical silo, the sum of losses from leak-dependent sources was found to be about an order of magnitude greater than those from leak-independent sources (Banks and Annis, 1984).

How well a silo is sealed is an important factor, but it has not been investigated to the same degree as the other parameters of fumigant loss. An attempt to model fumigant loss using the pressure decay time was made by Mann et al. (1999) who calculated an equivalent area of leakage. This technique, however, was not successful as it had errors in its area of leakage estimations ranging from -17.5% to 23.1%. Ultimately they concluded that the observed gas loss was inconsistent with the predicted values. A similar technique was used by Chayaprasert et al. (2010) to predict methyl bromide and sulfuryl-fluoride pressure decay half-life times. The model was mostly able to predict half-life times within one hour of the actual value.

The influence of fumigant loss from leakage and from sorption into the grain is clearly an important factor to be considered in a simulation that seeks to understand phosphine movement and concentrations in grain storage structures. In addition, how the scale of fumigant loss changes in response to environmental factors is also necessary to know if the relationship between environmental changes and fumigation success is to be understood. For this reason, a fumigation model that incorporates both phosphine sorption and silo leakage, while taking into account the influence of changing weather and operational conditions, would be a beneficial tool for simulating stored grain protection scenarios. A previous attempt at developing such a fumigation model was made by Isa et al. (2016) using the program Fluent instead of an

independent computer code. They also simulated vertical gas flow in a silo using Fluent and Comsol (Isa et al., 2011). While using any of the available fluid dynamics software packages has several advantages, such as ease of use and ease of visualizing results, it has disadvantages as well. Their fumigation model simulates both sorption and leakage losses, but the leakage losses are not influenced by weather condition or surrounding factors. Since the boundary conditions are set inside Fluent, loss was implemented with point losses only. The amount of loss was then controlled only by pressure half loss time. This strategy may be insufficient not only for fumigant loss that is affected by weather, but also in its inability to consider the combined effect of many small leaks over the entire surface of the silo.

Fumigation recirculation is an important factor in achieving a successful fumigation. Fumigations that recirculate gas have several advantages over passive fumigations, including reduced grain handling shrinkage, lower necessary dosages, faster fumigations, less required labor, improved worker safety, less phosphine in the environmental phosphine, reduced insect resistance, and reduced overall cost of fumigation (Noyes et al., 1998).

The objectives of this research were to build a model that is capable of accurately predicting fumigant concentration and movement throughout a grain storage silo that takes into account fumigant loss from leakage and sorption, and to validate this model with real world fumigation data.

Materials and Methods

1. Effect of Sorption

The M-L 3D ecosystem model developed by Lawrence and Maier (2011) that was used to investigate aeration strategies under Australian conditions in Chapter 3 was modified to

investigate fumigation concentrations and movement in a storage silo over the course of a fumigation. In order to accurately account for fumigant loss, the model was modified to include equations for fumigant sorption into the grain mass, and for leakage out of the storage silo.

In order to estimate sorption loss, a baseline equation relating phosphine concentration to fumigation time was used from Dargatzis and Pavic (2008). The equation is valid at a 1 mg/L application, and 0.75 fill ratio, resulting in an R^2 value of 0.96 at 25°C and 55% relative humidity. This baseline equation was used because a 0.75 fill ratio is reasonable considering the model consists of an entirely filled cylindrical section of wheat and no wheat in the headspace. The headspace that is not filled with grain in the silo represents the extra remaining 25% of the volume for the fill ratio. A phosphine concentration of 1 mg/L is reasonable for wheat fumigations based on typical Australian conditions. This equation also had one of the higher R^2 values available among equations presented in Dargatzis and Pavic (2008):

$$C = 1.5932 e^{-0.0416t} \quad \text{Eq 4.1}$$

Where,

C = fumigant concentration lost [mg/L]

t = time [days]

The time step for the simulations in the code is one hour, not one day, and the code also measures concentration in kg/m^3 instead of in mg/L. After revising Equation [4.1] to proper units for use in the code, equation [4.2] results:

$$C = 0.0015932e^{-0.0017t} \quad \text{Eq 4.2}$$

Where,

C = fumigant concentration lost [kg/m^3]

t = time [h]

The value listed by Daglish and Pavic (2008) is the value of the concentration in the flask, not the loss of phosphine. So in order to calculate the amount of phosphine lost due to sorption, the derivative of Eq [4.2] must be calculated, which results in equation [4.3]:

$$C = 0.0000026e^{-0.0017t} \quad \text{Eq 4.3}$$

Fumigant sorption also varies due to other factors that are important variables in our experiment, such as temperature and moisture content of grain. In order to account for these variables, Eq [4.3] was multiplied by factors dependent on temperature and moisture content. The effect of temperature on phosphine sorption was studied by Darby (2011) who determined sorption losses at 35°C were about five times as large as losses at 15°C , at a constant equilibrium relative humidity of 65%. Therefore, this result can be modeled with an exponential equation dependent on temperature, where the value at 35°C is five times the value at 15°C . The value for this expression is set to equal one when the temperature is at 25°C , because that is the temperature of the baseline equation from Daglish and Pavic (2008) (see Appendix 4.1). This means that when the temperature equals that of the baseline equation, the overall equation should be unchanged. The effect of moisture content on the sorption of phosphine was studied by Reed and Pan (2000). They determined fumigant loss for several temperatures at two values of wheat

moisture content, i.e., 11% and 13.5%. The sorption at the higher moisture content was 1.8 times greater than the sorption at the lower moisture content at 25°C. This was modeled with an exponential equation which was set to 11.5%, the equilibrium moisture content of the wheat from the baseline Darglish and Pavic (2008) equation (see Appendix 4.2). The resulting equation for fumigant loss due to sorption into the grain mass when modified to account for changing temperatures and moisture contents is therefore:

$$C = 0.0000026e^{-0.0017t} * 0.13365e^{0.0805T} * 0.067e^{0.235M} \quad \text{Eq 4.4}$$

Where,

C = fumigant concentration lost [kg/m³]

t = time [h]

T = temperature [°C]

M = moisture content [%], wet basis

In order to implement this equation into the computer code, the sorption calculated fumigant concentration lost due to sorption is subtracted from the current fumigant concentration at each node for each time step but only if the current fumigant concentration at that node is higher than the sorption amount to be subtracted. If the phosphine concentration at a node is less than the concentration that would be lost to sorption, the phosphine value at that node is set to zero instead.

2. Effect of Silo Leakage

2a. Effect of Wind Speed

In order to estimate the amount of fumigant lost due to leakage from the silo, a baseline equation that estimates fumigant loss as a summation of losses from various sources was used (Banks and Annis, 1984). The most significant sources of fumigant loss result from: (1) concentration differences between the inside of the grain silo and the ambient conditions, (2) chimney effects due to temperature differences, (3) chimney effects due to concentration gradients, and (4) wind effects. The category of ‘farm bin’ in the Banks and Annis (1984) paper was selected as it was the closest size to the silos used in our research (Cook, 2016), and the ‘silo bin’ category was based on concrete construction, while the ‘farm bin’ in our research was metal. The wind speed effect listed in Banks and Annis (1984) is estimated at 0.108/day. In order to convert this value into units of kg/m³/h, the expression must be multiplied by the initial concentration and changed into per hour values. In order to determine how this number changes with changing wind speed, experimental results reported by Cryer (2008) were used. In that experiment the half loss time of sulfuryl-flouride with most cracks closed and wind speed of 1 m/s, was one fourth the half loss time at 4 m/s. It was also noted that the type of fumigant did not have a significant effect on wind speed related leakage. Thus, that result can be reasonably extended to phosphine for the purpose of this estimation. Wind speed loss was then estimated by an exponential function with a value that was four times higher at 4 m/s than it was at 1 m/s. The value of 1 was set at a wind speed of 6.4 m/s, the base wind speed used in the estimations of Banks and Annis (1984) (see Appendix 4.3). The resulting equation for loss of fumigant due to wind effects is:

$$C = 0.0002233e^{0.4621S_w} * C_i \quad \text{Eq 4.5}$$

Where,

C = fumigant concentration lost [kg/m^3]

S_w = wind speed (m/s)

C_i = initial fumigant concentration [kg/m^3]

2b. Effect of Temperature

In terms of temperature, there are two sources of temperature-based loss described by Banks and Annis (1984). One is due to temperature-based chimney effect, which is denoted by T_c , and the second is loss due to temperature difference between the grain storage structure and ambient conditions, denoted by T_d . These estimates are placed in the equation as 0.019/day and 0.025/day, respectively. As in the wind speed example, these estimates must be adjusted to units of concentration per hour, and then the effect of changing temperature must be considered. In an experiment by Reed and Pan (2000), fumigant loss increased by a factor of approximately 4 when temperature increased from 20°C to 30°C. This can be estimated by an exponential equation where the value at 30°C is four times as high as the value at 20°C. The value at 25°C is set to one according to the calculations of Banks and Annis (1984) (see Appendix 4.4). This is a useful estimation of gas loss due to temperature-based chimney effect. However, no supporting literature for estimating the effect of temperature differences between the inside and outside wall has been found to investigate how leakage might be affected based on changing temperature differences. This should be further researched, but was outside the scope of this project. Thus, the same exponential equation was used to estimate the loss due to temperature difference. The resulting loss equation for temperature-based leakage is:

$$C = 0.0000248 e^{0.1386T_c} * C_i + 0.0000326 e^{0.1386T_d} * C_i \quad \text{Eq 4.6}$$

Where,

C = fumigant concentration lost [kg/m³]

T_c = temperature inside the grain silo [°C]

T_d = temperature difference between grain silo and ambient air [°C]

C_i = initial fumigant concentration [kg/m³]

2c. Effect of Concentration Differential

The final major effect to consider is the chimney loss due to concentration of fumigant. This effect was listed in Banks and Annis (1984) as 0.035/day. Again, this must be converted into hours and multiplied by initial concentration to arrive at values in kg/m³/h. The question of how fumigant loss depends on fumigant concentration is difficult to answer directly from literature, and no standardizing values are listed in Banks and Annis (1984). The value listed changes with respect to concentration, and all the values from Banks and Annis (1984) have an initial concentration multiplier in them, which suggests an equation of the form:

$$C = 0.0029962 C_i^2 \quad \text{Eq 4.7}$$

Where,

C = fumigant concentration lost [kg/m³]

C_i = initial fumigant concentration [kg/m³]

Combining the equations of all four effects (Eq 4.5, 4.6, 4.7) results in the following silo leakage equation:

$$C = 0.0002233e^{0.46215w} * Ci + 0.0000248 e^{0.1386Tc} * Ci + 0.0000326e^{0.1386Td} * Ci + 0.0029962Ci^2 \quad \text{Eq 4.8}$$

Where,

C = fumigant concentration lost [kg/m²]

In order to implement this equation into the computer code, the calculated fumigant concentration lost is subtracted from the current fumigant concentration at each node along the vertical silo wall at each time step but only if the fumigant concentration at that node is higher than the leakage amount to be subtracted. If the phosphine concentration is less than the amount to be subtracted, the concentration is set to zero. However, given that fumigant leakage from the silo is an effect that in the model is predicted to occur along the vertical silo wall, but the Banks and Annis (1984) values are calculated for loss based on the entire silo, Eq 4.8 must be multiplied by the ratio of the total number of nodes in the simulation model divided by the number of boundary nodes at which fumigant loss is calculated, assuming volumes associated with each node are of similar size:

$$N_c = N_n/N_b \quad \text{Eq 4.9}$$

Where,

N_c = node correction

N_n = number of nodes

N_b = number of boundary nodes

Banks and Annis (1984) stated that their definition of leakage was in reference to a silo that had a pressure half loss time of five minutes. Assuming that halving the pressure half loss time equates to doubling the leakage from the silo, the following leakage modifier results:

$$\text{Leakage Modifier} = 5/x \quad \text{Equation 4.10}$$

Where

X = pressure half loss time (minutes)

The final equation to predict fumigant leakage from the silo is therefore the result of multiplying equation 4.8 by equation 4.9 and equation 4.10:

$$C = \frac{5}{x} * \frac{Nn}{Nb} * (0.0002233e^{0.4621Sw} * Ci + 0.0000248 e^{0.1386Tc} * Ci + 0.0000326e^{0.1386Td} * Ci + 0.0029962Ci^2)$$

Eq 4.11

Where,

C = fumigant concentration lost [kg/m²]

X = pressure half loss time (minutes)

N_n = number of nodes

N_b = number of boundary nodes

3. Model Verification

Due to the difficulty of acquiring fumigation data from Australian sources that include all the necessary data needed to validate the derived equations, model verification was conducted using data collected during fumigation trials for another research project which was conducted at Kansas State University using an Australia-designed sealed silo and thermosiphon fumigant recirculation system (Cook, 2016). The silo constructed is a Bird's model 2250 from Bird's Silos and Shelters in Popanyinning, Western Australia, with a 4.4m diameter, 6.93m peak height, capable of storing 45.5 tonnes (1,793 bu) of corn. The cylindrical portion of the grain mass that was used in the simulation was 4.4m in diameter and 3.96m high. The fumigation that was chosen to validate the model was conducted from Aug 31 to Sept 9, 2015. During the first four days readings were taken approximately 10 times per day. Over the next six days readings were taken once every other day ending on September 9. The reported pressure half loss time was 31 seconds, as recorded the morning of the trial start. The targeted Concentration Time (Ct) product for this fumigation was 21,600 ppm-h. As shown in figure 4.1, sampling locations for the phosphine readings were arranged in five vertical columns throughout the grain bulk, one directly in the center of the silo, and four halfway from the center to the edge, one each on the North, East, South, and West side of the silo. As the simulation is not set up to predict readings in the cone, in the headspace, or in the thermosiphon, the reading points considered for this verification were the twenty reading points in the main cylinder of the grain mass, four from each of the five columns.

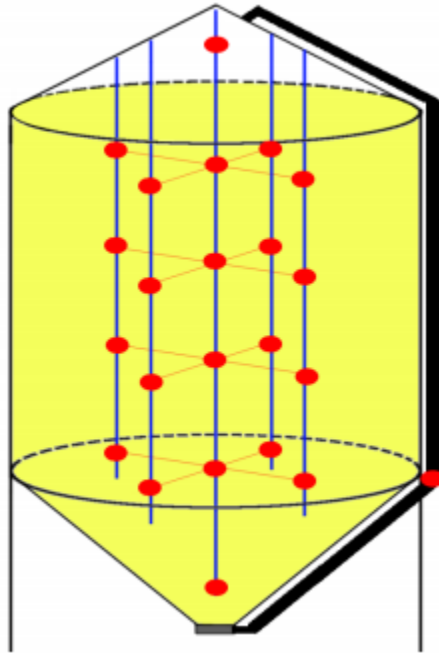


Figure 4:1 Fumigant sampling locations used in the experimental fumigation conducted in a sealed silo containing 45.5 tonnes of corn (Cook, 2016), each represented by a red dot.

A mesh with 2,587 nodes was created in the Abaqus finite element software for the simulation based on the dimensions of the silo supplied. While the dimensions were modeled precisely, the major discrepancy is that this silo contains a cone shaped bottom, and our model is limited to a flat bottom silo. For this reason, the cone was left off, but the extra distance may have provided space for more mixing of the fumigant before it arrived in the region of the simulation. For this reason, fumigant was applied across the entire lower boundary of the simulation, excluding boundary nodes. Weather data for the period in question was taken from the Kansas State University Mesonet database (<http://mesonet.k-state.edu/>). As phosphine cannot be directly input into the model, a phosphine application method was implemented in which the base nodes of the silo, excluding edge nodes, were set at a starting amount that was

held for 24 hours to approximate the phosphine release time in the experiment (Cook, 2016). Implementing a forced recirculation rate in the code would override more minor mixing effects, such as natural convection currents. Therefore, the effective recirculation rate used in the model will be larger than experimental rates in order to mimic results. Due to these dissimilarities between the coding environment and the real life experiment, the rate of recirculation from the thermosiphon and the starting concentrations of phosphine that were used were chosen based on the values that were best able to replicate experimental results. Unpublished thermosiphon data from Cook (2016) demonstrated a faster thermosiphon recirculation rate during day time hours of about twice the rate than was achieved during the night time hours. In order to match this effect, the recirculation rate in the simulation was doubled from 8 am until 4 pm to coincide with higher thermosiphon readings from warm periods of the day. The values chosen were a seeding phosphine value of 0.00065 kg/m^3 and a recirculation rate of 0.001 m/s during the day time and 0.0005 m/s during the evening and night time.

Results and Discussion

1. Verification Results for 24 h Phosphine Release

1a. Simulation Trends

With model parameters such as loss and leakage quantified, the model must be validated by comparison to the experimental values measured in Cook (2016). In discussion, the author indicated that he believed the phosphine to be released over a period of 24 h. This section discusses the results obtained from the model under a phosphine release time of 24 h and compares those values to the experimental results.

The verification results demonstrate reasonable agreement between the shapes and trends of the real world experimental data presented in figure 4.2 and the predicted data from the finite element model presented in figure 4.3-4.4. Figure 4.3 depicts the trends obtained when examining the same locations measured in the physical experiment, and figure 4.4 depicts the trends when examining all locations in the model. Both the experimental and simulated results indicate a rapid increase of phosphine at the beginning of the fumigation, followed by a loss of phosphine that continually slows until the end of the fumigation. Further discussion of fumigation trends can be found in appendix 4.5. While the trends are similar, the maximum average concentration is greater when only considering the points available in the experimental data. This effect demonstrates the potential for over predicting phosphine concentration when not measuring points along the sidewall of the silo.

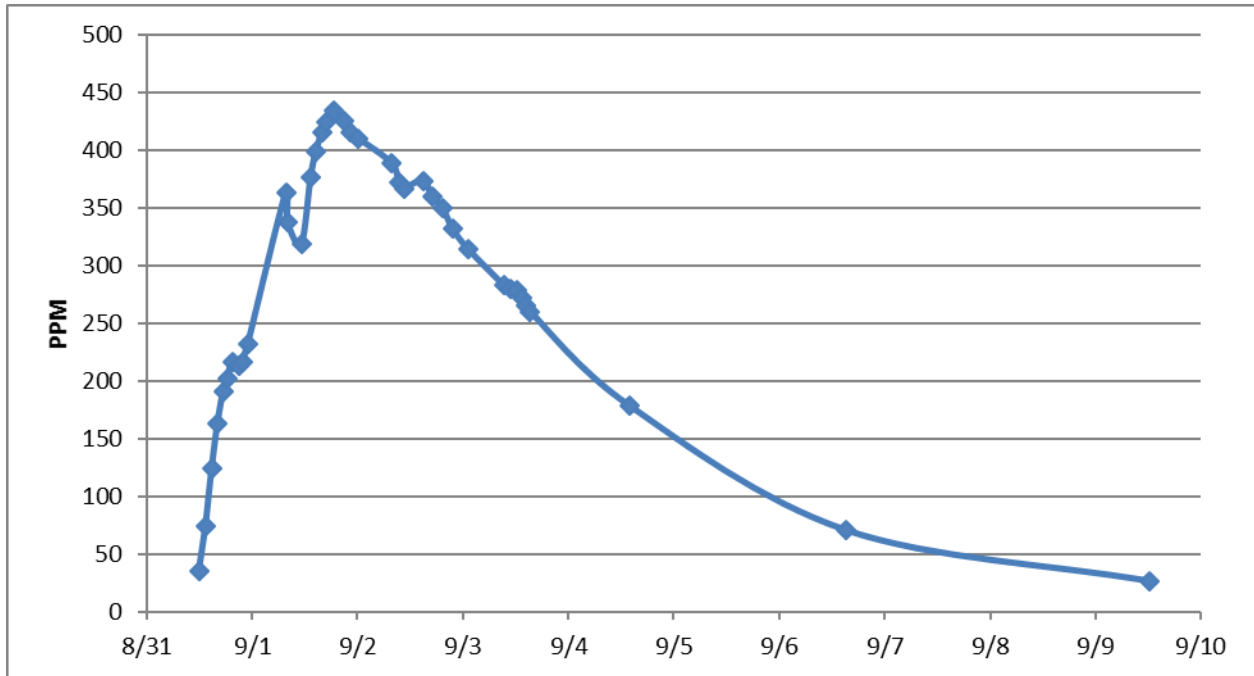


Figure 4:2 Average phosphine concentration (ppm) reported from the experimental results of Cook (2016) taken in the sealed silo between August 31 and September 9, 2015.

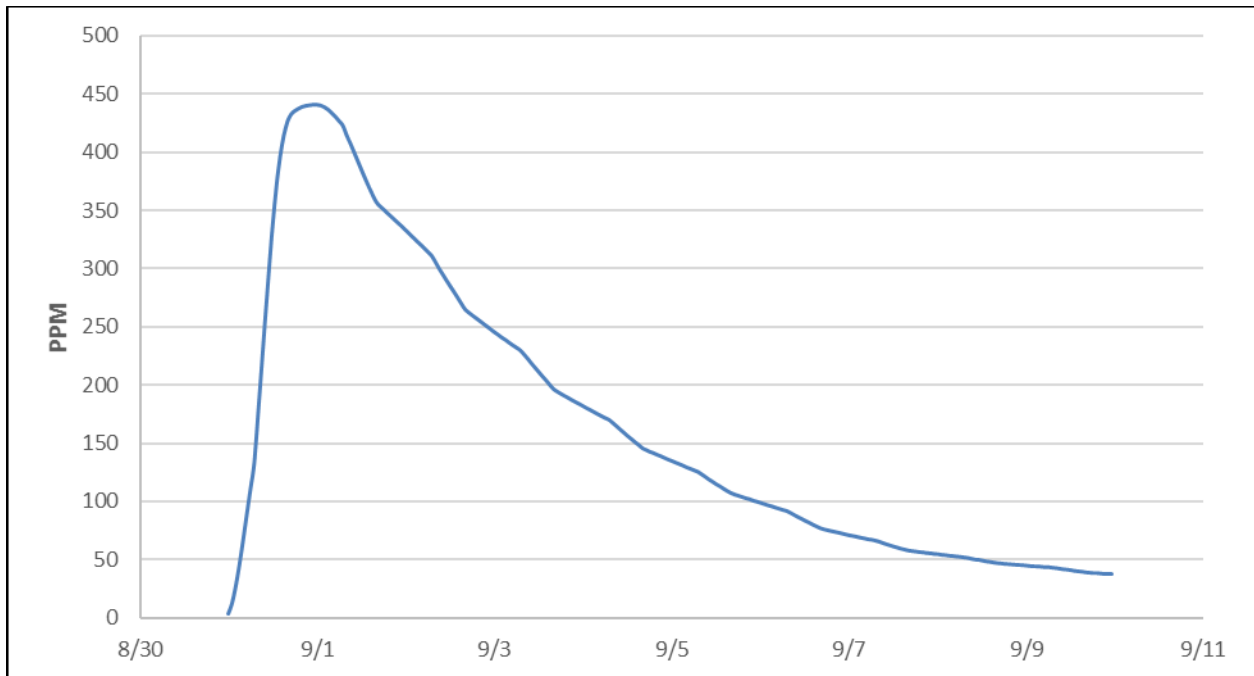


Figure 4:3 Average phosphine concentration (ppm) predicted by the simulation model considering only the same locations from which data were recorded by Cook (2016) between August 31 and September 9, 2015, with a 24h fumigant release.

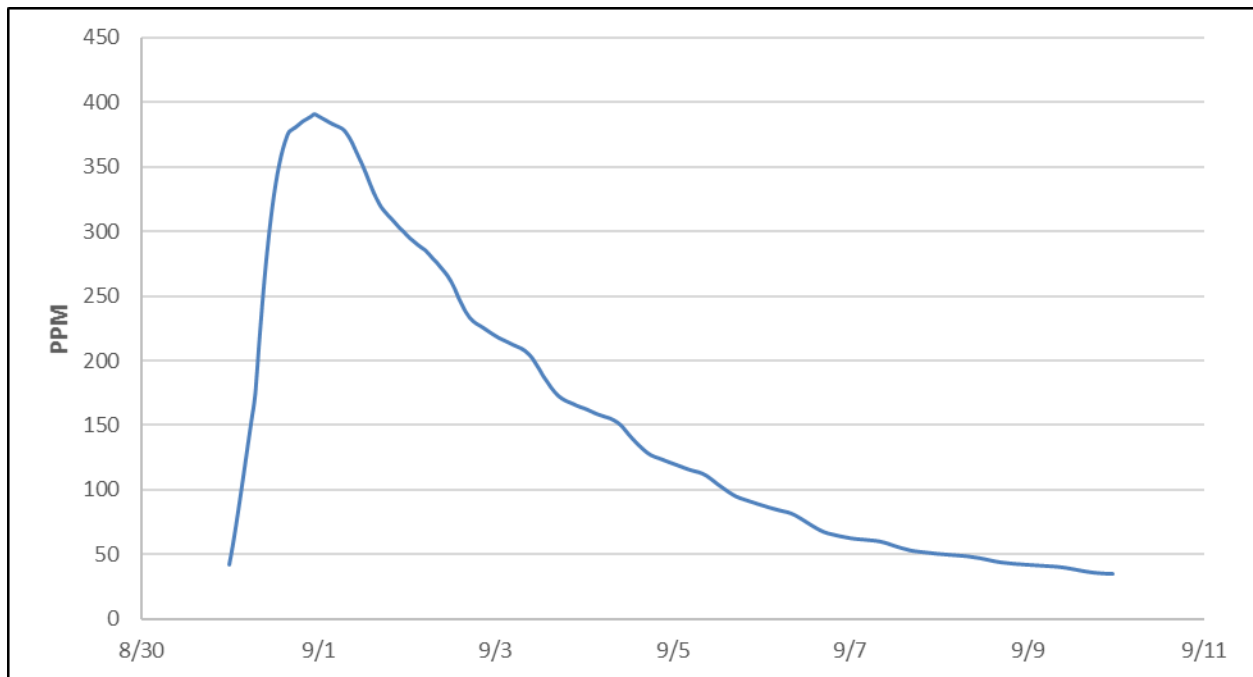


Figure 4:4 Average phosphine concentration (ppm) predicted by the simulation model when considering results from every node in the simulation between August 31 and September 9, 2015, with a 24h fumigant release.

The quantitative comparisons between the measured and predicted values are based on results reflecting the same locations and time readings, as shown in figure 4.5-4.7. The root mean square error of this verification was 47.5 ppm, the average difference was 0.1 ppm, and the average of the absolute values of the differences was 38.6 ppm. The overall average experimental fumigant concentration was 283.3 ppm, therefore, the average percentage error compared to predicted values was 13.6%. The major discrepancy between the results seems to begin the evening of the first day of fumigation, around 6:30 to 7:30 pm, when the increase in phosphine in the experimental data begins slowing and the predicted data do not. This coincides with the beginning of a decrease in night time temperature. This may be similar to the night time

phosphine drop noted in Australian experimental data, discussed in Appendix 4.5. This culminates in the largest difference between experimental and predicted data, at 11 am the next morning, after which the experimental phosphine readings begin to climb back to levels predicted by the simulation. The low temperature that night was 21.8°C, the afternoon highs for August 31st and September 1st were around 33°C. A similar effect appears to happen at a smaller scale the next night, with the values dropping slightly and then rebounding in the morning of September 2nd. The temperature that morning was around 25°C. After the second night, night time concentration drops are not seen in the experimental data, either because they did not happen, their effect was smaller due to lower phosphine values, or they were missed due to lack of night time phosphine sampling. The net effect, however, is that the predicted values appear to be a few hours ahead of the actual values. The night time decrease may also explain why the simulation slightly over predicted the amount of phosphine reported. This, along with an over prediction of the low phosphine levels seen late in the experiment, comprise the major differences between the simulation and experiment.

agreement suggests that the model is suitable for predicting fumigation trends and overall Ct-products. While the model is often accurate for predicting specific phosphine concentrations, it is less accurate for predicting concentrations during the first day of the fumigation, particularly at night.

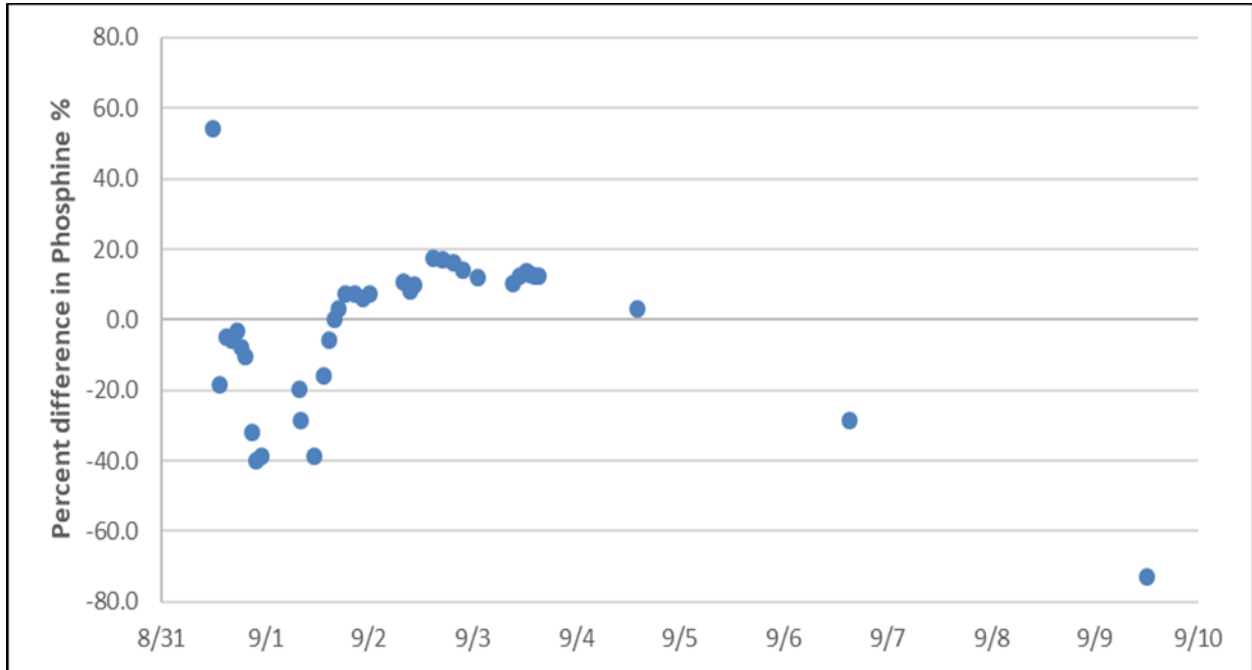


Figure 4:6 Percent difference (%) in phosphine concentration between simulated and experimental results considering only data at the same locations from which data were recorded by Cook (2016) between August 31 and September 9, 2015, with a 24h fumigant release.

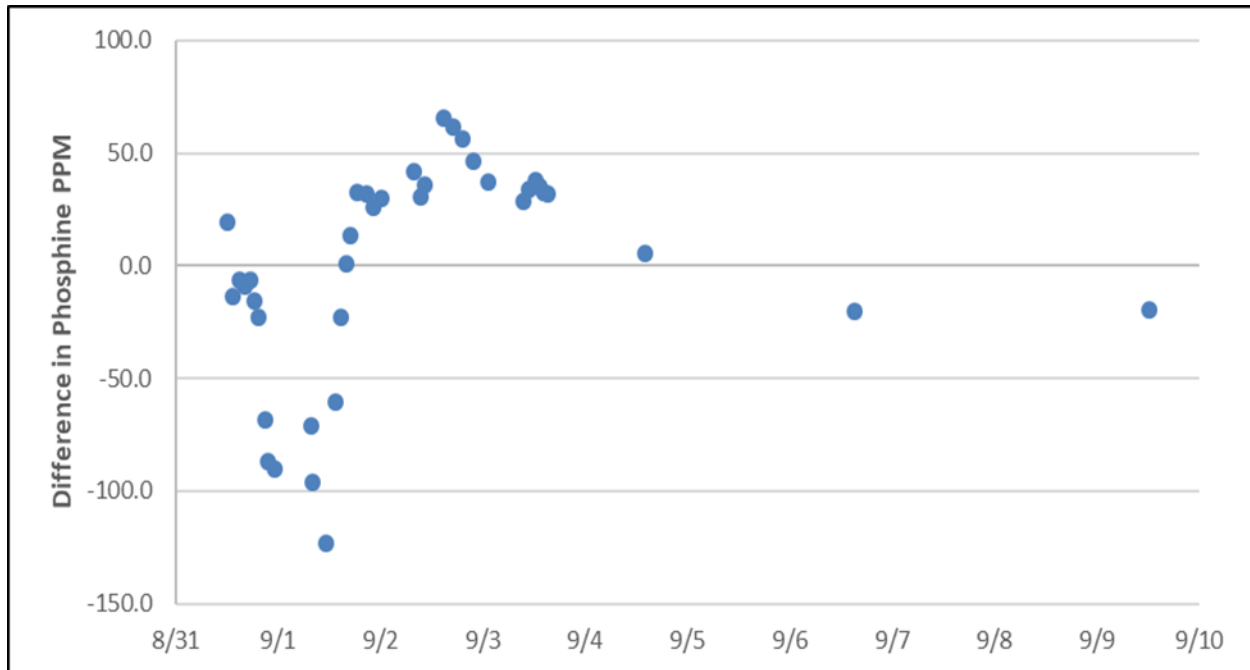


Figure 4:7 Difference in phosphine concentration (ppm) between simulated and experimental results considering only data at the same locations from which data were recorded by Cook (2016) between August 31 and September 9, 2015, with a 24h fumigant release.

The simulation calculates phosphine values at every location in the silo at an hourly time step, whereas the physical experiment data is only available at the 20 sampling points and at the reading times specified. Therefore, the model allows us to analyze the conditions in the silo at a level well beyond that available from the physical experiment. Ct-products calculated based on four different calculation methods are presented in table 4.1. When taking into account the additional reading times and location that were not measured, the predicted silo wide average Ct-product was 36,500 ppm-h. This value is less than the experimental value by a 15.5%. This result makes sense, though, because the experimental data points closest to the wall would have been halfway to the wall from the center of the silo, which means most of the silo volume would

be closer to the outside wall of the silo than the furthest reading points measured by Cook (2016).

Table 4:1 Cumulative Ct-product, experimental and predicted Ct-products based on four approaches: (1) simulated nodes and reading times are the same as those recorded by Cook (2016), (2) simulated nodes are the same as those recorded by Cook (2016) but reading times are hourly based on the simulation, (3) all nodes in the simulation code are included for hourly calculations, and (4) only the node in the simulation with the least phosphine concentration for hourly calculations.

	Experimental	Simulated same nodes and reading times	Simulated same nodes and hourly reading times	Simulated all nodes and hourly reading times	Simulated node with least phosphine hourly reading times
Cumulative Ct-Product (ppm-h)	43,200	43,600	39,900	36,500	11,600

In order to consider the locations in the silo that most likely would contribute to gas concentrations insufficient to kill all insects at all life stages, the results from the lowest concentration locations were analyzed. The lowest phosphine concentrations occurred at the top of the silo, along the silo wall, where concentrations never exceeded 175 ppm. Four of these locations were analyzed, the one pointing in each coordinate direction, and the results are presented in figure 4.2. The lowest Ct-product found was the North facing location. This

location had a predicted Ct-product of 11,579 ppm-h. This value does not meet the targeted Ct-product for this fumigation of 21,600 ppm-h, despite the fact that silo wide values were well above that amount. This result may imply that fumigations that appear successful may have regions of fumigation failure, contributing to fumigant resistance development in stored product insects.

Table 4:2 Cumulative Ct-product predicted at individual nodes along the top outer ring of the grain mass surface of the silo using hourly reading values for fumigation conducted between Aug 31 and September 9, 2015, with a 24h fumigant release.

	West	South	East	North
Cumulative Ct-Product (ppm-h)	15,400	12,300	12,600	11,600

1c. Horizontal Differences in Simulation

Cook (2016) also reported on the differences in phosphine concentration averaged vertically in the silo. The columns reported are north, south, east, west, and center. Figure 4.8 presents results recorded by Cook but not presented in his Master’s thesis. While there is variation, the largest of which is between the east and west sampling lines, reaching a maximum of 202 ppm at 10:50 am September 1, all lines follow a similar trend and the differences are mostly eliminated after the first two days of this 10-day fumigation. The predicted concentration values from the model do not show a significant difference between average values of columns

halfway to the silo wall, as seen in figure 4.9 in which values along the center, east, north, west, and south are all indistinguishable from each other at most times. Effect of radial position around the silo only appears clearly when comparing locations near the silo wall, as seen in figure 4.10. Phosphine values in the center column are shown to be higher than the values in any edge direction. This is clearly the result of the phosphine leakage equations, which are applied along the edge nodes, reducing phosphine values along the silo wall. The west side appears to be highest in phosphine concentrations when compared to the other locations along the silo wall. The east, south, and north locations are indistinguishable from each other. The reduced variability of phosphine concentrations horizontally in the silo is likely attributable to how the code handles the mixing velocities. While the experimental silo utilized a thermosiphon for recirculation, natural convection currents are also formed. In the simulation, the vertical recirculation values were set so as to provide a similar overall trend, but the loss of the effect of natural convection currents results in the reduction of horizontal variation in the silo. The remaining effect seen is likely due to the heating effects of solar radiation. The heating effect of solar radiation is not uniform across the silo surface, and would cause increases in leakage from the silo due to the temperature influence from equation 4.6. Increased daytime temperatures may also cause a reduction in leakage if it reduces the temperature differential between silo and environment also seen in equation 4.6.

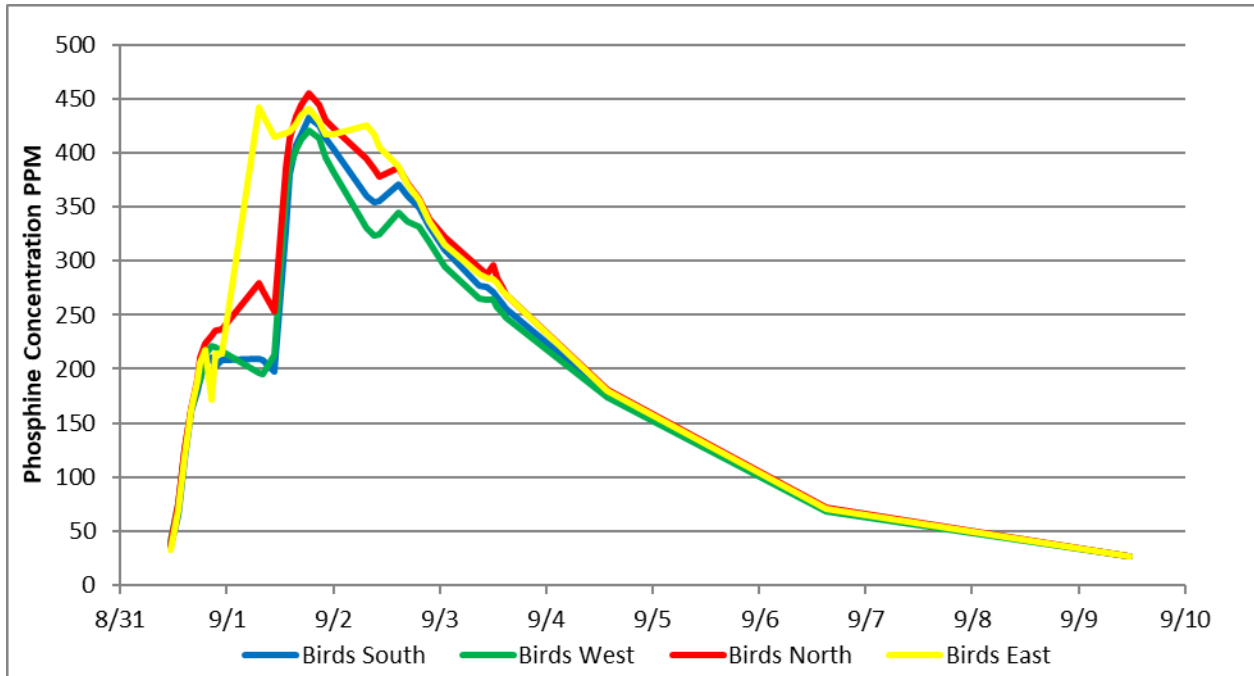


Figure 4:8 Vertical averages of experimental phosphine values (ppm) of columns located halfway to the edge of the silo recorded by Cook (2016) between August 31 and September 9, 2015.

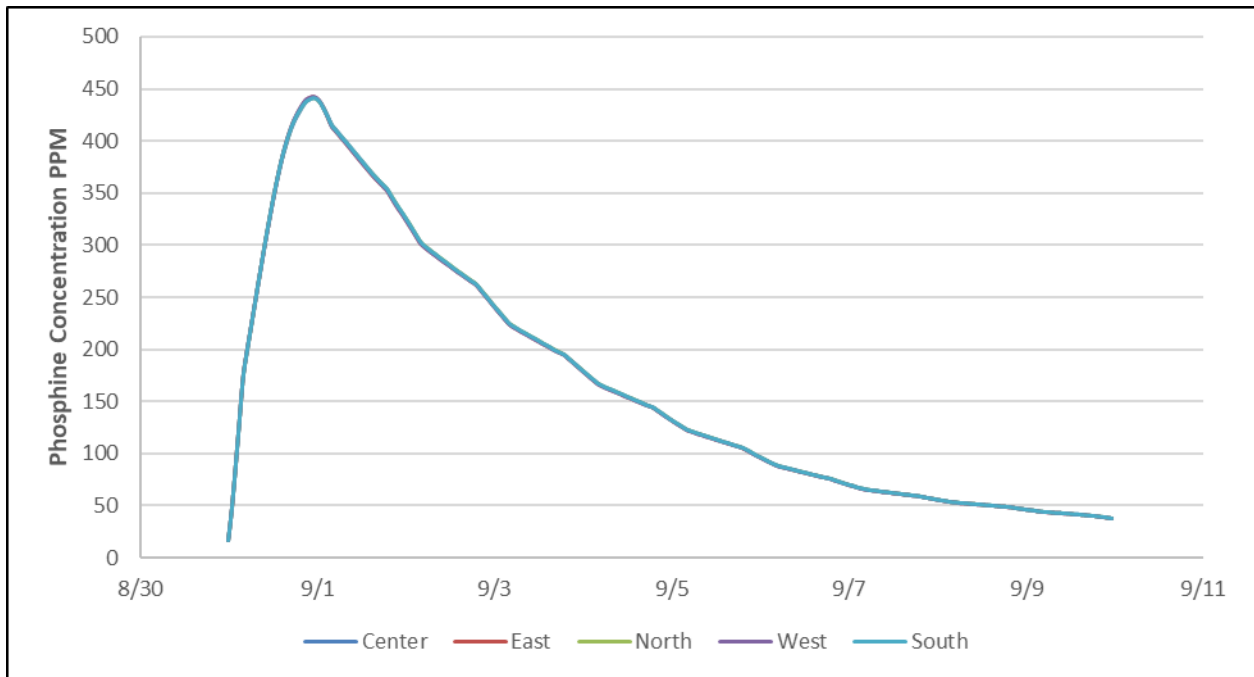


Figure 4:9 Vertical averages of predicted phosphine values (ppm) of columns located halfway to the edge of the silo considering only the same locations from which data were

recorded by Cook (2016) between August 31 and September 9, 2015, with a 24h fumigant release.

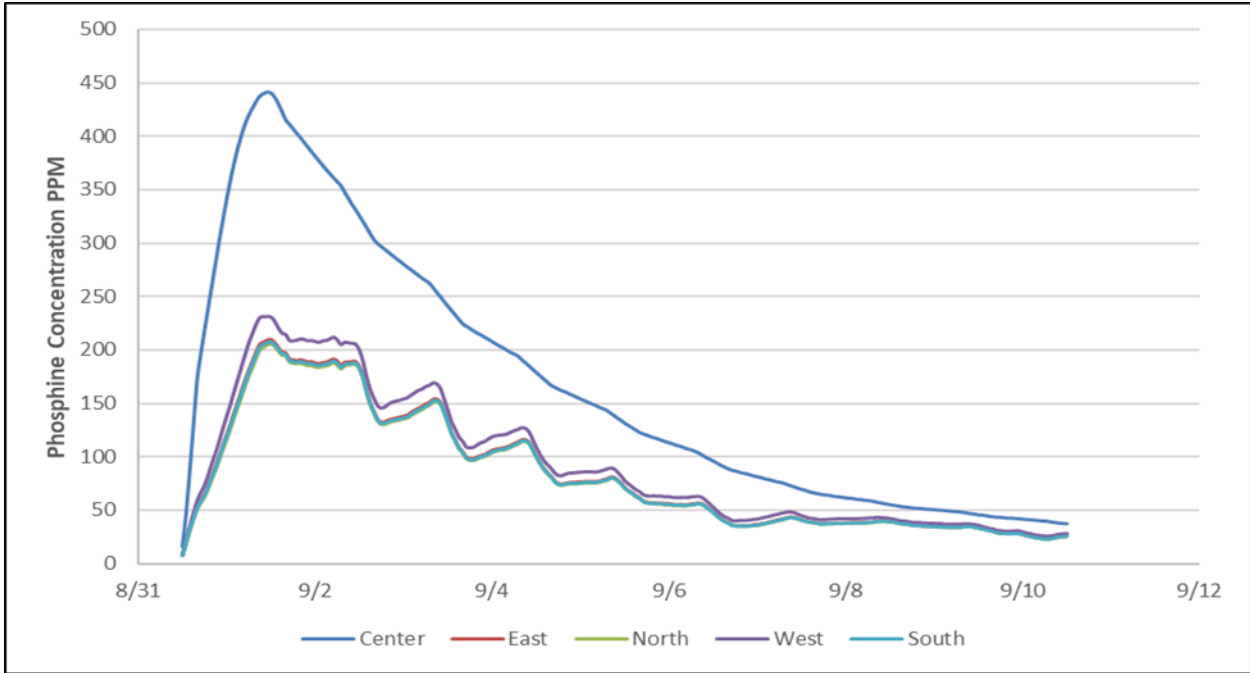


Figure 4:10 Vertical averages of predicted phosphine values (ppm) of four columns located along the edge of the silo, and one at the center considering only the same locations from which data were recorded by Cook (2016) between August 31 and September 9, 2015, with a 24h fumigant release.

The lowest phosphine concentrations occur along the side wall where the phosphine leakage equations are applied. The simulation model was used to investigate how far into the grain mass the wall leakage effect penetrates. Four nodes were examined 1.98 m from the bottom of the grain mass on the east side of the silo, and four locations from the center to the outer edge (2.2m, 1.9m, 1.6m, 0.7m). The cumulative Ct-products were 21,100, 51,300, 53,100 and 52,900 ppm-h, respectively. The largest effect of silo leakage is clearly seen along the silo wall (2.2m). The second node in from the silo wall (1.6m) also appears to be affected by the

leakage from the silo wall, as shown in figure 4.12. However, the values at that location are still closer to the rest of the silo than they are to the values at the edge of the silo wall. This effect indicates that the most of the leakage caused along the silo wall fails to penetrate 0.3m into the grain mass.

The trend at the silo wall is highly variable, particularly by time of day. The concentration at this location decreases during the day, reaching its lowest values in the late afternoon, and increases at night, reaching its highest values in the early morning. This seems to contradict some experimental results indicating low phosphine concentrations in the night time, which are more thoroughly discussed in appendix 4.5. A likely explanation for this effect in the simulations is that the greater temperatures and temperature differentials that occur during the day cause higher rates of leakage. However, because this daily temperature variation is seen only in the nodes directly on the side wall, it does not seem to have a large effect on overall phosphine concentrations. The trend at the center of the silo is that for the first few days, the concentration is flat and unaffected by changing concentrations in the rest of the silo. When the loss does reach the center of the silo, it has an immediate effect, followed by constant decline in concentrations.

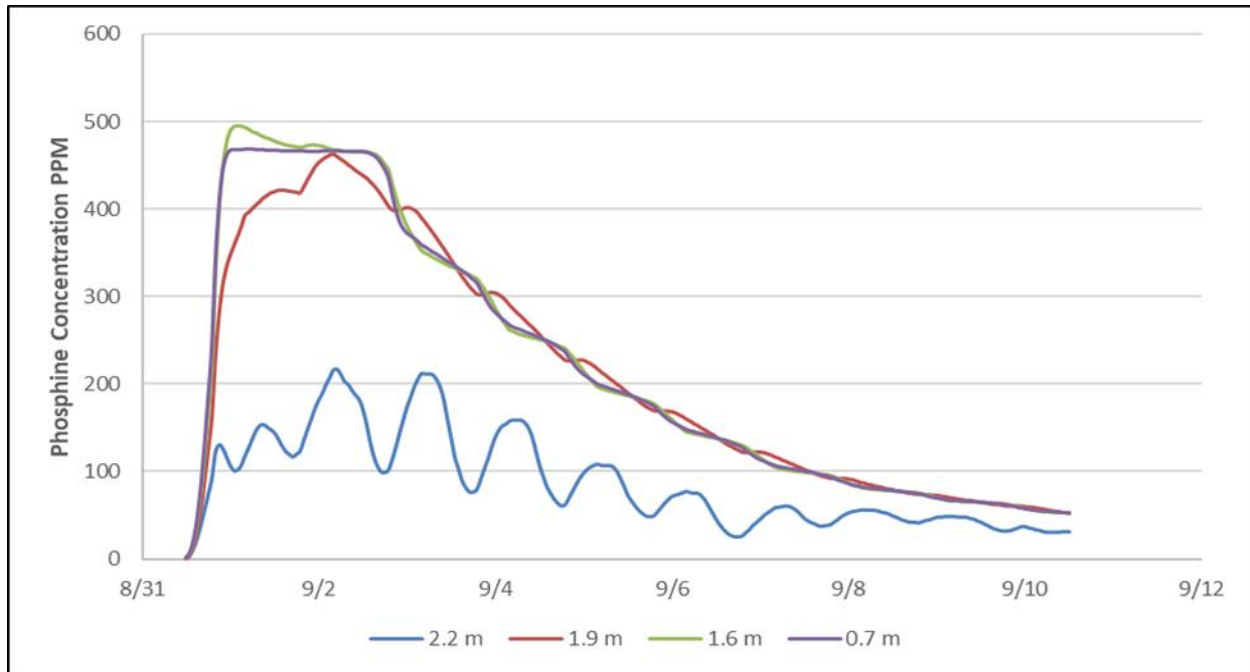


Figure 4:11 Comparison between predicted phosphine values (ppm) at specific nodes located 1.9m from the bottom of the grain mass and 0.7, 1.6, 1.9, and 2.2m from center of the silo fumigated between August 31 and September 9, 2015, with a 24h fumigant release.

1d. Scale of Sorption and Leakage

The simulation code estimates fumigant loss based on equations 4.4 and 4.11, which predict fumigant loss due to sorption and fumigant loss due to leakage. While specific values of fumigant lost from each node were not analyzed, the average amount of fumigant loss to sorption in the simulation was calculated to be 16.3ppm. The remaining phosphine lost from the simulation (>400ppm) was due to leakage, which indicates that fumigant leakage was the more important source of fumigant loss. As the leakage from the silo is dependent on overall concentration and on pressure half loss time, a fumigation with a high amount of fumigant or in a poorly sealed silo would result more leakage relative to sorption. A fumigation that is held at

lower concentrations in a well-sealed silo and at higher moisture contents would result in a greater amount of sorption relative to leakage.

2. Verification Results for 30 h Phosphine release

The verification replicated observed fumigation trends, however, the time at which maximum values were predicted to be reached occurred about 6h after the maximum values were reached in the experiment as seen in figure 4.5. In addition, the time required for the release of phosphine, which was estimated at 24 h from the beginning of the experiment, was approximated by Cook and may be inaccurate. Due to these factors, a second verification simulation was conducted in which the release of phosphine was extended to 30 h in order to align the maximum concentration values.

The results of this second verification are shown in Figures 4.12-4.14. This verification had a root mean square error of 50.6 ppm, an average difference of 21.8 ppm, and average of the absolute values of the differences was 34.8 ppm. The average difference and root mean square error is higher than the previous verification, however, the average of the absolute values of the difference is lower. The first verification, however, benefits more from the over predictions early in the predicted values canceling the under predictions later on. This can be seen in the difference and percent differences shown in figures 4.6 and 4.7 for the first verification, and figures 4.14 and 4.15 for the second verification. From September 1 through September 5, the highest differences are 65.6 ppm and 17.5% for the first verification, and 20.2 ppm and 8.09% for the second verification. Also, the first verification was more accurate during the first 12 hours, which was a period that is disproportionately impacting the statistics as readings were taken more frequently during that period than any other comparable time period in the

experiment. In comparison to the first verification, this one predicted phosphine concentrations lagged behind experimental values during the first day of fumigation by about 68 ppm on average compared to 45 ppm for the first fumigation.

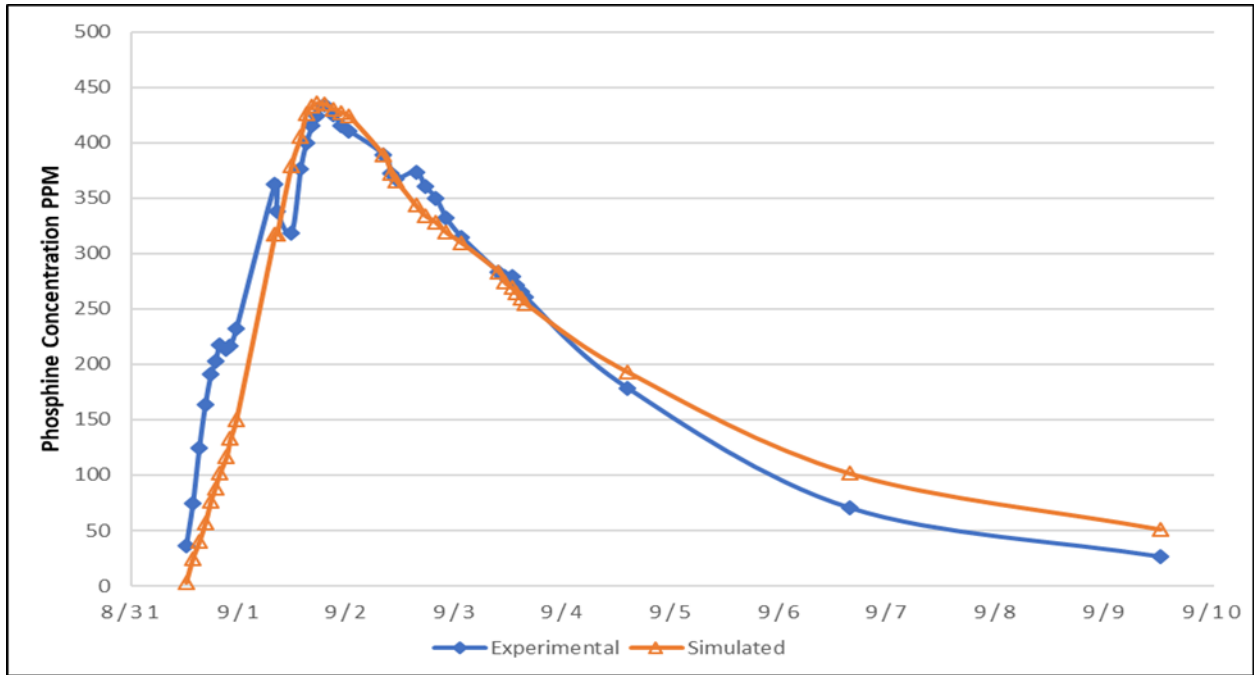


Figure 4:12 Comparison between average experimental and predicted phosphine concentration (ppm) results considering only data at the same locations and times recorded by Cook (2016) between August 31 and September 9, 2015, with a 30h fumigant release.

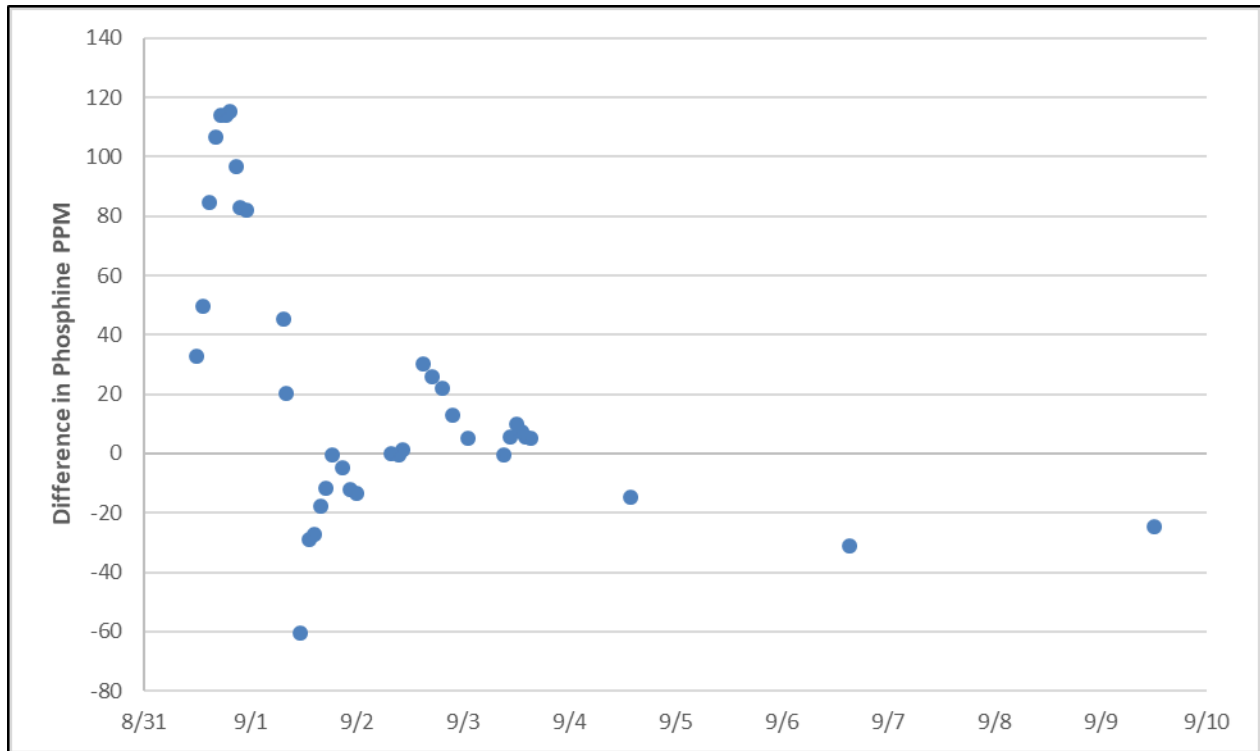


Figure 4:14 Difference in phosphine (ppm) concentration between simulated and experimental results considering only data at the same locations from which data were recorded by Cook (2016) between August 31 and September 9, 2015, with a 30h fumigant release.

As seen in figure 4.12, the second simulation under predicts-phosphine concentrations for the first twelve hours and over-predicts phosphine concentration values between September 1-5. For the 5-day period after the initial 12 h, this simulation predicts phosphine concentration with a high degree of accuracy, as seen in figures 4.13 and 4.14, with the percent difference in this period never surpassing 8.2%. This is the period when the fumigation is at its highest concentrations (175-435 ppm), and therefore the time of highest insect mortality, highest leakage rates, and period of most interest to stored grain managers. For instance, from the first reading on September 1st to the only reading on September 4th, the second verification simulation had an average percent difference of 0.1% and an average of the absolute values of percent difference of

4.4% compared to values from the first simulation of 4.1% and 12.4%, respectively. The Ct-product of this second simulation versus the experimental fumigation were 45,000 ppm-h and 43,200 ppm-h respectively, for the data points available in the experiment. While this Ct-product is still within 5% (4.3%) of the experimental Ct-product, it is not as close as for the first verification, which had an overall Ct-product of 43,600 ppm-h (0.9% difference). Based on these results, both simulations perform at a satisfactory level for predicting phosphine concentrations and trends, however, the second verification simulation is more useful for further experimentation and formation of recommendations because it has an increased accuracy during the days when fumigation efficacy is most critical and that are of greatest interest to stored grain managers.

Conclusions

An existing finite element model was expanded to simulate fumigant movement and loss by incorporating equations to predict phosphine leakage and sorption. This model was validated with data from an experimental fumigation conducted using a sealed Australian silo under U.S. weather conditions. The key results are:

- The verification demonstrates that the model effectively predicted the trend of phosphine concentrations, and accurately predicted the overall Ct-product of the fumigation. Based on a 24h phosphine release model the predicted Ct-product differed from the experimental value by 0.9%. A 30h release model predicted a Ct-product that differed by 4.3% from the experimental value.

- The fumigation model is most accurate during the times of highest phosphine concentration. However, the model under predicts phosphine concentrations during the first 12h of fumigation and over predicts phosphine concentrations beyond the first six days of fumigation.
- While silo average Ct-products were within 5%, the simulation was not able to accurately reproduce differences observed between the north, east, south, and west sides of the grain mass.
- Predicted Ct-products from areas in the silo not monitored during the experimental fumigation such as near the surface of the grain mass demonstrate the possibility that a fumigation that is ruled successful on average Ct-product might fail to control insects in these specific areas.

Chapter 5 - Sensitivity Analysis of a Fumigant Movement and Loss Model for Bulk Stored Grain to Predict Effects of Environmental Conditions and Operational Variables on Fumigation Efficacy

Introduction

An effective fumigation requires a specific concentration of fumigant being held for a specified amount of time in all areas of the silo, in order to kill all life stages of all insects present. Computer modeling is a useful tool to analyze the combined effect of the parameters that influence fumigant concentrations in a grain storage silo, and as a function of geographic locations and climatic situations (Casada and Noyes, 2000). Banks and Annis (1984) list a number of criteria to determine the success of a commercial fumigation, such as (1) the average maximum concentration of phosphine must be more than 50% of the theoretical amount of phosphine applied, (2) the concentration at the end of the exposure period must be greater than the minimum effective against insects, and (3) the ratio of minimum to maximum concentration must exceed 0.25 after not more than 25% of the exposure period.

Fumigant concentrations can be influenced by a variety of factors including ecosystem conditions such as moisture content of the grain mass (Reed and Pan, 2000), temperature of the grain mass (Banks and Annis, 1984; Darby, 2011; Reed and Pan, 2000), temperature differences between the grain mass and ambient air (Banks and Annis, 1984), and wind speed (Banks and Annis, 1984; Cryer, 2008). Wind and temperature based effects are considered leak dependent major forces in fumigant loss (Navarro, 1998). In addition, a fumigation is also influenced by a

number of engineering variables such as fumigant recirculation rate, amount of phosphine applied, rate of evolution of phosphine into gaseous form, and degree of the seal of the silo.

A better understanding of how environmental factors and operational procedures influence a fumigation would allow applicators to take more effective corrective actions to prevent fumigation failures. There are a number of factors that may deter the efficacy of a fumigation where enough fumigant was applied to theoretically control the insects, according to Banks and Annis (1986). These factors are excessive overall loss of fumigant, inadequate fumigant dosage in localized regions, excessive delay between application and fumigant reaching particular regions, or a combination of these factors occurring simultaneously. To observe whether any of these effects were occurring in a fumigation would be difficult and would require excessive monitoring of fumigant concentrations at a number of locations in the silo. Even with such controls, there could be regions that are not monitored and experience problems, or environmental conditions that are abnormal or unforeseen. For these reasons, simulation with a three dimensional ecosystem model that can predict phosphine values at key locations in the silo can be of use.

The objectives of this research were to use the mathematical model developed and validated in Objective 2 to investigate the effects of environmental conditions (i.e., temperature, relative humidity, and wind speed) and operational variables (i.e., recirculation rate, degree of silo seal, type of fumigant, and silo dimensions) on fumigation efficacy.

Materials and Methods

In order to quantify effects of environmental conditions on predicted fumigant movement and loss, the weather data from the 10-day fumigation conducted from Aug 31 to Sept 9, 2015 in

Manhattan, Kansas, was modified by changing each key parameter (wind speed, ambient temperature, relative humidity) by +/- 25%. The impact of weather conditions on silo size was also investigated on the Coreen, NSW silo investigated under objective 1. The effects of fumigant recirculation and silo leakage were analyzed with changes of +/- 25% and +/- 50%. All simulations were then compared to the validated results at the actual weather conditions and evaluated on the effect that the variation had on the average fumigation concentration.

Fumigation with phosphine was compared against fumigation using sulfuryl-fluoride. Sulfuryl-fluoride is an alternative fumigant of commercial interest particularly to manage resistance of stored product insects to phosphine. The overall approach to modeling sulfuryl-fluoride in the M-L-P finite element ecosystem model is similar to the procedure for modeling phosphine, but with minor changes for factors such as gas density and diffusivity. The sorption characteristics for sulfuryl-fluoride are different, however, and require new equations. Sriranjini and Rajendran (2008) showed that wheat sorbed 17.7% of sulfuryl fluoride after 24 h at 25°C at an initial 66 g/m³ concentration. Hwaidi et al. (2015) presented sulfuryl-fluoride sorption and desorption data at several temperatures and moisture contents. The estimated baseline sorption equation for 12% moisture content and 25°C is:

$$C = 12.81e^{-0.0046t} \quad \text{Eq 5.1}$$

Where,

C = fumigant concentration lost [mg/l]

t = time [h]

Hwaidi et al. (2015) also investigated the relationship of moisture content and temperature on the sorption rate constant. They determined that increasing temperature causes a linear increase in the sorption rate constant by 4.6 to 7.6 fold when temperature ranged from 15°C to 35°C and by about 1.5 to 3 fold when moisture content ranged from 12% to 15%. To include the temperature and moisture content dependencies in the model, a linear temperature term with slope of 3/10 was added along with a linear moisture content term with slope of 2/3. The resulting equation for modeling sorption of sulfuryl-fluoride as a function of temperature and moisture content is:

$$C = 0.01281e^{-(0.0046t + (0.3*(T-25)) + (0.667*(MC-12)))} \quad \text{Eq 5.2}$$

Where,

C = fumigant concentration lost [kg/m³]

t = time [h]

T = temperature [°C]

MC = moisture Content [% wet basis]

Fundamentally, this equation is in the same form as the sorption equation for phosphine. Put into the same format as the phosphine equation, Eq 5.2 can be rewritten as:

$$C = 0.01281e^{-0.0046t} * 0.000553e^{0.3T} * 0.000335e^{0.667MC} \quad \text{Eq 5.3}$$

This equation gives the concentration of sulfuryl-fluoride over time. In order to arrive at an equation for the change of sulfuryl-fluoride over time, the derivative of Eq 5.3 with respect to time must be calculated to arrive at the final equation:

$$C = 0.000058926e^{-0.0046t} * 0.000553e^{0.3T} * 0.000335e^{0.667MC} \quad \text{Eq 5.4}$$

Although leakage of sulfuryl-fluoride has been studied by some (Chayaprasert et al., 2012) it has not been investigated as in-depth as phosphine. Cryer (2008) focused on wind induced leakage rates of sulfuryl-fluoride and methyl-bromide, and observed that the type of fumigant does not have a significant effect on wind induced loss. Given that the guiding equations used previously to estimate phosphine leakage from Banks and Annis (1984) were not specific to phosphine but rather generalized equations, and because wind induced leakage rates should be similar to phosphine, it is a reasonable assumption to use the leakage equations adapted for phosphine also for sulfuryl-fluoride.

Results and Discussion

1. Effect of Operational Variables

1a. Effect of Changing Leakage Rate

A successful fumigation requires a well-sealed silo. Among other factors, the amount of leakage from a silo depends on the degree of silo seal that makes a fumigation either successful or a failure. Recommended values for pressure half loss time vary by size of silo and range from three minutes for a 500 m³ silo to 6 min for a 2,000 to 15,000 m³ silo (Navarro, 1998). An

approximate rule of thumb for silo fumigations in Australia is pressure half loss times of three minutes or greater tend to assure a successful fumigation, while two to three minutes might cause failure or success, and less than one minute would cause a failed fumigation (Manoj Nayak, Personal Communication).

Shown in figure 5.1 are the predicted average phosphine concentrations for five simulations with a varying leakage rate, expressed as percentages of the leakage rate from the model verification (i.e., 100%). As expected, phosphine concentrations were higher for silos with a lower leakage rate. The effect is not directly proportional, as halving the leakage does not result in halving of the concentrations in the silo. Instead, halving the leakage resulted in a phosphine concentration that when averaged over all locations and times was 30% greater than the concentration from the verification. At 1.5x the leakage rate, the same overall average phosphine concentration was 12% less than the overall average concentration from the verification. Fumigations with lower leakage rates achieved higher maximum phosphine concentrations (416, 407, 400, 393, and 388 for 50-150%, respectively), as leakage begins taking effect before the maximum values are reached. The trends of decrease are similar throughout, despite the changes to leakage rate.

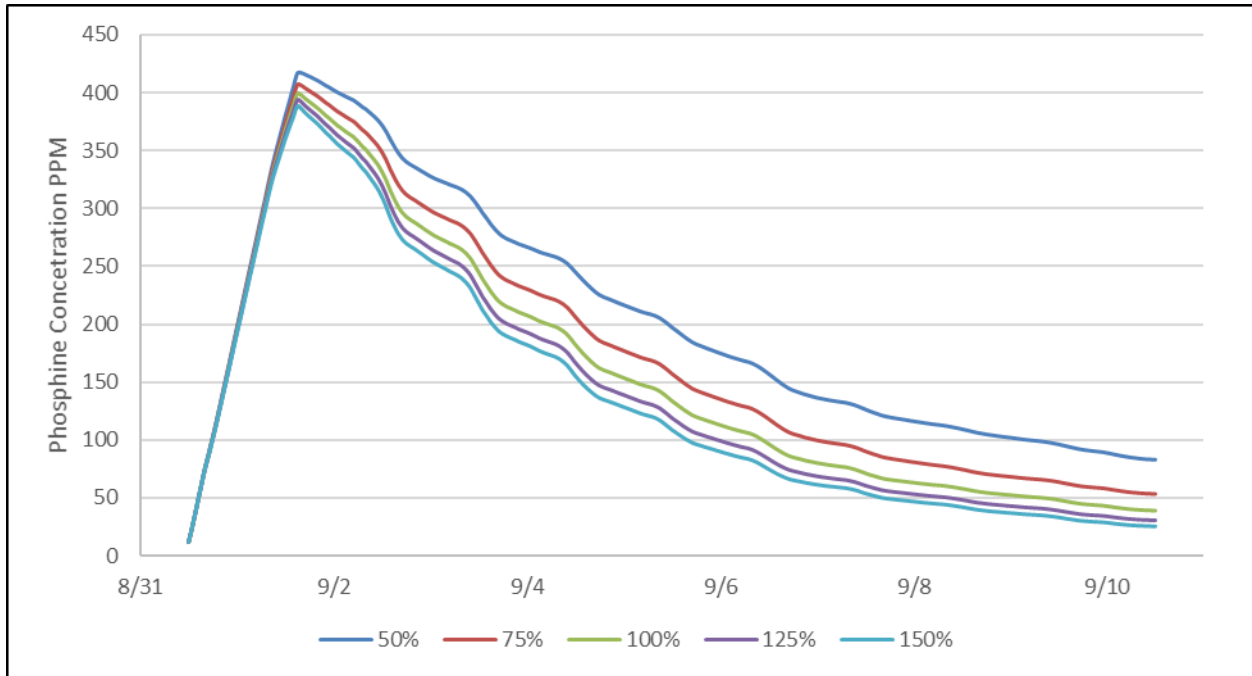


Figure 5:1 Overall average phosphine concentration (ppm) for five leakage rates, expressed as a percentage of the leakage rate (100%) used in the verification conducted between August 31 and September 9, 2015.

Percentage changes resulting from the five simulations are shown in figure 5.2.

Improving the degree of seal by a factor of three (i.e., from 150% to 50%) increased the overall average Ct-product by 47%, i.e., from 33,300 ppm-h to 48,900 ppm-h. Doubling the leakage rate of the silo (i.e., from 75% to 150%) increased overall average Ct-products by 39%, from 35,100 ppm-h to 48,900 ppm-h as seen in table 5.1. By the end of the simulation the percentage differences from original were 111%, 36%, -21%, and -34% for the 50%, 75%, 125%, and 150% leakage situations, respectively. As the leakage from the silo increases, the resulting decreases in concentration are reduced. This result makes sense because the amount of phosphine lost from any location is dependent on the concentration. However, it is not relative to the concentrations in the rest of the silo. Additionally, a point on the side of the wall can only lose phosphine at the

rate the leak allows for. Therefore, at high rates of leakage, loss of phosphine from the silo wall can become rate limited not by the phosphine loss equations, but by the speed of phosphine movement from within the grain mass. Thus, even if phosphine loss from the wall doubles in rate, that will not correlate with the phosphine concentration totals in the silo being cut in half. This also suggests that improving sealing of a relatively well sealed silo has a greater positive impact than small improvements to a leaky silo.

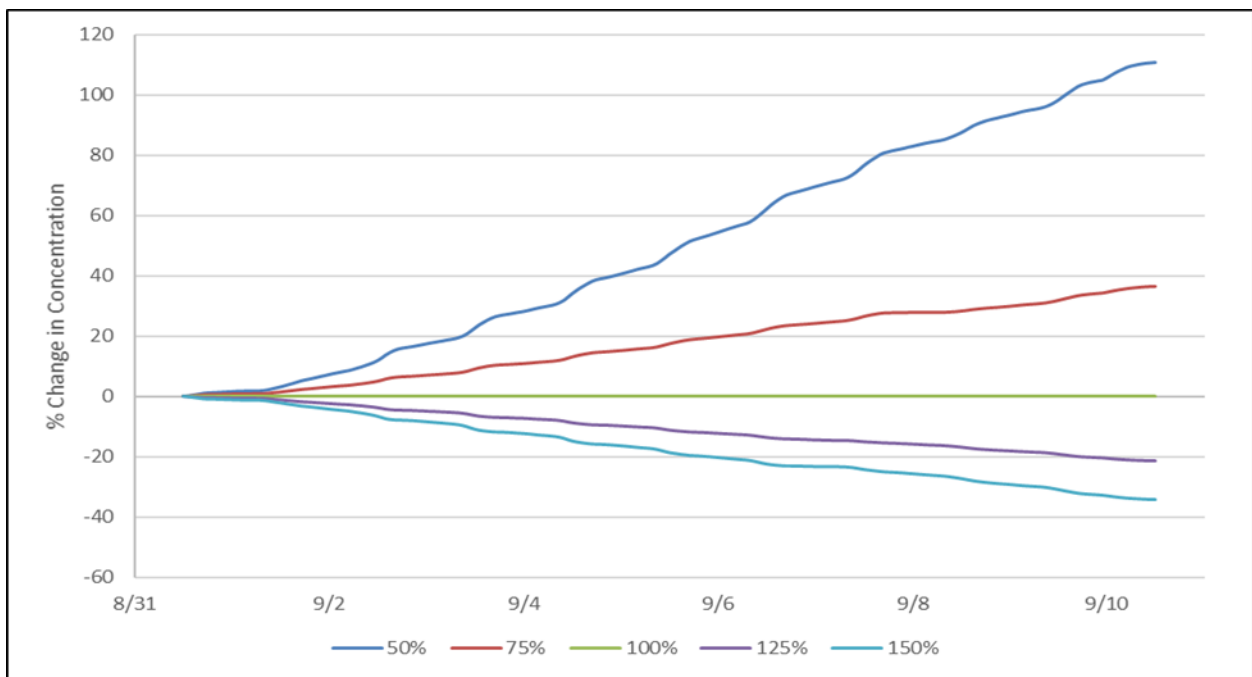


Figure 5:2 Change in overall average phosphine concentration (%) compared for varying leakage rates, expressed as a percentage of the leakage rate (100%) used in the verification conducted between August 31 and September 9, 2015.

Improving the degree of seal by a factor of three (i.e., from 150% to 50%) increased the overall average Ct-product by 47%, i.e., from 33,300 ppm-h to 48,900 ppm-h. Doubling the

leakage rate of the silo (i.e., from 75% to 150%) increased overall average Ct-products by 39%, from 35,100 ppm-h to 48,900 ppm-h as seen in table 5.1.

Table 5:1 Cumulative average Ct-products (ppm-h) and the difference from original (%) for five leakage rates, expressed as a percentage of the leakage rate (100%) used in the verification conducted between August 31 and September 9, 2015.

	50%	75%	100%	125%	150%
Ct-product	48,900	41,700	37,700	35,100	33,300
Percent Difference	22.9	9.7	0.0	-7.4	-13.1

These results should be of interest to grain handlers and fumigation applicators in both the U.S. and Australian contexts. According to Cook (2016) a vast majority of grain stores in the U.S. are not designed to be sealed, and temporary sealing occurs only prior to fumigation. Extensive efforts were undertaken by Cook (2016) to permanently seal a Scafco brand silo that was not designed to be airtight. Cook was only able to achieve pressure half loss times of 0-50 seconds, which were well below the minimum of three minutes recommended to achieve a successful fumigation. Cook recorded similar results for a Bird's brand silo that was designed to be sealed, although the silo constructed on location never achieved Bird's factory specifications. Based on the results of this modeling work, temporary sealing techniques that fail to achieve significant sealing improvements are not likely to lead to substantial improvements in fumigant concentrations. Additionally, this result underlines the importance of designing and constructing well-sealed silos and of pressure testing constructed silos to ensure quality of seal. If a silo is constructed with a high pressure half loss time, achieved fumigant concentrations will be higher, and temporary sealing activities will be more impactful in increasing fumigant concentrations.

1b. Recirculation Rate

Another factor with a high degree of influence on fumigation efficacy is fumigant recirculation rate. Shown in figure 5.3 are the predicted average concentrations of phosphine for five simulations with a varying leakage rate, expressed as percentages of the leakage rate from the model verification (i.e., 100%). A higher recirculation rate results in better mixing of fumigant as it reenters the silo and more uniform movement of fumigant through the grain mass. A higher recirculation rate will bring more phosphine in contact with the leakier silo wall and grain surface, increasing the exposure of insects in those areas to the fumigant. The negative effect is that more phosphine leaks from the wall and silo roof. Thus, the total amount of fumigant loss increases and the average amount of phosphine decreases. Increases in the recirculation rate aided by the thermosiphon have a similar effect on overall average fumigant concentration as the increases in leakage rate. Similarly, increasing recirculation rates have progressively smaller impact on concentration decrease. Halving the leakage resulted in a phosphine concentration that when averaged over all locations and times was 44% greater than the concentration from the verification. At 1.5x the leakage rate, the same overall average phosphine concentration was 27% less than the overall average concentration from the verification. Fumigations with lower recirculation rates achieved higher maximum phosphine concentrations (465, 430, 400, 365, and 336 for 50-150%, respectively), as recirculation begins taking effect before the maximum values are reached. The trends of decrease are similar throughout, despite the change in recirculation rate.

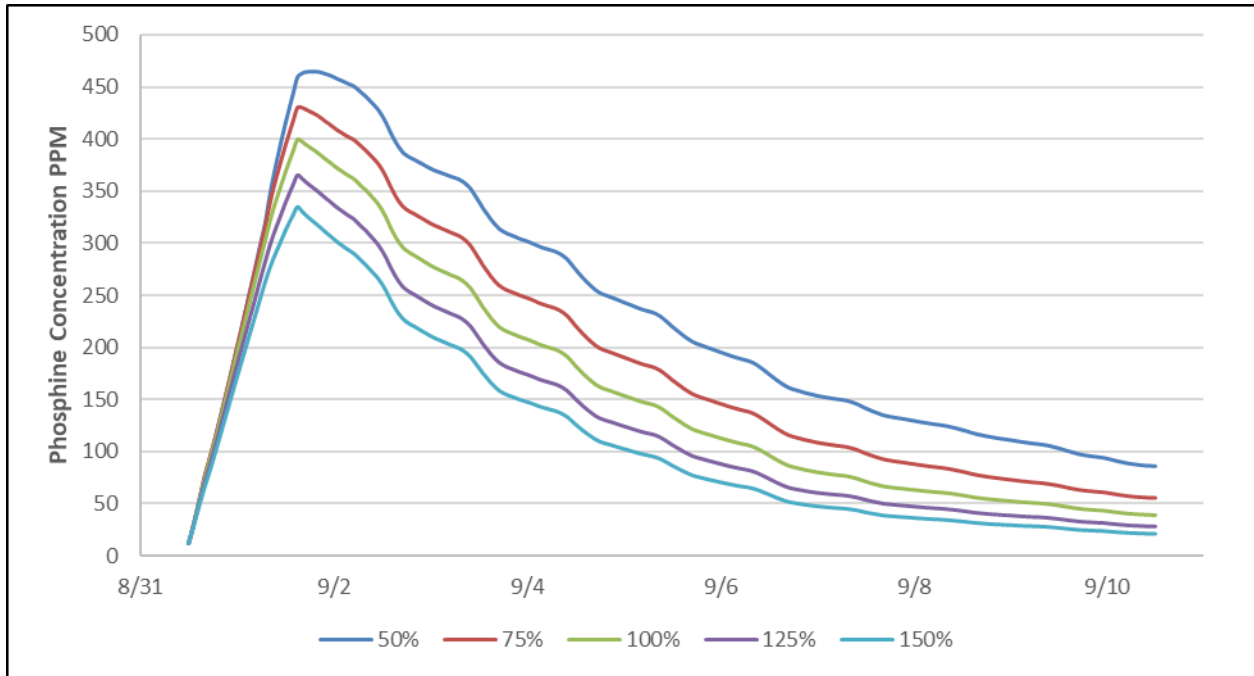


Figure 5:3 Overall average phosphine concentration (ppm) for five recirculation rates, expressed as a percentage of the recirculation rate (100%) used in the verification conducted between August 31 and September 9, 2015.

Percentage changes resulting from the five simulations are shown in figure 5.4. By the end of the simulation the percentage differences from original were 118%, 41%, -28%, and -47% for the 50%, 75%, 125%, and 150% recirculation rates, respectively. As with the leakage analysis, as the recirculation increases, the increased loss in fumigant decreases.

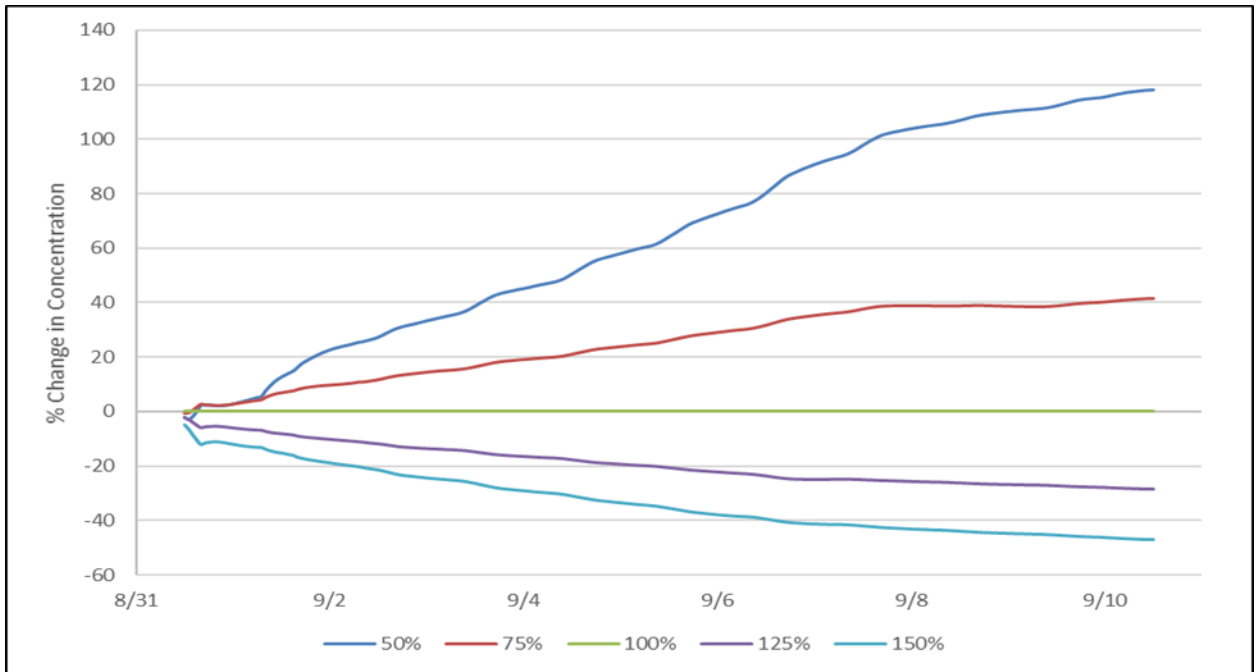


Figure 5:4 Change in overall average phosphine concentration (%) for five recirculation rates, expressed as a percentage of the leakage rate (100%) used in the verification conducted between August 31 and September 9, 2015.

Increasing the recirculation rate by a factor of three (i.e., from 50% to 150%) decreased the overall average Ct-product by 97%, i.e., from 54,400 ppm-h to 27,600 ppm-h. Doubling the recirculation rate of the silo (i.e., from 75% to 150%) decreased overall average Ct-products by 38%, from 44,500 ppm-h to 27,600 ppm-h.

Table 5:2 Cumulative average Ct-products (ppm-h) for the whole silo, expressed as a percentage of the recirculation rate (100%) used in the verification conducted between August 31 and September 9, 2015.

	50%	75%	100%	125%	150%
Ct-product	54,400	44,500	37,700	32,000	27,600
Percent Difference	44.3	18.0	0.0	-15.2	-27.8

When making management decisions about which recirculation rate to use, one of the most important factors is the effect on the areas of the silo that are most vulnerable to insect survival because of receiving insufficient fumigant. While an increase in recirculation rate results in an overall decrease in fumigant concentrations, the decision to recirculate will be the correct one if it results in increased concentrations in the areas of the silo with the least amount of fumigant. In the previous objective, four locations with the lowest Ct-product were investigated. In table 5.3, Ct-product values are presented for each of those four locations along the top upper edge of the grain mass for nine recirculation rates, listed as a percentage of the verification recirculation rate.

Table 5:3 Cumulative Ct-products (ppm-h) for the nodes along the top outer edge of the grain mass by location for nine recirculation rates, expressed as a percentage of the recirculation rate used in the verification (100%) conducted between August 31 and September 9, 2015.

	West	South	East	North
12.5%	15,200	12,100	12,400	11,400
25%	18,600	14,700	15,000	13,800
37.5%	19,700	15,600	15,900	14,600
50%	19,100	15,200	15,500	14,300
62.5%	18,400	14,800	15,000	13,800
75%	17,500	14,100	14,300	13,200
100%	17,800	14,400	14,600	13,500
125%	14,500	11,800	12,000	11,100
150%	13,100	10,800	10,900	10,200

There is a clear tradeoff between delivering phosphine to vulnerable areas in the silo and the resultant increase in leakage. The greater the recirculation rate is, the more there will be increased fumigant leakage. The lower the recirculation rate is, the more insufficient will be the fumigant distribution, with the top of the silo taking an increased amount of time before the fumigant concentration increases sufficiently. The Ct-products at the top of the silo reach a maximum value at 37.5% of the verification recirculation. This recirculation rate resulted in the highest maximum concentrations of all rates tested, and maintained a higher average concentration than the simulations at lower recirculation rates for the initial 49h of the simulation.

The benefits of closed loop recirculation fumigation systems over systems without recirculation have been documented extensively (Noyes et al., 1998). These simulation results

indicate that there is an optimum flow rate to maximize fumigation efficacy. In this simulation, the optimum recirculation rate for both overall maximum concentrations and for Ct-products in the most vulnerable areas of the grain silo was 37.5% of the verification airflow rate. This airflow rate (0.0001875 m/s night time and 0.000375 m/s day time) is lower than any of the airflow rates (0.026 m/s to 0.0062 m/s) discussed in Noyes et al. (1998). However, the smallest silo discussed in Noyes et al. (1998) was 100x larger than the silo used in this research (5,000 tonnes vs 45.5 tonnes). The ideal recirculation rate is likely silo specific due to the effect of variations in silo dimensions and silo seal. To further investigate this relationship, the 1,500 tonne Australian silo previously discussed in chapter 3 was tested under two recirculation rates, the original rate used in the verification of the model, and the lowest fan powered recirculation rate suggested in Noyes et al. (1998). The results of this test are shown in figure 5.5, and demonstrate that while the higher airflow rates disperse the phosphine into the grain mass more rapidly, there is a substantial increase in leakage from the silo.

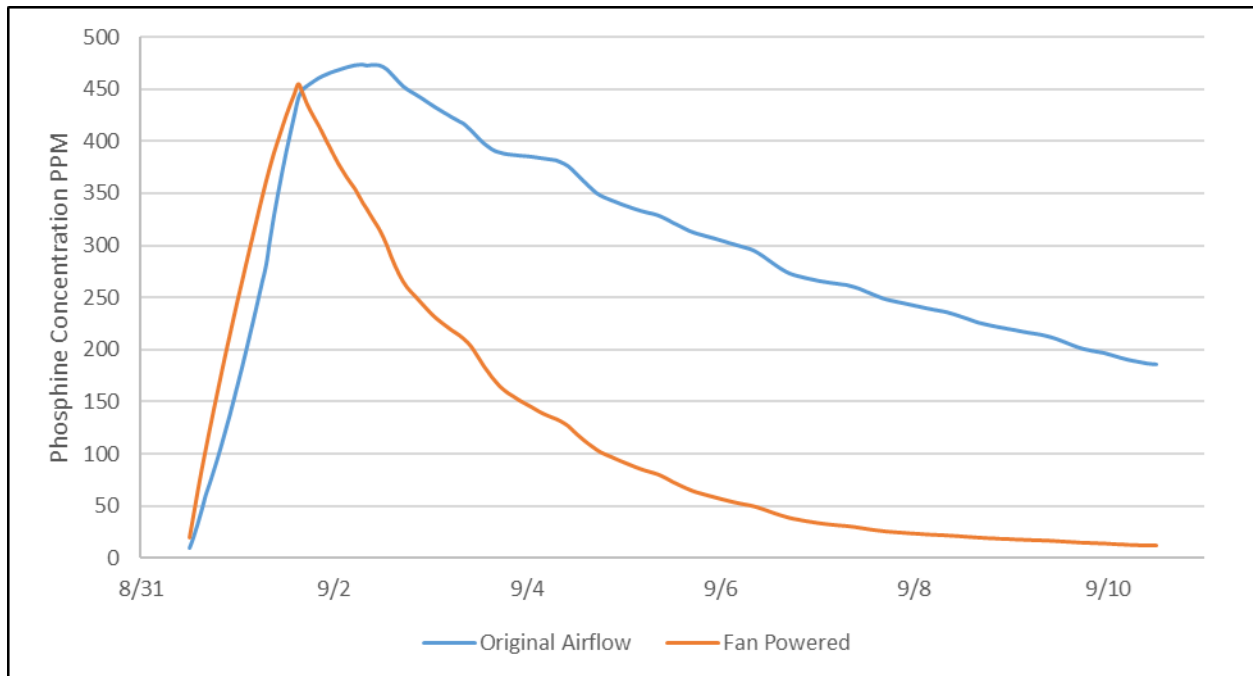


Figure 5:5 Overall average phosphine concentration (ppm) for two recirculation rates, the original airflow used in the verification (0.001-0.005 m/s) and fan powered recirculation (0.0062 m/s) in a 1,500 MT wheat silo

The resultant Ct-product of the fumigation under fan forced recirculation (i.e. 30,095 ppm-h) is less than half that of the fumigation under the recirculation rates used in the verification (i.e. 72,643 ppm-h), which was based on a thermosiphon system. Given the well demonstrated benefits for pest control due to gas recirculation, and the result from this simulation that suggests high recirculation rates can be detrimental, a small to moderate recirculation rate is likely the best management practice. This result suggests that a stored grain manager of a small on-farm silo should utilize passive recirculation technology such as the thermosiphon, because higher recirculation rates such as those provided by powered recirculation fans likely will not result in improved fumigant concentrations. On the other hand, further research is needed to investigate ideal recirculation rates for larger silos such as those investigated by Noyes et al. (1998)

1c. Sulfuryl-Fluoride

Figures 5.6 and 5.7 show the simulated concentrations when using sulfuryl-fluoride versus phosphine under the conditions of the validated experiment. The simulation model calculates fumigant concentration in kg/m^3 . Figure 5.8 shows the results when converted into units of parts per million. This seemingly large difference in concentrations achieved is due the difference in molecular weights of the two gases (i.e, 34 g/mol for phosphine versus 102 g/mol for sulfuryl-fluoride). The higher molecular weight of sulfuryl-fluoride has a less significant effect in a simulation with forced convection currents than in a simulation without forced recirculation. The effect of sorption, as seen in equation 4.4, is not dependent on the concentration and decreases slowly with respect to time. Functionally this means that the sorption differences between phosphine and sulfuryl fluoride will have a larger effect in longer fumigations, such as are common in Australia. The verification data used in this case, however, came from a ten-day fumigation under U.S. conditions. As discussed in more detail in the relative humidity section, sorption has a less significant effect relative to leakage. The final sorption amount totaled over the silo, in kg/m^3 , was 0.0603 for phosphine and 0.0141 for sulfuryl-fluoride. The lower rate of sorption for sulfuryl-fluoride would result in higher fumigant concentrations, further offsetting the effect of the reduced diffusivity and increased molecular weight. The results in figure 5.6 show that phosphine concentrations were slightly higher in kg/m^3 than the sulfuryl-fluoride concentrations. As seen in Figure 5.7, this difference grew gradually over the course of the fumigation to a maximum of 6.1% by the end. The Ct-products, in $\text{kg h}/\text{m}^3$, were 130 and 133 for sulfuryl-fluoride and phosphine, respectively, and 12,580 and 36,930 ppm-h, in ppm-h respectively

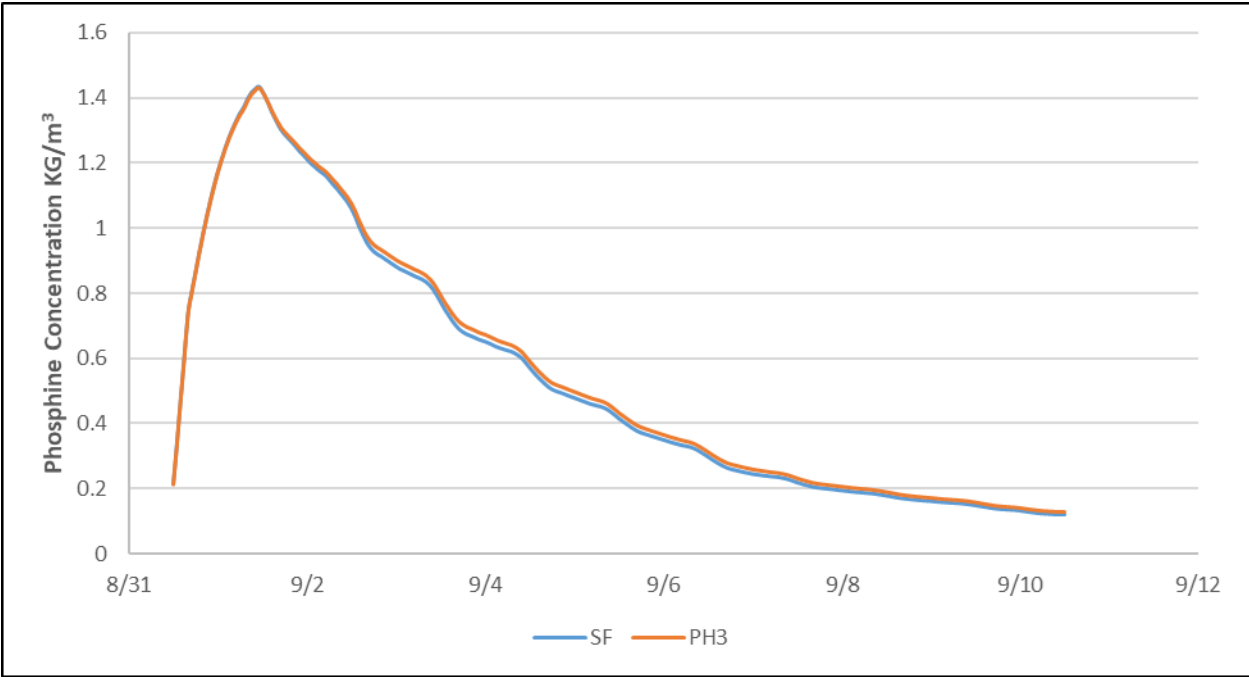


Figure 5:6 Overall average fumigant concentration (kg/m3) of phosphine and sulfuryl-fluoride fumigations, based on the verification conducted between August 31 and September 9, 2015.

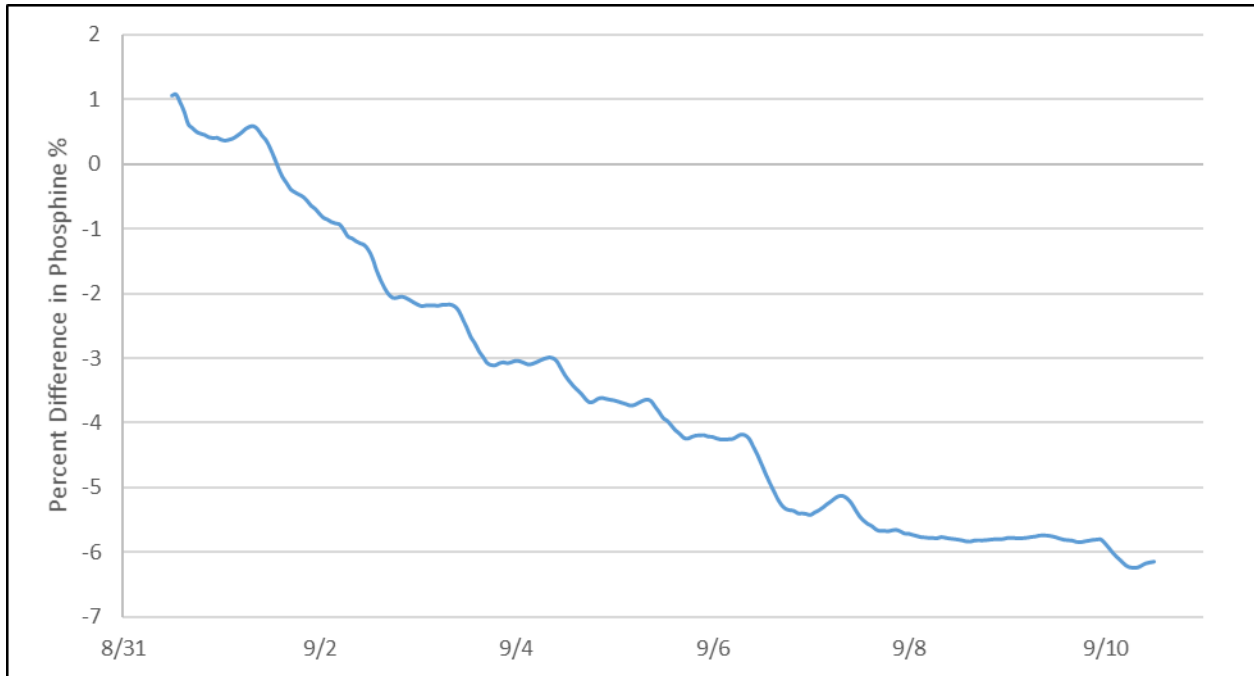


Figure 5:7 Change in overall average fumigant concentration (%) of phosphine and sulfuryl-fluoride fumigations, using kg/m³, based on the verification conducted between August 31 and September 9, 2015.

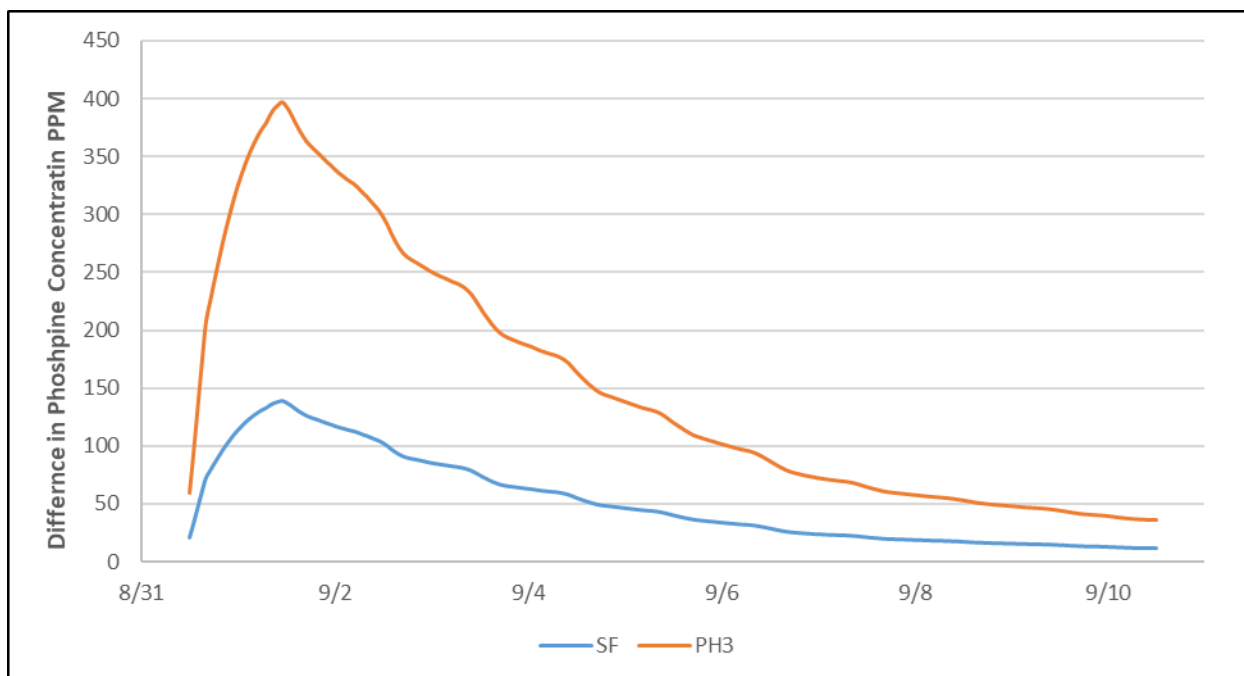


Figure 5:8 Overall average fumigant concentration (ppm) of phosphine and sulfuryl-fluoride fumigations, based on the verification conducted between Aug 31 and September 9, 2015.

The results of this simulation experiment demonstrate that the higher molecular weight of sulfuryl-fluoride has a negative impact on its distribution throughout the grain mass. The scale of this effect was more than enough to cancel out the reduced loss due to fumigant sorption. Additionally, without forced recirculation, fumigant distribution would have been even poorer. This demonstrates that utilizing recirculation technology is more important for improving efficacy of fumigations with sulfuryl-fluoride than with phosphine. This should be especially true for larger storage structures typically found at commercial facilities in the U.S. and Australia.

2. Effect of Environmental Conditions

2a. Temperature of Ambient Air

Shown in figure 5.9 are the predicted average concentrations of phosphine for five simulations with a varying ambient temperature, expressed as percentages of the ambient temperature for the model verification (i.e., 100%). As expected, when ambient temperatures were increased, total average phosphine concentrations in the silo decreased. The effect of increasing temperatures is not directly proportional, as the effects of temperature changes decrease as the temperature increases. When temperatures were decreased, total average phosphine concentrations increased by a higher amount. Halving the ambient temperature resulted in a phosphine concentration that when averaged over all locations and times was 26% greater than the concentration from the verification. At 1.5x the ambient temperature, overall average phosphine concentration was 27% less than the overall average concentration from the verification. Fumigations with lower ambient temperatures achieved higher maximum phosphine concentrations (416, 410, 400, 380, and 364 for 50-150%, respectively). The scale of the effects builds with time, becoming larger as the simulation progressed (Figure 5.10). By the end of the simulation the percentage differences from original were 101.6%, 57.3%, -47.1%, and -67.9%, for the 50%, 75%, 125%, and 150% ambient temperature situations, respectively. The temperature decreases caused 57% and 102% increases in phosphine concentration for the 75% and 50% temperature cases, respectively.

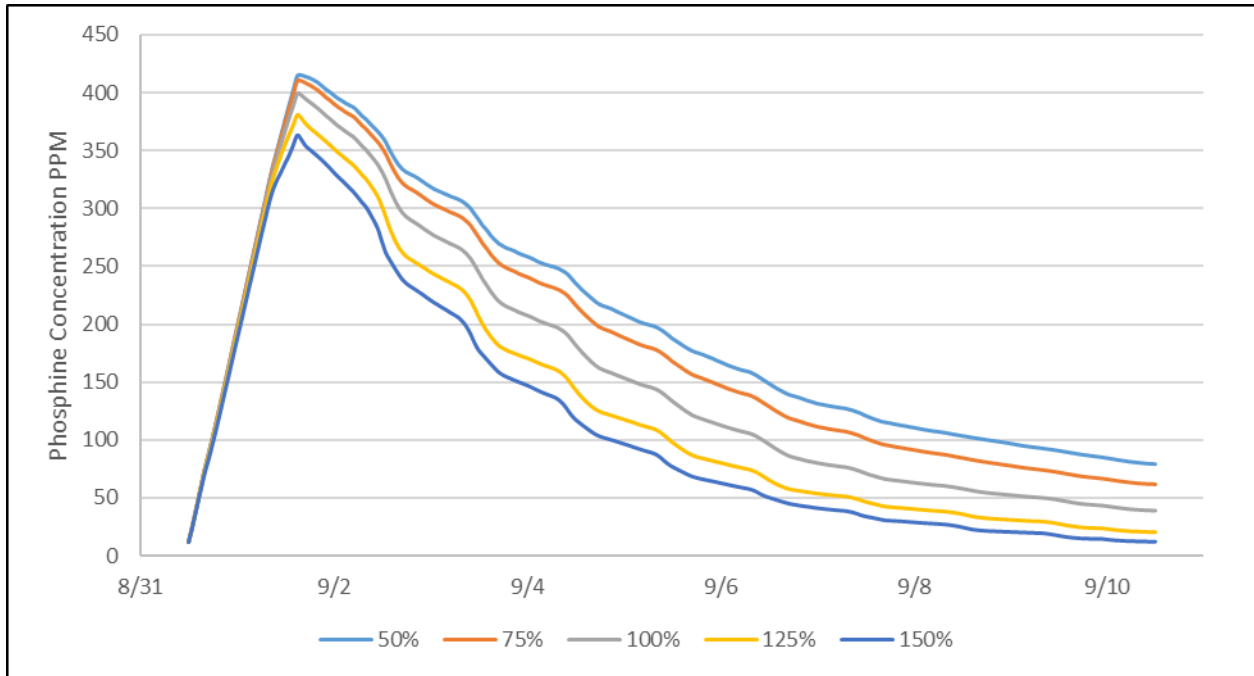


Figure 5:9 Overall average phosphine concentration (ppm) for five varying temperature conditions, expressed as a percentage of the temperatures (100%) used in the verification conducted between August 31 and September 9, 2015.

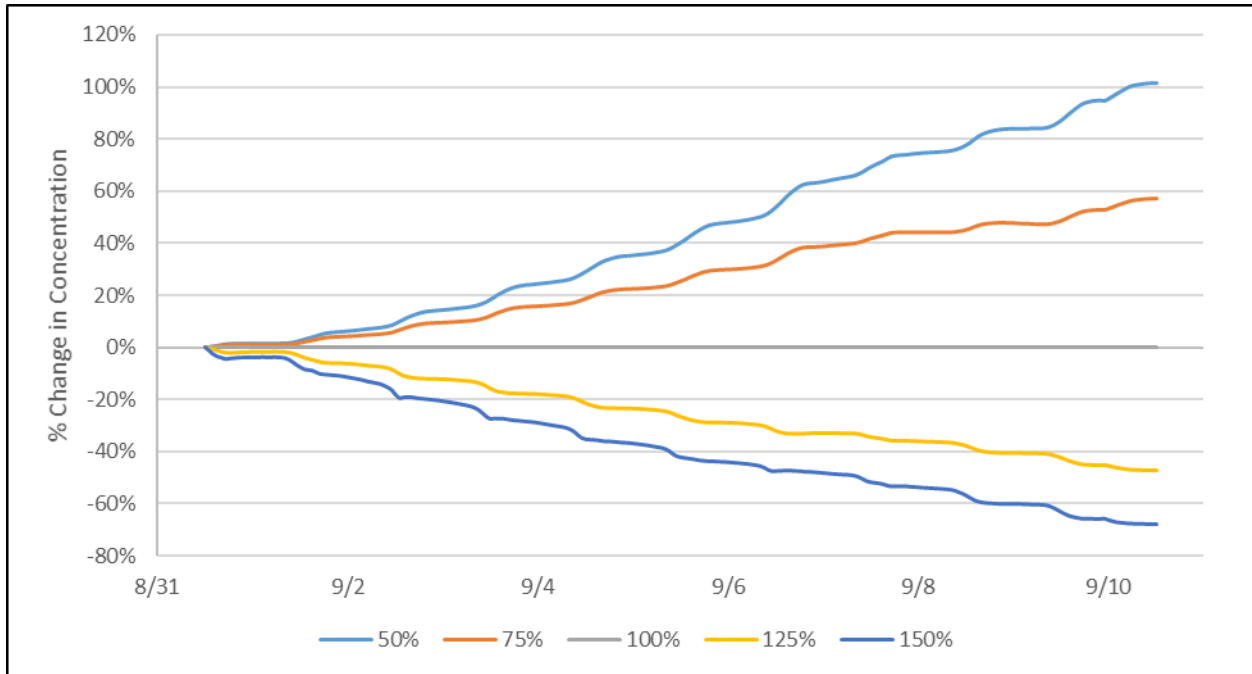


Figure 5:10 Change in overall average phosphine concentration (%) for five temperature conditions, expressed as a percentage of the temperatures (100%) used in the verification conducted between August 31 and September 9, 2015.

Increasing the ambient temperature by a factor of three (i.e., from 150% to 50%) decreased the overall average Ct-product by 71.5%, i.e., from to 47,500 ppm-h to 27,600 ppm-h (Table 5.4). Doubling the ambient temperature of the silo (i.e., from 75% to 150%) decreased overall average Ct-products by 39.1%, from 43,800 ppm-h to 27,700 ppm-h.

Table 5:4 Cumulative average Ct-products (ppm-h) and the difference from original (%) for five ambient temperatures, expressed as a percentage of the ambient temperatures (100%) used in the verification conducted between August 31 and September 9, 2015.

	50%	75%	100%	125%	150%
ppm-h	47,500	43,800	37,700	31,400	27,700
Percent Difference	26.0	16.1	0.0	-16.6	-26.6

The primary reason for this relationship is found in the fumigant loss equation and its reliance on temperature. Based on equation 4.6, fumigant concentration loss increases as a function of grain temperature along the silo wall, and with increases in the difference between the silo temperature and ambient temperature. Additionally, temperature increases also increase the fumigant loss due to sorption as detailed in equation 4.4. Increasing and decreasing ambient temperature does not have an equal influence on overall fumigant concentrations. This is due to the previously discussed effect on increasing leakage from the silo. As the leakage rates increase at high temperatures, the effect diminishes because the leakage effect due to temperature difference comprise only two terms in the overall leakage equation, which is additive. This can be seen clearly in table 5.4, as increasing from the 100% case to 125% had a larger effect than increasing from 125% to 150%, and decreasing from 100% to 75% had a larger effect than decreasing from 75% to 50%.

The effect of temperature is of particular interest in subtropical grain growing regions such as Australia, where temperatures are high and grain is commonly fumigated in the summer. Higher temperatures cause increased gas leakage, making sealing even more important. While high temperatures cause a decrease in phosphine concentrations in the grain mass, phosphine is more effective against insects at higher temperatures (Bond, 1989; Sun, 1946) in large part due to their increased activity and higher respiration rates. If, however, the silos were well sealed,

increased leakage caused by higher temperatures would be mitigated and insect susceptibility to the fumigant would be maximized.

2b. Relative Humidity of Ambient Air

Changing the relative humidity of the ambient air by manipulating the weather data had no effect on simulated phosphine concentrations (data not shown). Effects from increased relative humidity could have an effect on phosphine concentrations through increased moisture contents in the grain mass. Increased moisture contents would affect the concentrations in the silo through the sorption equation (Equation 4.4). However, the impact of sorption was small compared to leakage losses. Sorption accounted for an overall average loss of only 17 ppm by the end of the simulated verification trial, compared to 343 ppm lost due to leakage.

As shown in chapter 3, moisture content changes take substantially longer than temperature changes to develop in a grain mass. Given there was no aeration of the grain with ambient air and only ten days were simulated, ambient relative humidity changes had no effect on moisture content in the grain silo. Recirculation of air as part of the air-gas mixture through dry wheat at 11.3% moisture content, dry basis, maintains equilibrium conditions between the air temperature and relative humidity and grain temperature and moisture content. Therefore, for most closed-loop fumigation applications, relative humidity of the ambient air will not have an appreciable impact on fumigant concentrations.

2c. Wind Speed

Shown in figure 5.11 are the predicted average concentrations for phosphine for five simulations with varying wind speeds, expressed as percentages of the wind speeds from the

model verification (i.e., 100%). As expected, phosphine concentrations were higher for silos with lower wind speeds. Halving wind speed resulted in a phosphine concentration that when averaged over all locations and times was 10.4% greater than the concentration from the verification. At 1.5x, the same overall average phosphine concentration was 13.3% less than the overall average concentration from the verification. Fumigations with lower wind speeds achieved higher maximum phosphine concentrations (407, 404, 400, 393, and 386 for 50-150%, respectively), as leakage begins taking effect before the maximum values are reached.

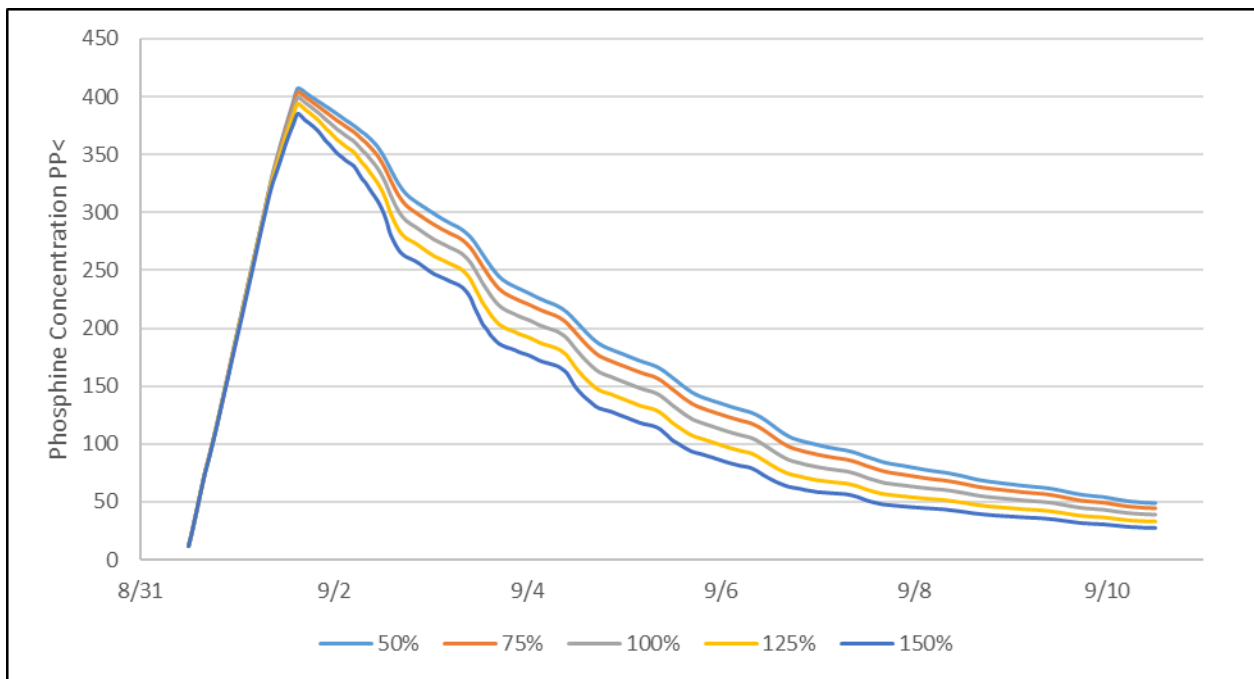


Figure 5:11 Overall average phosphine concentration (ppm) for five wind speeds, expressed as a percentage of the wind speeds (100%) used in the verification conducted between August 31 and September 9, 2015.

Percentage changes resulting from the five simulations are shown in figure 5.12. By the end of the simulation the percentage differences from original were 25%, 14%, -15%, and -29% for the 50%, 75%, 125%, and 150% wind speed cases, respectively.

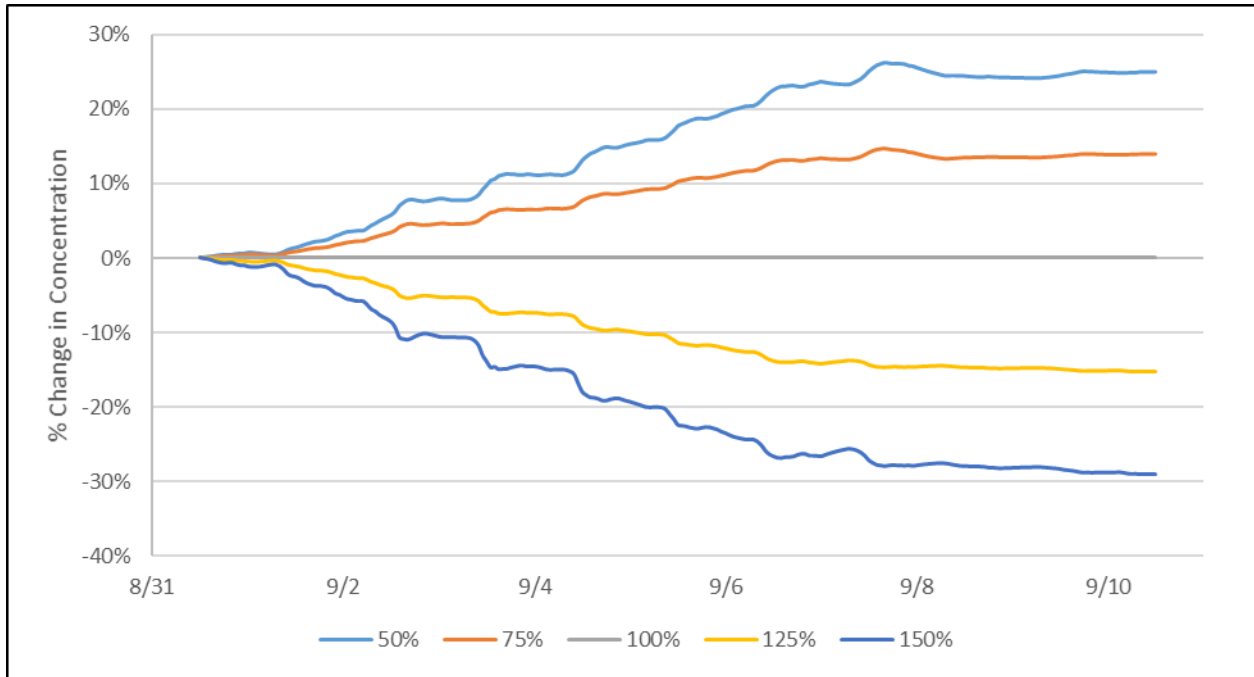


Figure 5:12 Change in overall average phosphine concentration (%)for five wind speeds, expressed as a percentage of the wind speeds (100%) used in the verification conducted between August 31 and September 9, 2015.

Increasing the wind speed by a factor of three (i.e., from 50% to 150%) decreased the overall average Ct-product by 27%, i.e., from 41,600 ppm-h to 31,700 ppm-h (Table 5.5). Doubling the wind speed of the silo (i.e., from 75 to 150%) decreased overall average Ct-products by 21%, from 39,9200 ppm-h to 31,700 ppm-h.

Table 5:5 Cumulative average Ct-products (ppm-h) and the difference from original (%) for wind speeds, expressed as a percentage of the wind speeds (100%) used in the verification conducted between August 31 and September 9, 2015.

	50%	75%	100%	125%	150%
Ct-product	41,600	39,900	37,700	35,200	31,700
Percent Difference	10.4	6.0	0.0	-6.7	-13.3

For temperature and leakage effects, any change in conditions that resulted in an increased loss of fumigant had a smaller proportional change as higher amounts of loss were reached. In this case, the effect of increased wind speeds did not decrease at higher wind speeds, and in fact had a slightly larger impact on phosphine concentrations. The value in the exponent of the wind speed equation (Equation 4.5) is more than three times the exponent in the temperature equations. Thus, the exponential effect of increasing wind speed will be much more pronounced than changes in temperature or leakage as seen previously in sections 1a and 1b of this chapter. The exponential increase in fumigant concentration loss due to higher wind speeds was slightly more than enough to overcome the diminishing returns of increasing leakage. Additionally, wind speeds are usually low and more variable than ambient temperature on a day-to-day basis. Thus, the influence of wind speed on a fumigation is more variable than the influence of ambient temperature. While the temperature effect continued to increase consistently over the course of the simulation, the wind effect was more dependent on varying weather conditions. The low wind speed conditions that were observed beginning on September 8 caused the effects of changing wind speed to level off, as seen in figure 5.12. These results indicate that weather events that cause high wind speeds are capable of having a large impact on phosphine concentrations in a silo. This points to the importance of best fumigation

management practices such as seal testing a silo before a fumigation and monitoring gas concentrations during a fumigation. Monitoring phosphine concentrations helps detect increased fumigant loss due to sudden increases in wind speed.

2d. Impact of Environmental Conditions on Silos of Different Dimensions

The effect of ambient temperature and wind speed on a silo are also influenced by silo dimensions, specifically the surface area to volume ratio. The silo used for verification has a main cylindrical section of 4.4 m diameter and 3.96 m height, resulting in a volume of 60.21 m³ and an external surface area of 85.15 m². This equates to a surface area to volume ratio of 1.41 m²/m³. The silo used in Coreen, NSW, has a diameter of 13.7 m and a height of 12.4 m, giving it a volume of 1,825.2 m³ and a surface area of 827.7 m², for a surface area to volume ratio of 0.45 m²/m³. The larger silo reflects the size of a larger on-farm storage silo, but is still smaller than the size of steel tanks used at grain holding terminals, such as those discussed in Noyes et al. (1998), which had diameters of 20-30 m.

The effects of changes in ambient temperature were smaller in the silo with the smaller surface area to volume ratio, as seen in figure 5.13 and figure 5.14 (Figure 5.14 indicates that all concentration data is within 15% of original values, whereas figure 5.10 indicates much larger changes in concentration because of the larger surface area to volume ratio). The final percentage changes were -10.9%, -7.31%, 8.35%, and 14.4% for the 150%, 125%, 75%, and 50% temperature conditions, respectively. The effects of changes in wind speed were also smaller for the silo with the smaller surface area to volume ratio, as seen in figures 5.15 and 5.16 (Figure 5.16 indicates that concentration data is within 4% of original values, whereas figure 5.12 indicates much larger changes in concentrations of up to 30% difference because of the

larger surface area to volume ratio). The final percentage changes for the larger silo were - 3.14%, -1.6%, 1.5%, and 2.6% for the 150%, 125%, 75%, and 50% wind speeds, respectively. The influence of environmental changes is most dominant on the wall and roof the silo, while the core areas are not affected. Therefore, it is not a surprise that silos with smaller surface area to volume ratios are less affected by changes in weather conditions. These results suggest that environmental factors affect fumigation efficacy more substantially in silos with large surface area to volume ratios. This result concurs with Montross (1999), who found that in silos exposed to solar radiation, the average and core temperatures of a larger silo would be lower than in a smaller silo because the smaller surface area per unit volume meant slower warming of grain especially in the core grain mass.

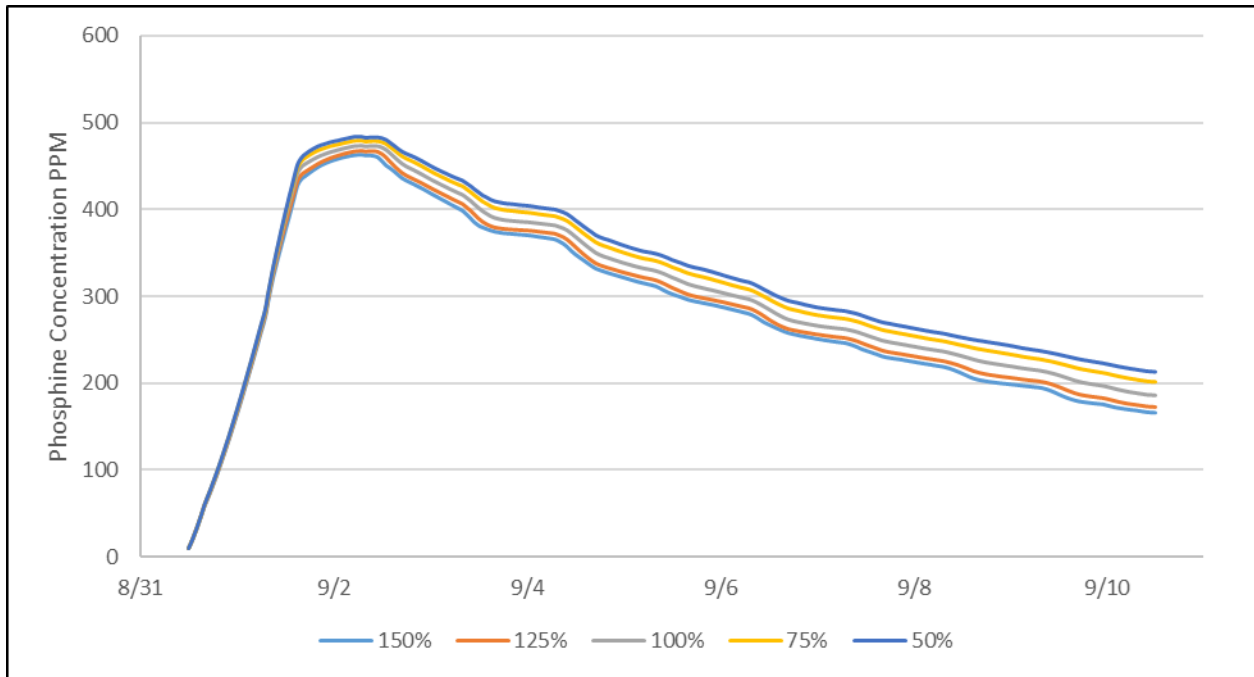


Figure 5:13 Overall average phosphine concentration (ppm) for five temperature conditions, expressed as a percentage of the temperatures (100%) used in the verification conducted between August 31 and September 9, 2015, for the 1500 MT silo with a surface area to volume ratio of 0.45 m²/m³.

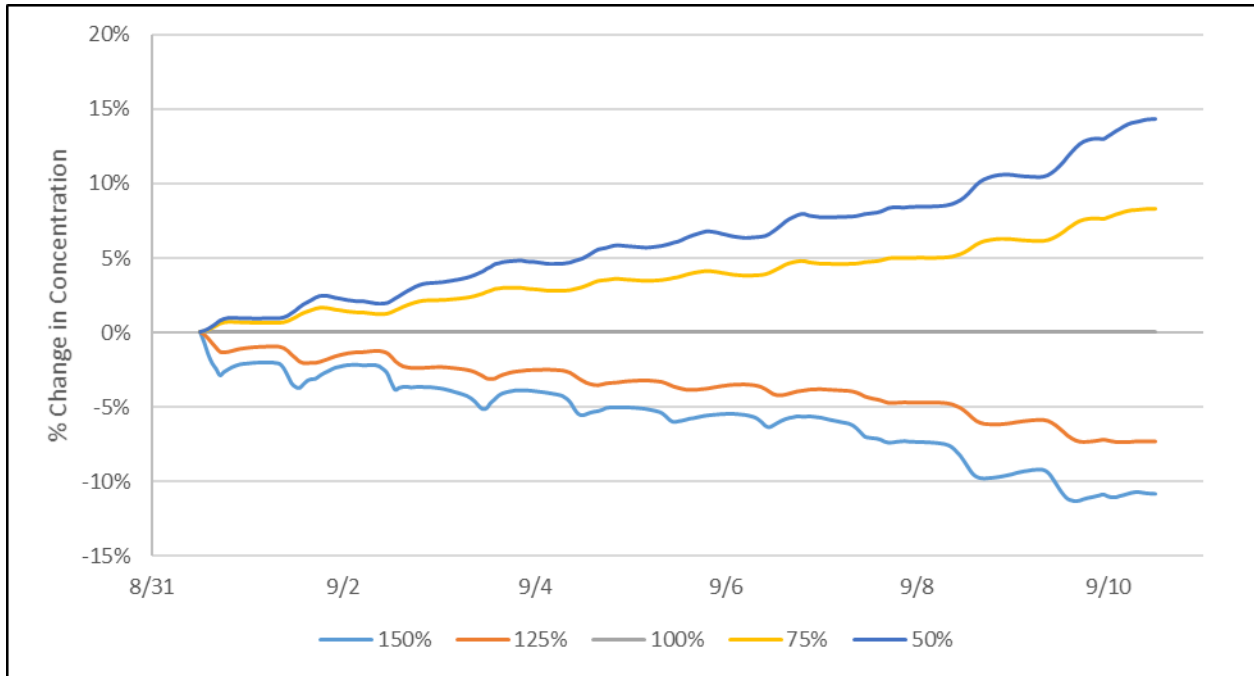


Figure 5:14 Change in overall average phosphine concentration (%) for five temperature conditions, expressed as a percentage of the temperatures (100%) used in the verification conducted between August 31 and September 9, 2015, for the 1500 MT silo with a surface area to volume ratio of 0.45 m²/m³.

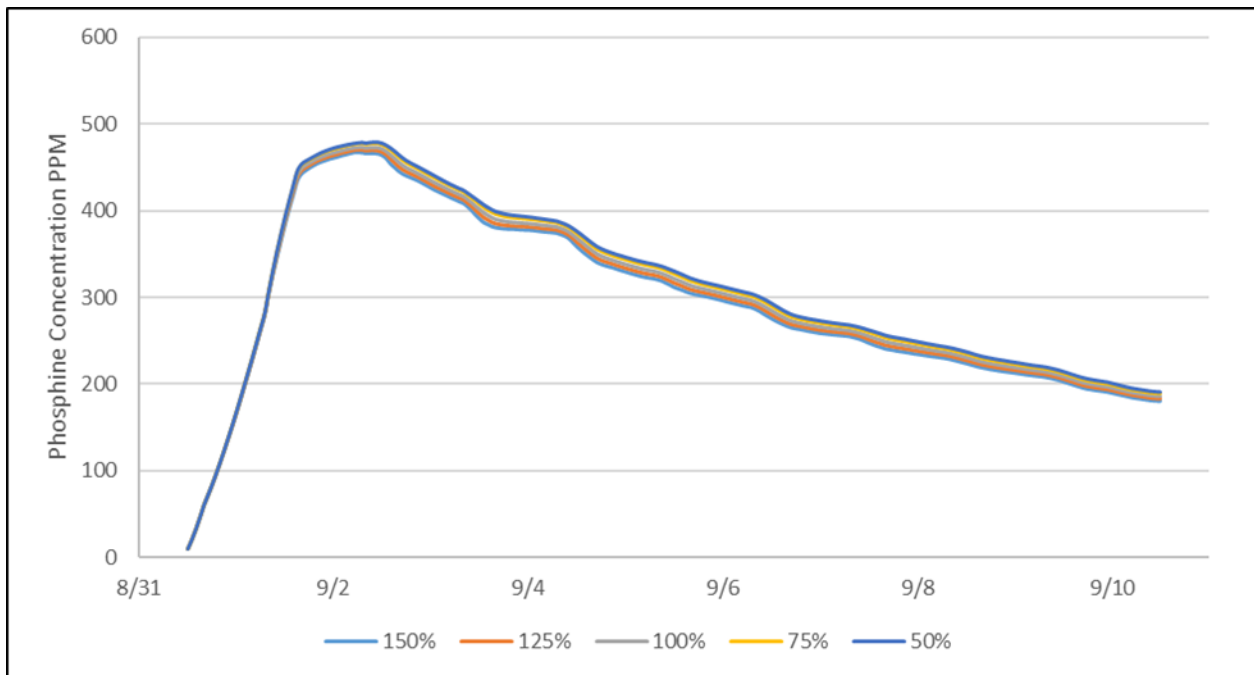


Figure 5:15 Overall average phosphine concentration (ppm) for five wind speeds, expressed as a percentage of the wind speeds (100%) used in the verification conducted between

August 31 and September 9, 2015, for the 1500 MT silo with a surface area to volume ratio of 0.45 m²/m³.

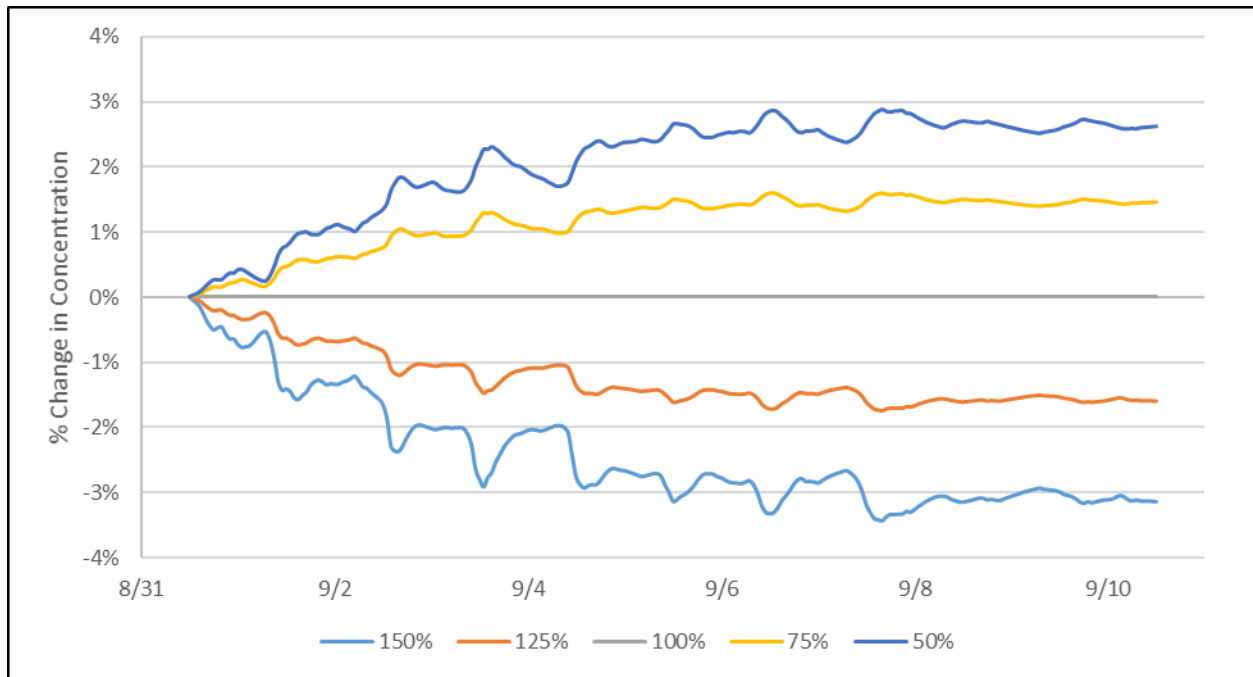


Figure 5:16 Change in overall average phosphine concentration (%) for five wind speeds, expressed as a percentage of the wind speeds (100%) used in the verification conducted between August 31 and September 9, 2015, for the 1500 MT silo with a surface area to volume ratio of 0.45 m²/m³.

The results of these simulations indicate that increases in temperature and wind speed cause increased fumigant loss. These results correspond with the mathematical predictions by Banks and Annis (1984), and with the results of Chayaprasert et al. (2015). These simulations also show that changes in temperature have greater impact on fumigant concentration than changes in wind speed over the conditions examined in this research. Chayaprasert also examined the relationship between these effects, and found that there was a greater wind speed effect than temperature effect. However, that result was seen most clearly in a trial using

constant wind speeds ranging from 4 m/s to 12 m/s. In the original weather data for the verification in Manhattan, Kansas, the peak wind speed recorded was 5.4 m/s, and wind speeds were only over 5 m/s for 2 hours over the course of the entire fumigation. Additionally, increasing wind speeds were shown to have an increasing effect, demonstrating the potential impact of high wind speed conditions. Therefore, the conclusion that temperature has a greater impact than wind speed on the weather conditions tested is not a direct contradiction of the finding by Chayaprasert et al. (2015) because the range tested was smaller than that tested in Chayaprasert et al. (2015).

Conclusions

The validated M-L-P 3D ecosystem model was successfully applied to investigate the sensitivity of fumigation efficacy as a function of ambient temperatures, relative humidity, and wind speed, recirculation rate, type of fumigant, and degree of silo seal. The key results are:

- Improving degree of seal in a poorly sealed silo has less impact on improving fumigant concentrations than reducing leakage rate in an already moderately well sealed silo. Reducing leakage rate to 50% and 75% increased fumigant concentrations by 111% and 36% compared to -21% and -34% for 125% and 150% leakage rate changes, respectively.
- Increasing fumigant recirculation rates resulted in decreased overall Ct-products. However, Ct-products did not increase proportionally in the most vulnerable areas of the silo (i.e., where the silo wall meets the headspace). The optimum recirculation rate was found around 37.5% of the original recirculation rate. By the end of the simulation,

average phosphine concentrations changed by 118%, 41%, -28%, and -47% for the 50%, 75%, 125%, and 150% recirculation rates investigated, respectively.

- Sulfuryl-fluoride concentrations (in kg/m³) were slightly lower than phosphine concentrations under the same conditions. Sulfuryl-fluoride sorbed less and moved more slowly due to its greater molecular weight. By the end of the simulation, sulfuryl-fluoride concentrations were predicted to be 6.1% lower compared to phosphine concentrations.
- Increasing temperature and wind speed decreased phosphine concentrations, with temperature changes having a more significant impact overall than wind speed changes. However, given the larger variability of wind effects and the greater impact of increasing wind speeds relative to temperature, high wind weather events such as thunderstorms have the potential for significant impact on phosphine concentrations. Changes in relative humidity had no effect in the closed loop fumigation system.
- Larger silos with smaller surface area to volume ratios dampened the impact of changing weather conditions on phosphine concentrations. This is an important consideration for farmers especially in Australia where thermosiphon fumigation of smaller hopper silos with larger surface area to volume ratios is common.

Chapter 6 - Modeling Post-Fumigation Desorption of Phosphine in Bulk Stored Grain

Introduction

Phosphine is a dangerous gas commonly used as a fumigant that is known to adsorb onto the surface of grain kernels during fumigation. It is important to understand the process of phosphine desorption in order to ensure safe handling of fumigated grain in silos and during shipments. Grain that has not fully released the phosphine it absorbed during fumigation may continue to desorb phosphine into the headspace of a railcar, shipping container, river barge, or ship hold, and the surroundings it is openly exposed to. If this happens at a different rate or quantity than expected, the grain storage or holding structure may continue to contain phosphine at a detectable level when it is believed to be free of fumigant. This can endanger people handling such grain as well as lead to shipping delays because grain must be below a certain fumigant concentration before safe handling and offloading. OSHA standards specify a long term exposure limit of 0.3 ppm (Occupational Safety and Health Administration, 1988), while the UK lists a short term handling limit of 0.28 ppm and a longer exposure limit of 0.14 ppm. The Australian government also advises a phosphine handling limit of 0.3 ppm. Exposure to residual phosphine in treated grain can also lead to dangerous working conditions because phosphine is toxic to humans. Inhalation exposure to phosphine gas liberated from aluminum phosphide fumigants presents risks of major morbidity and mortality.

While exposure to phosphine is not common, it is not a rare occurrence either, with 88 cases of illness from phosphine exposure reported in California between 1994 and 2005 (Fong et al., 2005). The symptoms of phosphine inhalation are nonspecific and transient, but can rapidly

become life-threatening (Sudakin, 2005). There is also limited data on the efficacy of therapeutic interventions (Sudakin, 2005) which make phosphine poisoning a potentially serious problem. As such, it is beneficial to gain a better understanding of the desorption rates of phosphine in bulk stored grain.

A report by the Plant Biosecurity Cooperative Research Center (Collins, 2009) states that grain stored above 12% moisture content should be aerated, but states no time requirement. The report also states that grain fumigated under 12% moisture content can remain sealed if not immediately needed. The Queensland Department of Agriculture and Fisheries (2010) recommends a venting time of 24 h, although no enforced regulation is cited. The degree to which this guideline is followed is unknown. In the U.S. context, the California Environmental Protection Agency states that grain should be vented after fumigation but provides no further guidelines (Gurusinghe, 2014).

Adsorption refers to chemicals that merely adhere to the grain surface, whereas absorption refers to chemicals that are drawn into the grain kernel. Sorption is used as a blanket term to refer to both processes. In many articles sorption values are calculated based on chemicals lost from the headspace above the product due to the relative ease of measuring gaseous concentrations (Daglish and Pavic, 2008; Darby, 2011; Dumas, 1980). Such investigations do not quantify the difference between phosphine adsorbed and absorbed due to the chosen method of measuring the value. For the purposes of this analysis, the primary interest is in the concentrations of fumigant in the interstitial air spaces. Therefore, the general term ‘sorption’ is used and literature that does not differentiate between adsorbed and absorbed chemicals can be used.

The Langmuir equation (Langmuir, 1918) models adsorption as a series of bonding locations on a surface under the assumption of an isothermal ideal gas. Some of these bonding sites will become filled, and some will remain empty. In the Langmuir model there are only a set number of bonding sites available. Once all bonding sites are filled there is no more adsorption, and because all bonding sites are considered equal, they are bound with the same energy amount. The BET or Brunauer, Emmett and Teller equation (Brunauer et al., 1938) is an extension of the Langmuir equation that describes multilayer adsorption. The BET equation applies the Langmuir equation to additional layers assuming that adsorption can continue infinitely and there is no interaction between layers. In the BET model, each subsequent layer is held more loosely than the one above it.

According to Banks (1986) and Dumas (1980), not all adsorbed phosphine molecules are held with the same strengths. Some are held loosely and some are held firmly. The loosely bound fumigant is lost quickly during desorption, while the firmly bound is held longer. This would seem to be consistent with the BET model of adsorption, i.e., multiple layers of molecules adsorbed with different amounts of energy. However, Dumas (1980) determined in phosphine sorption on wheat that the initial wave of desorption is consistently more than two orders of magnitude greater than the second wave of desorption.

The total amount of phosphine sorbed by wheat in experiments conducted by Dumas (1980) was around 10% for a range of concentrations, with longer phosphine fumigation times resulting in a greater amount of sorbed phosphine. After 8 days of fumigation with constantly supplied phosphine varying from 0.1 to 1.5 mg/L, the terminal concentrations were greater than 90% of the concentration supplied (Daglish and Pavic, 2008). The total chemisorbed phosphine recorded by Berck (1968) showed that the percent of total sorption was influenced heavily by

temperature and exposure time. The amount of sorption varied with temperature, moisture content, and the time of exposure. Whole wheat kernels at 12.5% moisture content that had been stored for 3 days had sorbed between 4.8% to 33.2% at 4°C and 35°C, respectively. Most of the adsorbed phosphine was desorbed within 4 days, but small amounts of desorption continued for many weeks, with 0.01 ng/g found after 35 days of aeration, and 0.004 ng/g still being found after 220 days of aeration (Dumas, 1980). Banks (1986) reported that detectable quantities of unchanged fumigant desorb over several weeks after a fumigation. Some phosphine is taken up irreversibly in chemisorption and not released (Banks, 1990). However, from these results, we can confirm that physisorption is the dominant type of sorption in phosphine fumigations on wheat under most cases, a conclusion also reached by Dumas (1980). This is a reasonable assumption because chemical reactions take time and energy inputs greater than physical adherence.

Applying higher dosages of phosphine during fumigation led to higher rates of desorbed phosphine with an upper limit around 4.5 µg of phosphine for 10 g of wheat (Dumas, 1980). For other fumigants such as ethylene dibromide, trichloroethylene, chloroform, and carbon tetrachloride, desorption was faster at cold temperatures than at warm temperatures. For example, ethylene dibromide residue left on corn after seven days was 1.7 g/m³ at 17°C and 5.6 g/m³ at 37°C, out of an applied 300 g/m³ (Bielorai and Alumot, 1975). A faster desorption from cooler wheat would provide the added benefit of using aeration to cool the grain and potentially ship earlier if desired. However, this conclusion is contradicted by Dumas (1980) who observed higher temperatures were shown to yield a faster, less complete desorption of phosphine. Dosage of phosphine did not have an effect on the percentage of phosphine recovered from wheat flour (Rauscher et al., 1972) where all desorption tests yielded greater than 98% recovery

with little change coming from higher phosphine application concentrations. Ultimately, 99% of the phosphine administered in the room temperature study was recovered. This demonstrates the low amount of chemically altered phosphine that was unrecoverable. Higher concentrations were shown to have had an effect in some experiments by Dumas (1980), who demonstrated a lower percentage of recovery with an increased phosphine exposure. The final phosphine concentration was never less than 90% of the dosage applied during the fumigation after 8 days (Daglish and Pavic, 2008). The daily percent losses ranged between 1 and 10% depending on initial phosphine dose and filling ratio (the proportion of the container that was filled with grain).

Hwaidi et al. (2015) stated that sulfuryl-flouride desorbs rapidly, and that there was no significant desorption of sulfuryl-flouride in their tests long term. Those consisted of aerating the grain in a fume hood for 10 minutes, and then storing it at 25°C and testing for sulfuryl-flouride daily for three weeks, and then monthly for 18 months. After the initial 10 minutes, sulfuryl-flouride readings remained below detectable levels. This indicates that investigating modeling of sulfuryl-flouride desorption is not useful and was thus not further pursued in this dissertation research.

In order to model phosphine desorption, analogous equations to the ones created for sorption would need to be generated. Unfortunately, there are relatively few literature sources focused on phosphine desorption compared with phosphine sorption. Dumas (1980) indicated that the quantity of desorbed phosphine depends on a number of factors. These include the concentration of phosphine applied and the length of time of the application. They arrived at the conclusion that longer exposures to phosphine caused deeper penetration into the grain, while during short exposure periods most of the phosphine was merely adsorbed to the surface.

The objectives of this research were to expand the M-L-P 3D ecosystem finite element model to investigate post-fumigation phosphine desorption, perform a silo scale experiment and use the experimental data to verify the expanded M-L-P model, and then apply the model to predict post-fumigation desorption of phosphine in bulk stored grain.

Materials and Methods

1. Changes to Sorption Model

In the previous chapter, estimates of the sorption loss were created using a baseline from the Daghli and Pavić (2008) equation relating phosphine concentration to fumigation time based on a 1 mg/L application as seen in Eq 4.1.

$$C = 1.5932 e^{-0.0416t} \quad \text{Eq 4.1}$$

Due to the increased concentrations of fumigant observed in the Lake Grace fumigation when compared to the fumigation by Cook (2016), it is more reasonable to use a baseline equation from Daghli and Pavić (2008) that is based on a 1.5 mg/L phosphine application. The most applicable baseline equation for this experiment is:

$$C = 2.4157 e^{-0.0319t} \quad \text{Eq 6.1}$$

Where,

C = fumigant concentration lost [mg/L]

t = time [days]

As in previous chapters, the time step for the simulations is one hour, not one day, and also uses concentration in kg/m³ instead of ppm, so after adjusting to proper units, the equation is:

$$C = 0.0024157e^{-0.0013t} \quad \text{Eq 6.2}$$

Where,

C = fumigant concentration lost [kg/m³]

t = time [h]

The fumigation concentrations listed by Daghli and Pavic (2008) is the value of the concentration in the flask, not the loss of phosphine. So, to calculate the amount of phosphine lost due to sorption, the derivative of Eq 6.2 must be calculated:

$$C = 0.0000032e^{-0.0013t} \quad \text{Eq 6.3}$$

Eq 6.3 represents the updated equation for the new baseline, analogous to Eq 4.3 previously described. The next step is to apply the temperature and moisture content factors. As only the base equation was changed, these factors will be the same as previously calculated in Appendix 4.1 and Appendix 4.2. When combined with the other factors used previously, namely temperature and moisture content, the new equation is:

$$C = 0.0000032e^{-0.0013t} * 0.13365e^{0.0805T} * 0.067e^{0.235MC} \quad \text{Eq 6.4}$$

Where,

C = fumigant concentration lost [kg/m³]

t = time [h]

T = temperature [°C]

MC = moisture content [% dry basis]

2. Desorption Modeling Strategies

The 3D ecosystem model developed by Lawrence and Maier (2011) and expanded in this dissertation was used to investigate the effects of desorption following a fumigation event. In the absence of conclusive and appropriate experimental data for estimating desorption two different methods of calculating fumigant desorption were tested. Case 1 was based on the assumption that fumigant desorption is analogous to fumigant sorption in the reversed direction, and that 100% of sorbed phosphine will eventually desorb back into the interstitial air space. In order to accomplish this, the phosphine sorption equations previously calculated are used but instead of removing fumigant from the interstitial air space and assigning it to the grain mass, fumigant is removed from the grain mass and returned to the air. This process continues at each node in the simulation until all phosphine is released. In Case 2 two coupled ordinary differential equations were used that describe an equilibrium of phosphine concentration between the grain mass and interstitial air space. These equations were developed in Darby (2008) and were used in the Fluent modeling approach by Isa et al. (2016). All constants required for the equations are given in Darby (2008).

$$\frac{dc}{dt} + \frac{ssorpkf}{Bfill} c - \frac{ssorpkf}{BfillF} C = 0 \quad \text{Eq 6.5}$$

$$\frac{dC}{dt} - \frac{ssorpkf}{1-\epsilon} c + \frac{ssorpkf}{(1-\epsilon)F} C + kbindC^N = 0 \quad \text{Eq 6.6}$$

Where,

Bfill = constant determined by filling ratio and porosity

C = fumigant concentration in grain [g/m³]

c = fumigant concentration in air [g/m³]

F = partition factor, 0.196

kbind = 0.0344

kf = linear mass transfer coefficient

N = 0.76

ssorpkf = 0.0153

t = time [h]

ε = porosity of the grain

3. Model Verification

Experimental results for post-fumigation venting were obtained from a fumigation experiment conducted in Lake Grace, Western Australia from April 12 through April 20, 2016 with post-fumigation venting taking place on April 20 and 21. The fumigation was conducted in a Bird's brand well-sealed (pressure half loss time greater than 5 minutes) 100-ton hopper-bottom wheat silo. Concentration readings were taken approximately hourly during week days

between 7 am until around 6 pm. During periods of venting, readings were taken approximately every half hour. Readings were taken with a DragerSensor XXS PH3HC brand chemical monitor, with a stated measuring range of 1-2000 ppm and a resolution of 1 ppm through tubes that were run into the grain mass. Concentrations were measured in a vertical column down the center of the grain mass in the headspace, 0.5m, 1.5m, and 3m below the grain surface, as well as 0.5m from the wall of the silo 7m below the grain surface, in the North, East, South, and West directions. Venting was carried out with an aeration fan blowing vertically through the grain mass and out the opened top hatch of the silo. After phosphine readings dropped below the 1 ppm detection limit in some parts of the silo, venting stopped and the silo was closed. This cycle was repeated three times for a total of approximately 7 hours of silo venting.

Weather data was collected for April 12 through April 21, 2016 from the Australian Bureau of Meteorology Climate data services. Weather data was available hourly from the nearby town of Newdegate, Western Australia. Hourly solar radiation data was more difficult to acquire because no nearby weather stations recorded solar radiation hourly. In order to account for latitude, a station at Adelaide airport was chosen over the nearest station in Broome, Western Australia.

Results and Discussion

1. Experimental Results

Table 6.1 shows phosphine concentrations at all reading points from the beginning of silo venting until the completion of the experiment. Due to the well-sealed silo, phosphine fumigant

readings were maintained at more than 1000 ppm at all reading locations until the end of the fumigation. During venting, phosphine concentrations decreased rapidly, with results first noticeable near the bottom of the silo (i.e., North, West, South, East) and to a lesser degree in the headspace. The decrease in phosphine concentration due to the venting process begins in the lowest portion of the grain mass and works its way up the silo. The drop in concentrations is faster at the radial points away from the center of the silo. For most of the venting and holding periods, phosphine concentrations are highest in reading locations that are closest to the center of the grain mass, i.e., the one that is 3m below the grain surface. This is true despite the fact that the concentration at 3m begins dropping before the concentrations in the headspace and at 0.5m. For example, the 3m location is the lowest from 7:30 am to 9:15 am, but is often the highest throughout the rest of the experiment, the most notable exception being 1 pm on April 20. Evidence of phosphine desorption was observed, with the average silo concentration across all reading locations increasing from 10.25 ppm to 38.25 ppm during the first holding period (11:45 am to 3 pm on 4/20/16). During the second holding period, concentrations increased from an average of 6.13 ppm at 6 pm to an average of 35.13 ppm at 8:30 am the next morning. Both of these increases were far higher than the 0.3 ppm handling limit for phosphine and would have created an unsafe environment had grain been cleared for handling. While the venting procedure in this experiment did not meet the 24 h venting standard advanced by the Queensland Department of Agriculture and Fisheries (2010), the previous recommendation was only that aeration be used if moisture content was above 12% (Collins, 2009). It is also possible that a farmer or grain handler may have decided to end the venting cycle as soon as two hours and fifteen minutes after the start of the venting (9:45 am), as concentrations near the edge of the silo (West and South locations) were below detectable levels with handheld monitors. Such a

decision could have resulted in the grain maintaining phosphine concentrations well above acceptable limits.

Table 6:1 Experimental phosphine concentrations (ppm) in the silo headspace and 0.5m, 1.5m, and 3m below the grain surface in the core of the grain and at the North, West, South, and East locations in the grain mass 7m below the grain surface for periods of venting (bolded) and periods of sealed holding (not bolded) after conclusion of a fumigation in Lake Grace, Australia, April 20-21, 2016.

	Headspace	0.5m	1.5m	3m	North	West	South	East
4/20/16 7:30	1630	1600	1530	1500	1650	1190	1090	1250
4/20/16 8:15	446	1510	1500	1430	50	19	21	34
4/20/16 8:45	370	1330	1190	1250	23	12	12	13
4/20/16 9:15	252	370	107	216	6	5	5	6
4/20/16 9:45	27	69	64	82	3	0	0	2
4/20/16 10:15	16	46	45	58	2	0	0	3
4/20/16 10:45	14	32	29	51	2	0	2	3
4/20/16 11:15	11	27	24	28	2	0	2	2
4/20/16 11:45	10	21	20	25	2	0	2	2
4/20/16 13:00	25	57	70	19	19	14	14	15
4/20/16 14:00	20	48	50	50	27	18	20	21
4/20/16 15:00	27	48	55	58	37	26	26	29
4/20/16 16:00	25	38	47	34	45	23	29	34
4/20/16 17:00	18	35	28	47	0	0	0	0
4/20/16 18:00	3	14	10	18	0	0	0	0
4/20/16 20:00	7	15	16	21	6	3	0	4

4/21/16 7:30	31	35	42	53	42	32	34	36
4/21/16 8:30	32	36	36	37	37	34	34	35
4/21/16 9:00	17	31	34	36	0	0	0	0
4/21/16 9:30	9	32	16	28	0	0	0	0

2. Validation Results

The validation results for both desorption modeling cases (Case 1, reversed sorption equations and Case 2, equilibrium differential equations developed in Darby, 2008) are presented in Figures 6.1-6.2. The Case 2 simulation over predicted phosphine concentrations in the first holding period (12 pm to 3 pm April 20), while Case 1 under predicted phosphine concentrations during that period. Both simulations under predicted phosphine concentrations at the end of the second holding period (6 pm April 20 to 8:30 am April 21). During the first holding period, average concentrations were 28.8 ppm, 11.2 ppm, and 71.2 ppm for the experiment, Case 1, and Case 2, respectively. During the second holding period, the average concentrations were 9.0 ppm, 1.1 ppm and 16.2 ppm, respectively. The Case 1 simulation showed phosphine concentrations that increased continually throughout the holding periods. In Case 2, however, the phosphine concentration increased immediately after venting, and then slowly decreased over the storage period due to silo leakage. The experimental data show a trend that more closely resembles that of Case 1, with phosphine values increasing slowly during venting periods.

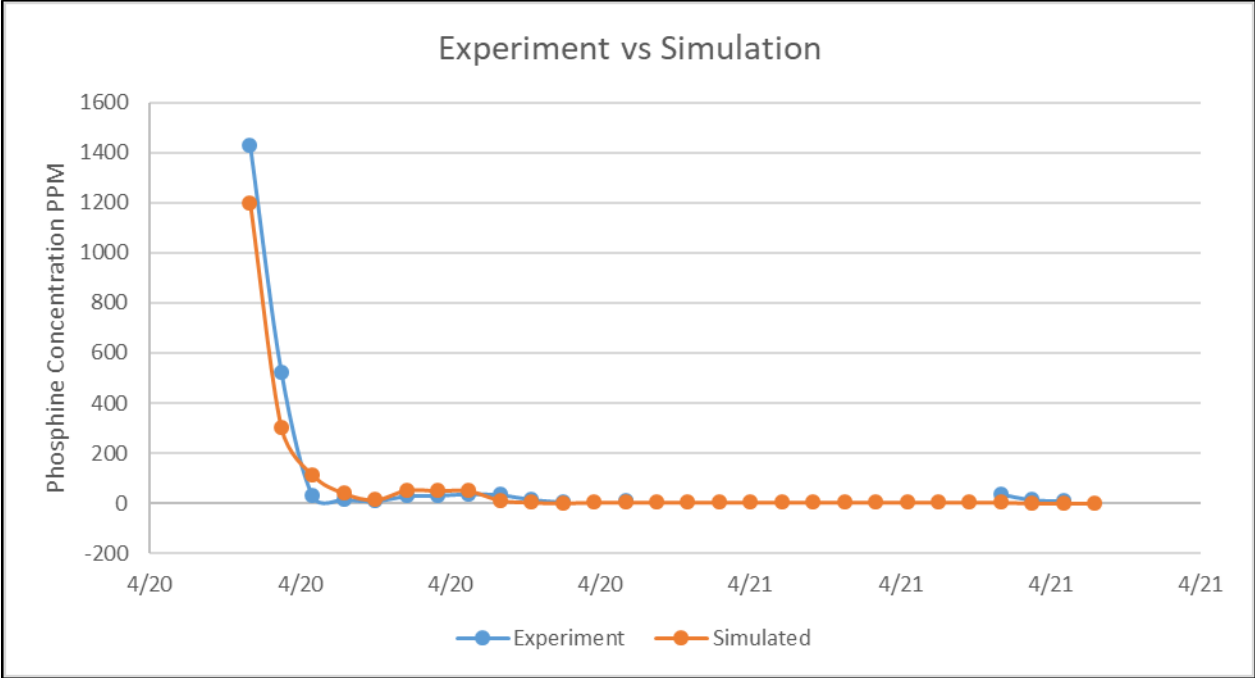


Figure 6:1 Experimental and predicted phosphine concentrations (ppm) for a reversed sorption equation model (Case 1) after conclusion of a fumigation in an 80 ton wheat silo located in Lake Grace, Australia, April 20-21, 2016.

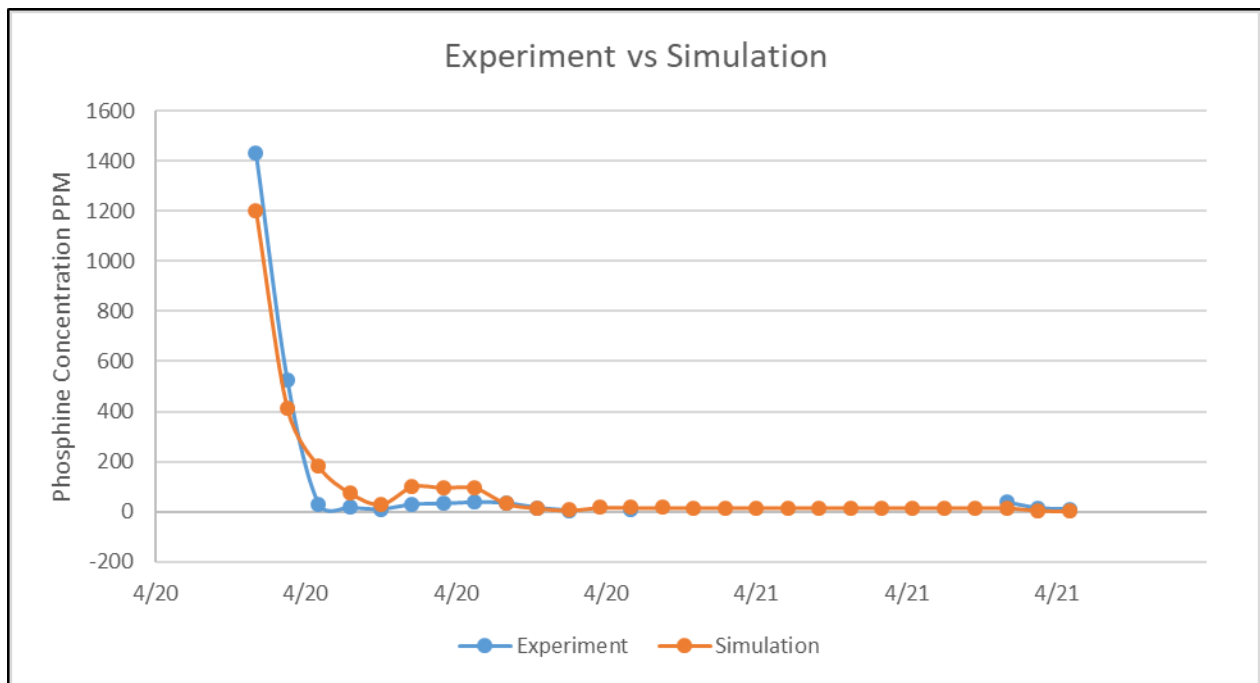


Figure 6:2 Experimental and predicted phosphine concentrations (ppm) for an equilibrium differential equations sorption model (Case 2) after conclusion of a fumigation in an 80 ton wheat silo located in Lake Grace, Australia, April 20-21, 2016.

A comparison of the two simulations with the experimental results at lower concentrations is shown in figure 6.3. In the experiment and with the Case 2 simulation, the final phosphine concentrations were greater than the exposure limit of 0.3 ppm, but Case 1 was below the limit. The final experimental reading was an average of 10.6 ppm, while Case 1 had an average of 0.17 ppm and Case 2 an average of 2.4 ppm. Over the course of a 13 h period simulated after the end of the experimental values, however, the average concentration in the Case 1 simulation exceeded the safe handling limit, ending at 0.9 ppm, compared to 5.4 ppm for Case 2. Overall, Case 2 provided the more accurate prediction of experimental results as seen in figure 6.3, with an average % error of -89.5% compared to the average % error of 86.3% in Case 2. The absolute values of the % error for Case 1 and Case 2 were 89.5% and 121.3%,

respectively. Overall, however, both models demonstrated errors that are large in comparison to the fumigation validation results. The increased error is a reflection both of the increased complexity of the desorption process and the relative lack of literature on the topic to reference.

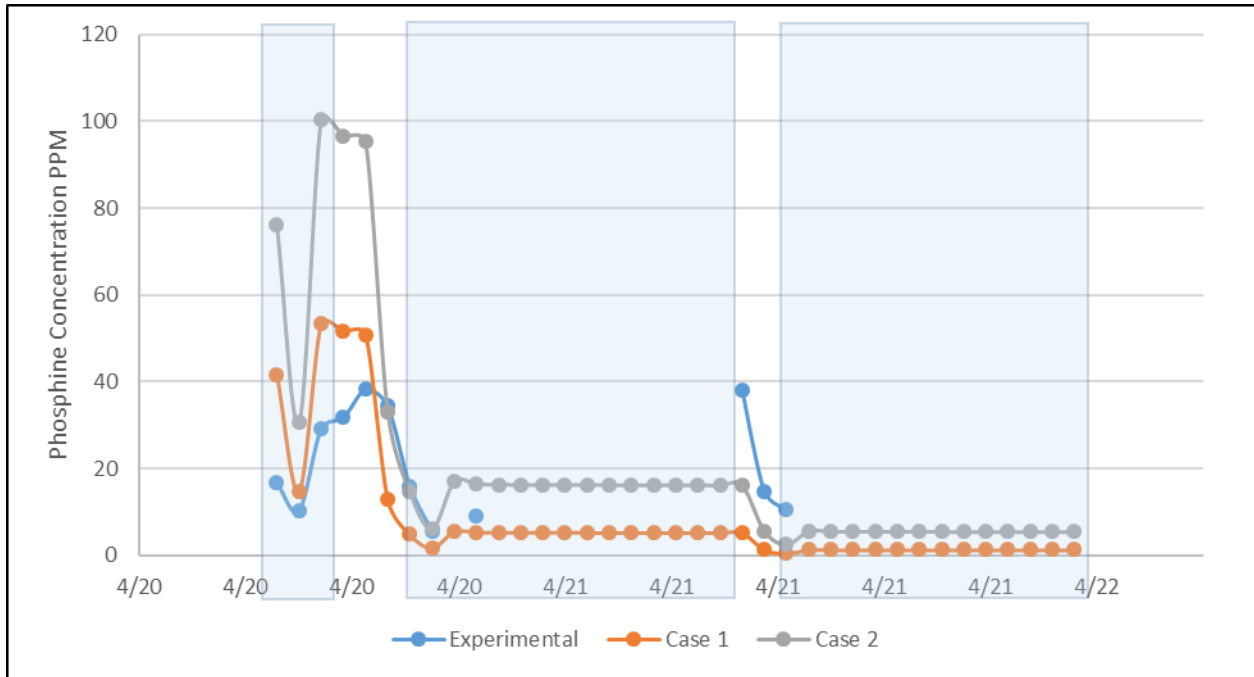


Figure 6:3 Experimental and predicted phosphine values (ppm) for Case 1 and Case 2, 2h after conclusion of a fumigation in an 80 ton wheat silo located in Lake Grace, Australia, April 20-21, 2016. Periods without venting are shaded.

For Case 1, the assumption was made that desorption occurs at the same rate as sorption, but in the reversed direction. The use of the reversed sorption equation (Case 1) generated results with trends that were consistent with the trends of the experimental data. In Case 1 it was assumed that all of the sorbed phosphine would eventually desorb, yet at the end of the simulated Case 1 fumigation, only 5 ppm of the 23.3 ppm sorbed into grain had been desorbed. If the simulation had continued until all of the phosphine had desorbed, the result would be a

phosphine concentration greater than that of Case 2, and much higher than the safe handling limit. The fact that significant quantities of phosphine remain in the grain mass makes a direct comparison between the predictions of Case 1 and Case 2 simulations difficult. Additionally, given the under predicted phosphine concentrations from the experimental data and a continual increase in concentration at the end of the simulation, it appears that the assumption that the desorption rate for phosphine is the same as the sorption rate is a poor assumption. The Case 1 model would have predicted the experimental results more accurately and resulted in a closer comparison with the Case 2 model had the same sorption relationships been used but with a faster desorption rate.

For Case 2, the differential equations from Darby (2008) were developed for sorption environments based on an equilibrium model between the grain and interstitial air. Due to their form they should have been well suited to model desorption without the need for additional assumptions. However, the Case 2 simulations did not match the overall trends as well as the Case 1 simulation during the holding phases, as previously mentioned, because there was no time component to the trends. During both holding phases, the experimental data showed phosphine concentrations gradually increasing after the silo was sealed, whereas the Case 2 estimated phosphine concentrations reached a relative maximum immediately. The Case 2 predictions were, however, more accurate in predicting concentrations than Case 1 starting from the second venting phase.

3. Improving Case 1 Desorption Equation

The evidence discussed in the previous section demonstrated that the Case 1 approach predicted more accurate trends than Case 2, but that the assumption that the governing equation

was the same for sorption led to inaccuracy because the fumigant concentrations were too low shortly after desorption. Thus, the grain presumably retained fumigant long after the simulation was complete. Based on these observations, a higher rate of desorption would better match the experimental data and the values from the Case 2 simulation, as well as liberate more of the phosphine from the grain faster, allowing for a more direct comparison with the Case 2 venting times. For this reason, simulations were conducted for the Case 1 desorption model in which the desorption equation was multiplied by a constant factor in order to speed up desorption. After several simulations in which the desorption equation was multiplied by a constant, a multiple of 10 best reproduced the experimental values. The results of this simulation are shown in figures 6.4 and 6.5.

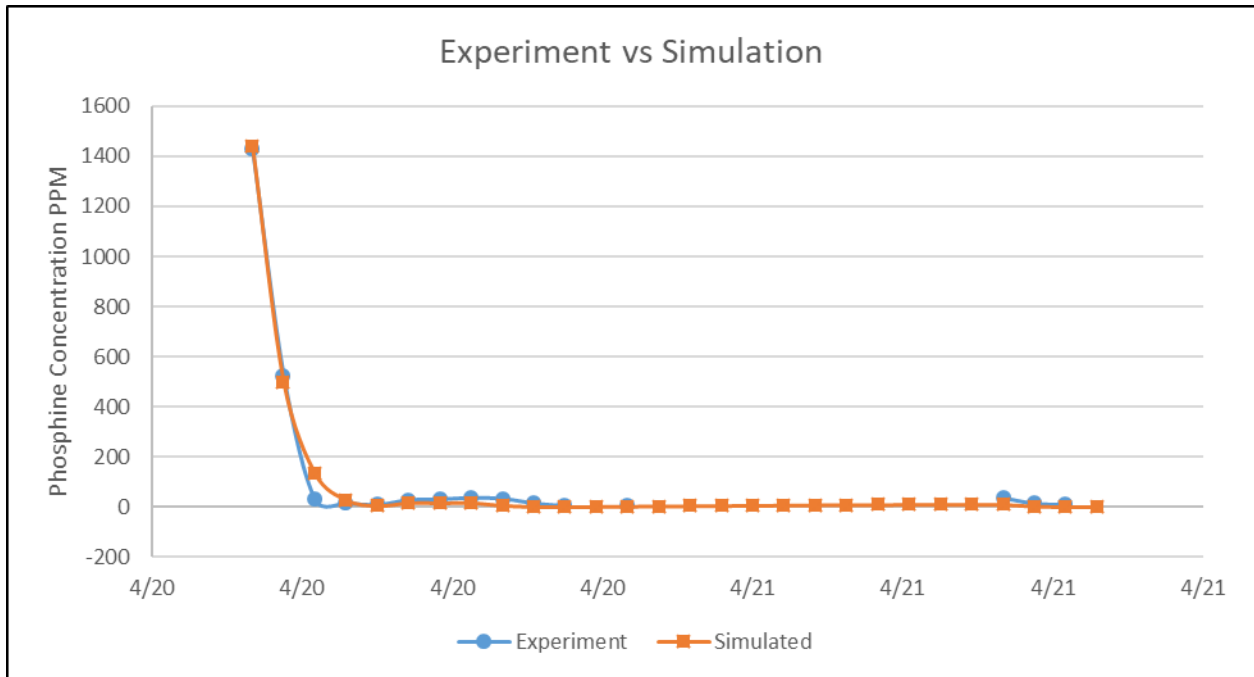


Figure 6:4 Experimental and predicted phosphine concentrations (ppm) for a reversed sorption equation model with a 10x multiplier for desorption rate (Modified Case 1) after conclusion of a fumigation in an 80 ton wheat silo located in Lake Grace, Australia, April 20-21, 2016.

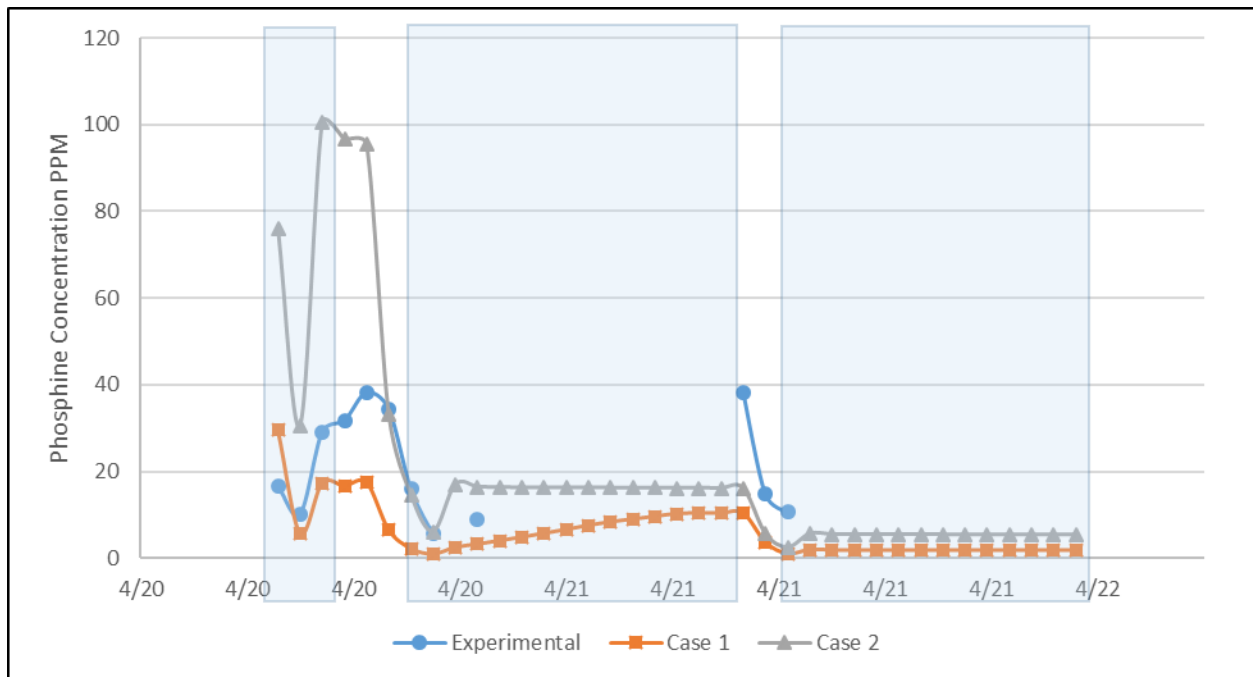


Figure 6:5 Experimental and predicted phosphine values (ppm) for Modified Case 1 and Case 2, 2h after conclusion of a fumigation in an 80 ton wheat silo located in Lake Grace, Australia, April 20-21, 2016. Periods without venting are shaded.

In this simulation, the final phosphine concentration in the modified Case 1 was above the safe handling limit, as was the experimental data and the Case 2 simulation. The final experimental reading was increased to 0.97 ppm, an increase of 0.17 ppm from the original Case 1 simulation. Overall, the modified Case 1 provided the more accurate prediction of experimental results as seen in figure 6.5, with an average percent error of -55.5% compared to the average percent error of 86.3% in Case 2. The absolute values of the percent error for Case 1 and Case 2 were 68.4% and 121.3%, respectively. While Case 1 predicted values that were closer overall to the experimental values, an under prediction of phosphine values is more troubling when making conclusions about safety procedures than an over prediction. While the phosphine values for the modified Case 1 simulation are still too low, this modification increased

the accuracy of the simulation. Additionally, the modified Case 1 simulation further highlighted trends that were missing in the Case 2 simulation. For instance, the continual increase during the second holding period is clearly seen in the modified Case 1 simulation, increasing from 0.9 ppm to 3.2 ppm over the first 2 h, and then from 3.2 ppm to 10.4 ppm over the next 12 h. For comparison, the Case 2 simulation increased from 6.1 to 16.9 in the first hour after closing the silo, and then decreased slowly over the remainder of the holding period. The experimental simulation increased from 5.6 ppm to 9.0 ppm over the first 2 h, then from 9.0 to 38.1 ppm over the next 12.

4. Fumigation Safety Simulations

Table 6.2 summarizes to what extent venting was predicted to be successful or not to meet certain Australian and U.S. fumigation safety requirements. The U.S. results were obtained by inserting a venting and holding phase in the last day of the validated U.S. fumigation conducted in the silo fumigated in Manhattan, Kansas, from Aug 31 to Sept 9, 2016, which was discussed in objective 2. The Lake Grace, Australia, and Manhattan, Kansas fumigations were examined by simulating a continuous venting strategy of 24 h in line with the guidelines from the Queensland Department of Agriculture and Fisheries (2010), a 7 h venting strategy in line with experimental results but without multiple phases, and a 3 h venting strategy in order to simulate minimum venting based on the recommendations of Collins (2009) and Gurusinghe (2014), who recommended venting but did not specify a time period. While there was a difference between the U.S. and Australian fumigations, there was also a noticeable difference between the predictions of Case 1 and Case 2. The most notable differences between prediction methods

came for predictions of 7 h venting times. In the Australian simulation, both versions of the model predicted unsafe conditions, but Case 1 predicted maximum concentrations of 13.1 ppm compared to only 1.5 ppm for the Case 2 simulation. In the U.S. case, the 7 h venting time yielded maximum concentrations of 10.0 ppm in Case 1 and 0.04 ppm in Case 2. Case 1 fumigations were unsuccessful for the 7 h and below venting times. Case 2 had a similar overall outcome, with the only safety disagreement between the two simulations appearing in the U.S. silo that was vented for 7 h. Case 1 simulations predicted higher residual phosphine concentrations than Case 2 simulations under all conditions except the Australian simulation with only 3 h of venting. The resulting simulations predicted that phosphine levels with the 24 h venting time would have been judged safe under both simulations and in both locations.

Table 6:2 Overall safety analysis with Safe (average phosphine concentration less than 0.3 ppm at conclusion of simulation) and Not Safe (average phosphine concentration more than 0.3 ppm at conclusion of simulation) based on fumigations performed in Lake Grace, Australia, April 12-21, 2016 (Australian Simulation) and Manhattan, Kansas between August 31 and September 9, 2015 (U.S. Simulation) (Cook 2016).

Simulation	Conclusion
Australian Experiment with 7.25h venting time	Not Safe; 10.6 ppm average
Australian Simulation Modified Case 1 with 3h venting time	Not Safe; Up to 81.6 ppm
Australian Simulation Case 2 with 3h venting time	Not Safe; Up to 128.8 ppm
Australian Simulation Modified Case 1 with 7h venting time	Not Safe; Up to 13.1 ppm
Australian Simulation Case 2 with 7h venting time	Not Safe; Up to 1.5 ppm
Australian Simulation Modified Case 1 with 24h venting time	Safe, Below 0.06 ppm
Australian Simulation Case 2 with 24h venting time	Safe; Below 0.0001 ppm
U.S. Simulation Modified Case 1 with 3h venting time	Not Safe; Up to 33.1 ppm
U.S. Simulation Case 2 with 3h venting time	Not Safe; Up to 16.1 ppm
U.S. Simulation Modified Case 1 with 7h venting time	Not Safe; Up to 10.0 ppm
U.S. Simulation Case 2 with 7h venting time	Safe; Below 0.04 ppm
U.S. Simulation Modified Case 1 with 24h venting time	Safe; Below 0.002 ppm
U.S. Simulation Case 2 with 24h venting time	Safe; Below 0.000000042 ppm

The major difference between the U.S. and Australian case studies was how well sealed the Australian silo was (pressure half loss times greater than five minutes), leading to phosphine

concentrations much higher than were found in the fumigation in Manhattan, Kansas, (maximum concentration recorded of 1,700 ppm vs 510 ppm). The higher phosphine concentration achieved in the Australian experimental fumigation, and the length of time that concentration was maintained in contact with the stored grain mass resulted in a greater amount of sorption to occur. For both desorption cases modeled, this increase in sorption caused a corresponding increase in time required for desorption. This result indicates the influence of factors such as maximum fumigant concentration and length of fumigation. With the continued spread of phosphine resistant insects, grain fumigators will resort to utilizing higher phosphine concentrations and longer exposure times to kill all insect life stages. This decision would result in increased phosphine desorption time from the grain mass, and thus would require longer venting times to achieve safe levels for handling grain post-fumigation.

In order to further explore the necessary venting times required for fumigations, the fumigation in Lake Grace, Australia, was tested under five different venting times with four different pressure half loss times under both simulation cases. The results for desorption Modified Case 1 are listed in table 6.3, and those for desorption Case 2 are listed in table 6.4. Both tables list results as the greatest average concentrations obtained in the first 24 h after venting. Modified Case 1 consistently predicted higher phosphine values than Case 2, with the highest concentration found in Case 2 (1.1 ppm) lower than the Case 1 values for 8, 10, and 12h of venting at each pressure half loss time. This agrees with previous results shown in table 6.2.

Table 6:3 Maximum average phosphine concentrations (ppm) post-venting for fumigations with four pressure half loss times (30 s, 1 min, 3 min, and 5 min) and five venting times (8h, 10h, 12h, 18h, and 24h) under simulation Modified Case 1 (reversed sorption model) based on fumigation performed in Lake Grace, Australia from April 12-21, 2016.

	8h	10h	12h	18h	24h
30 s	11.0	9.8	8.3	2.8	0.043
1 min	11.8	10.2	8.6	2.9	0.05
3 min	12.2	10.5	8.9	3.0	0.059
5 min	12.2	10.6	9.0	3.0	0.059

Table 6:4 Maximum average phosphine concentrations (ppm) post-venting for fumigations with four pressure half loss times (30 s, 1 min, 3 min, and 5 min) and five venting times (8h, 10h, 12h, 18h, and 24h) under simulation Case 2 (Equations from Darby, 2008) based on fumigation performed in Lake Grace, Australia from April 12-21, 2016.

	8h	10h	12h	18h	24h
30 s	0.59	0.099	0.019	0.00053	0.000015
1 min	0.70	0.109	0.021	0.00065	0.000019
3 min	0.96	0.13	0.022	0.00062	0.000017
5 min	1.10	0.14	0.028	0.00055	0.000015

For both desorption cases, maximum average phosphine concentrations after completion of silo venting are lower for longer periods of venting. Maximum average phosphine concentrations after completion of silo venting are also lower for fumigations with lower pressure half loss times, although there are exceptions. Decreases in maximum average phosphine concentration with increasing pressure half loss time are seen Case 2 at the highest venting times (18h and 24h). Under both cases, these increases occur at phosphine concentrations well below the safe handling limit of 0.3 ppm. Additionally, differences are small enough that they may be the results of rounding errors in model calculations. Under both prediction cases, the 24h silo venting recommendation by the Queensland Department of

Agriculture and Fisheries (2010) was sufficient to lower phosphine concentrations to safe handling levels independent of the pressure half loss time. Case 2 simulations indicate that safe handling levels had been achieved after only ten hours of venting. After 12 h of venting, Case 2 predicted phosphine levels more than an order of magnitude lower than the hazardous limit for all pressure half loss times tested. These results indicate that the 24 h venting guideline may be more strict than is necessary to guarantee worker safety under the Case 2 predictions, although the Case 1 simulations suggest the longer venting times are needed. Under the Case 1 equations, however, the fan venting time is not as important as the desorption time, and a similar venting effect could have been achieved under fewer fan run hours. If the aeration fans had been run long enough to achieve one complete air exchange through the silo, and then the silo was left at rest for 24 h, at which time the fans were turned back on long enough to run one more complete air exchange through the silo, full venting would still be achieved despite lower fan run times.

Ultimately, these results indicate the importance of following guidelines for the venting of fumigated grain. A minimum number of hours of forced fan venting are required to achieve phosphine concentrations below 0.3 ppm so that the grain is safe to handle. The reports which indicate that grain should be vented but provide no guidelines for minimum length of ventilation (Collins, 2009; Gurusinghe, 2014) are not sufficient and may endanger grain handlers. Both the experimental and simulated results demonstrate that phosphine readings taken at a single point or a single time may be misleading to the fumigator or grain handler who may incorrectly conclude that safe phosphine levels have been reached. These results underline the importance of specific guidance on minimum venting times in grain handling standards to ensure worker safety, especially considering fumigant sorption and quality of silo seal. There is a necessity for continued research in order to better understand fumigant desorption and more closely identify

associated venting times in order to assure minimum venting times. In particular, a baseline equation of the form developed for sorption by Daglish and Pavic (2008) would be useful in determining the impact of fumigant sorption. A baseline equation of the kind used for sorption would have been particularly helpful in improving the simulation of Case 1, which had trends that were in some ways more accurate than Case 2.

Conclusions

An experimental fumigation trial that included monitoring fumigant venting and holding grain was conducted in Lake Grace, Australia. The M-L-P 3D ecosystem model was modified to include two estimates for phosphine fumigant desorption. Both approaches were validated using the experimental data. Simulations were conducted to test minimum times of post-fumigation grain venting to reach phosphine desorption levels below 0.3 ppm that are considered safe for handling grain. The key results are:

- The sealed silo showed phosphine concentration increases during two consecutive periods after venting, resulting in 28 ppm and 29 ppm increases, respectively.
- Simulations were able to reproduce overall desorption trends, but consistently over predicted initial desorption values and under predicted desorption values after the second period of venting.
- Two equations estimating fumigant desorption were tested, with an average of -55.5% error for Case 1 (reversed sorption equations) and 86.3% error for Case 2 (equations from Darby, 2008).

- The assumption that desorption rate was the same as sorption rate proved to be inaccurate. The simulation analysis indicated desorption rate was 10x as large as the sorption rate. As a result, the initial Case 1 approach was modified accordingly.
- Simulations with Modified Case 1 equation indicated that a 3 h or 7 h venting periods were not sufficient in either the U.S. or Australian context. Further investigation under the Australian context showed that 8 h, 10 h, 12 h, and 18 h venting times were insufficient but a 24 h venting time would have been sufficient to reduce phosphine concentrations below 0.3 ppm for the safe handling of grain post-fumigation.
- Simulations with the Case 2 equation indicate that the 3h or 7h venting periods were not sufficient in the Australian context, but the 7 h venting period would have been sufficient in the U.S. context. Further investigation under the Australian context showed that 8 h, venting times were insufficient but 10 h, 12 h, 18 h, and 24 h venting times would have been sufficient to reduce phosphine concentrations below 0.3 ppm for the safe handling of grain post-fumigation.
- Given the incomplete and somewhat contradictory literature and grain handling standards in the U.S. and Australia, there is a need for additional research into fumigant desorption and venting of post-fumigation grain to achieve levels safe for grain handling, especially when considering higher gas concentrations, longer exposure times, and better sealed silos to overcome phosphine resistance in stored product insects.

Chapter 7 - Contributions and Model Improvements

Introduction

The original M-L 3D ecosystem model was substantially expanded by this dissertation research. This chapter will summarize the key contributions and how they were coded, as well as the limits of their application and the future work needed to address them. A user guide on how to run the code and make modifications in the code and then compile it in order to use it in different size silos and with historic weather data from different geographic locations is being developed separately.

Numerical Solver Improvements

The first key contribution was to change the technique used in the numerical solvers in order to increase speed and reliability of the code. The finite element method requires a system of equations that describes the governing equations (conservation of mass, conservation of energy, conservation of momentum) to be solved for each time step in the simulation. To achieve this, the equations are modified into a matrix of coefficients and a matrix of variables and solved using the techniques of matrix mathematics. The original code provided by Lawrence (2010) used an LU decomposition solver that was not producing accurate results in preliminary chemical movement simulations. The LU solver takes the coefficient matrix, which will be referred to as A , and decomposes it into a lower triangular matrix and an upper triangular matrix. From this decomposition, forward and backward substitution can be used to solve the system of equations. This was replaced with an iterative solver and as a failsafe, the more stable PLU solver was added to replace the LU solver. The PLU solver is very similar to the LU solver except partial pivoting is performed, in which the matrix is transformed in order to make it easier

to compute. This is done to assure the diagonal entry of $A(i,i)$ is the largest in magnitude of column i . This makes the PLU solver more stable than the LU solver which makes computing easier due to negative instead of positive feedback. Both the LU and PLU solvers are fixed cost solvers, in that the same amount of computation goes into solving the matrix regardless of whether it is sparse or not. Due to this restraint, Gauss-Seidel solvers were implemented but were not completely successful. After exploring the Gauss-Seidel solver, the code was modified with other iterative solvers, such as the Biconjugate Gradient Stabilized method with L-steps of GMRES (Generalized Minimum Residual), or `Bi_CG_Stab_L`.

`Bi_CG_Stab_L` is the work horse of the linear solvers used. `Bi_CG_Stab_L` is an iterative solver that uses the last known solution as a starting point to solve the new system of equations. This solver makes use of a sparse system of equations. Thus the first step is to convert $A(i,j)$ into the three vectors $R(k) = i$, $C(k) = j$, and $V(k) = A(i,j)$ where k ranges from 1 to the number of non-zero entries in A . This allows the solver to make use of sparse matrix-vector multiplication, which resulted in a substantial speed up in the code. The solution is then found to a given relative error tolerance ($1e-5$ for 32-bit operations and $1e-10$ for 64-bit operations, Visual Studios allows for either format). `Bi_CG_Stab` is similar to `Bi_CG_Stab_L` but does not include the L steps of GMRES. Additionally, there is also an ordinary differential equation solver module that makes use of the following methods; RK45 (same as the one used in MATLAB's ODE45), and the TR-BDF2 (half step using trapezoidal method then uses BDF2 method to finish the step). Both of these methods are adaptive step solvers, meaning that the solvers calculate an error term and adjust the time step used. With these solver methods, the code was able to compile faster and correctly operate the chemical movement simulations.

Insect Modeling

A second key contribution was the implementation of an insect model which was derived from Driscoll et al. (2000). This mathematical model differs from the Throne (1994) insect model used in previous versions of the code which was a biological-based model. This mathematical model was easier to code because it condenses the insect model into a clear governing equations. It also allows for easy modification of variables. For example, while the Throne (1994) model was only applicable to the maize weevil (*Sitophilus Zeamais*), the model based on Driscoll et al. (2000) can be applied to four additional insect species (i.e, *Rhyzopertha Dominica*, *Sitophilus Oryzae*, *Oryzaephilus Surinamensis*, *Tribolium Castaneum*). A limitation of this mathematical model is that it can only calculate population growth rates as an aggregate and cannot differentiate between life stages of the insect (i.e, eggs, larvae, pupae, adults). This mathematical model also calculates percentage change of insects, rather than the overall number. As insect population limits are often given in terms of the number of live insects per kg, the ability of this model to make specific predictions is based on the degree of initial infestation specified.

Additionally, neither the biological nor the mathematical model can account for insect movement within the grain mass or into or out of the grain silo. The code is sufficiently flexible to handle insect introductions, native populations, and movement within the grain silo, but useful equations to govern these phenomena have not yet been identified. The successful implementation of those additional components would enable a more comprehensive analysis of insect populations in a stored grain mass. Updating the model with insect movement and infestation predictions would also allow for reinfestation after the conclusion of a fumigation.

The model output of overall insect populations could be used to calculate insect damage to the grain and related dry matter shrink cost. The likelihood of detecting insect infestations in the grain could also be calculated. If the amount of insect damage were combined with an economic analysis that would assign a specific cost per insect per hour, then the predicted costs of insect damage could be calculated by multiplying the cost of each insect per hour by the total number of insects in the model at each hour. This calculation would give a running economic cost of insect infestation. The predicted cost could be combined with other costs (i.e, moisture shrink, fan electricity costs, dry matter loss) in order to compare aeration strategies and their efficacy in suppressing insect development at minimum cost while maximizing stored grain quality. These aspects were beyond the scope of this dissertation research but should be addressed in the future.

Grain Chiller Modeling

The third key contribution to the code was the modification to allow for air conditions other than ambient to be used in aeration strategies in order to simulate the use of a grain chiller. Grain chillers are a technology of interest for improving aeration in many tropical and subtropical regions that has not been previously demonstrated. The approach that was used to investigate the use of grain chillers is similar to ambient aeration except that the input file is modified to allow aeration to be conducted with an alternate air stream comprised of air with a relative humidity and temperature representing the exit conditions of the grain chiller. This does not include modeling the conditions of the refrigeration cycle of the grain chiller, as described by Maier (1992), but instead uses data that was collected from a grain chiller as Morales-Quiros (2017) did. This expanded capacity modeling was incorporated into a project that investigated

grain chillers as a tool to improve rice storage conditions in Costa Rica, as reported in Morales-Quiros (2017), as well as in Thailand, which is work in progress.

Fumigation Modeling

The fourth key contribution was the addition of the fumigation model. Lawrence (2012) had added a fumigant distribution model towards the end of his dissertation research, but it was not fully functional, nor was it validated. This was in part due to lack of access to fumigation data. In order to achieve a working fumigation code, the capacity to account for fumigant loss due to sorption and leakage effects was added, as described in Chapter 6. Also, the capacity of the code to account for air recirculation through the grain silo and mass was added to better simulate closed loop fumigation.

The equations coded into the model are capable of accurately predicting gas concentrations vertically throughout the silo, but they do not accurately predict differences in gas concentrations horizontally across a silo. As a consequence, the leakage effects had little influence on the fumigant concentrations except for nodes directly along the silo walls. The forced convection velocities used to simulate forced gas recirculation via thermosiphon override the influence of natural convection currents and diffusion occurring in the grain mass. This error is small in aeration simulations, as the forced air convection velocities were large in comparison. However, the loss of these influences was seen more clearly in the closed loop fumigation trials as the natural convection currents lost were larger in comparison to the smaller velocity recirculation caused by the thermosiphon. As a result, the air and gas mixing that occurs due to thermosiphon recirculation of the gas was the primary mechanism for distributing fumigant to the boundary nodes. This likely limited the horizontal impact of gas leakage out of the silo, as it

limited the horizontal exchange of fumigant. In order for the model to more accurately predict concentration differences across the horizontal sections in the silo, the code would need to be modified in how it calculates forced convection currents and incorporate effects from natural convection currents and gas diffusion.

Another factor that would improve the accuracy of the fumigation model is analyzing thermosiphon behavior in closed loop fumigation systems and how it is influenced by ambient temperature and solar radiation. The only literature on thermosiphon functionality is Cook (2016), who reported differences in thermosiphon velocity throughout the day, but did not investigate governing equations for fluid flow. In this model, Cook's observations were used but thermosiphon velocities were assumed constant, except for during the warmest hours of the day, during which they were doubled. Solar radiation and ambient temperature were not directly taken into account in determining thermosiphon velocity. If representative equations were produced to describe the velocity and direction of fumigant movement through a thermosiphon, they could be coded with existing data that is already used in the model.

Fumigant Desorption Modeling

The fifth key contribution was the addition of modeling the fumigant desorption effect after the fumigation is complete and the silo is vented. The literature on this effect is incomplete and contradictory, especially compared to research on the sorption effect. The results of this work demonstrated that the Case 1 predictions had more accurate trends, but that the Case 2 equilibrium model was more accurate in values. A more accurate version of the Case 1 assumptions was created by increasing the desorption effect by a factor of 10 based on what values would best match experimental conditions. It would be more accurate if literature values

were available. It would therefore benefit the understanding of desorption and the ability to make predictions via modeling if baseline desorption equations were calculated of the kind available for sorption (Daglish and Pavic, 2008).

CO₂ Production Modeling

In addition, further coding has been done to simulate the release of chemicals into the grain mass. By changing the way that the model inputs chemicals into the grain to be additive instead of hard setting values, the model has the potential for multiple nodes to be used as release points without them being interfered with by other release points nearby. This means that the coding and results for chemical release into the model is more responsive and realistic. This improvement is being applied in practice to analyze carbon dioxide production from insect pests in stored rice in Thailand. The successful conclusion of this work would allow the model to be used to analyze factors such as carbon dioxide monitors as a means of detecting and quantifying insect infestations, and insect suppression through controlled atmosphere storage. Additional progress in these areas would further contribute to the overall goal of increased optimization of best grain storage management practices to reduce insect infestations despite growing phosphine resistance in insects.

Future Modeling Opportunities

A novel and interesting future model would be one that combines the aeration and fumigation capacities of the current model into one system that can monitor the entire grain storage system. This was attempted as a part of this dissertation, but was ultimately not successful. The model was successfully modified to allow for the code to change during

simulation between aeration, fumigation, and desorption functionalities, which was the main work necessary to produce a combined model. Insect populations would be the most consistent and important response variable used to analyze the impact of such a combined model. In order to utilize insect populations in this way, the insect growth model would need to be modified to include insect death equations as a result of phosphine concentration. In order to achieve this, accurate equations based on literature sources would need to be produced that can relate percentage insect death to phosphine concentration for each hour of exposure. Such literature is difficult to find due to the fact that success or failure of a fumigation is not judged on a per hour basis. Also, such a model would be an oversimplification of the biological effects of fumigant on insects.

A combined fumigation and aeration model was produced that avoided this issue by modeling the insect response to fumigant based on a running Ct-product. In this model complete insect death was assumed to occur at each node when the node was exposed to the designated Ct-product of fumigant. No insect deaths would occur until that level of fumigant was reached. Ultimately, this version of the code was unsuccessful due to the combined influence of previously stated limitations. Due to the assumption of complete death or complete survival based on Ct-product, the resultant insect populations were either unaffected by the fumigation or completely killed. This limited the ability of the model to analyze factors such as time of year of the fumigation. Due to the previously stated limitation of no insect movement, all nodes receiving sufficient Ct-product were not able to be reinfested and became meaningless to insect populations throughout the rest of the simulated storage period. Due to the difficulty in accurately predicting horizontal fumigant distributions, which limited the leakage effect to the side walls, most of the grain storage volume had a similar cumulative Ct-product. The result was

that the model produced largely binary results of either nearly complete insect death or no insect death.

Were an effective version of the combined model to be developed, the fumigation component of the model could report directly on resultant insect populations instead of fumigant concentrations, and aeration and fumigation could be sensibly combined. This would allow a more in-depth look at a variety of factors such as timing of fumigation and effect of increased phosphine resistance among stored grain insects that have not been explored in this dissertation.

Chapter 8 - Conclusions

Aeration Modeling Under Australian Conditions to Preserve Stored Grain Quality and Minimize Insect Activity

The effectiveness of six aeration strategies for the cooling of stored wheat under East Australian weather conditions were examined. The strategies were compared on the basis of time required to cool grain to 15°C or less, moisture content and uniformity in the grain mass, fan motor electricity usage, temperature uniformity in the grain mass, and insect populations.

The key results are:

- An effective strategy at airflow rates of 0.105 m³/min/t to 0.42 m³/min/t that does not require complex controls would be to run the aeration fan to cool stored grain whenever the ambient air temperature is below 20°C (Strategy 3), and switch to maintenance aeration once the targeted grain temperature of 15°C or less is reached.
- A more effective but more complex strategy where the aeration fan is turned on whenever the ambient temperature is less than the grain temperature at the center of the grain mass (Strategy 5) will cool the grain to 15°C one day later, 26 days earlier, and 41 days earlier for 0.105, 0.21, and 0.42 m³/min respectively, and require 23%, 49%, and 66% fewer fan run hours, respectively.
- For the higher airflow rate of 0.42 m³/min when compared to a lower airflow rate of 0.105 m³/min proved to be a tradeoff between faster wheat cooling and higher energy costs (achieved 15°C 101 days earlier with Strategy 5 compared to a 594% increase in kWh)

- Placing wheat into a silo at increased initial temperatures of 20°C-27°C does not substantially increase the cooling time of the grain with the 3°C temperature differential between ambient and internal grain temperature (Strategy 5 modified). However, it does increase fan run hours (from 2,214 to 2,555 at 0.21 m³/min/t, +15.5%) and insect development (an overall average of 52% of original at 20°C to 179% of original at 27°C, +244%).
- The three strategies tested to mitigate insect growth rates all successfully reduced insect numbers to less than 5% of their original value by the end of the simulated storage period. While strategies 3 and 5 were most effective in controlling insect populations in 3 of the 6 tested situations each, strategy 5 had the lowest energy usage in all scenarios.
- While the 3°C temperature differential strategy (modified strategy 5) had the most efficient energy use (using the fewest fan run hours, and reaching 15°C an average of 11 days after the fastest strategy, strategy 5), it performed comparatively poorly on overall insect growth. This was seen most notably at the highest airflow rate of 0.42 m³/min ton, where total average insect numbers increased from strategy 5 levels, where overall average insect levels increased by 28% at 20°C and by 66% at 27°C.
- Overall, the temperature differential strategy based on internal grain temperature (strategy 5) performed the best out of all strategies tested. It was able to cool the grain mass the fastest, used fewer fan run hours than every strategy except strategy 5 modified, and also controlled insect populations as well as any other strategy. This strategy is recommended under East Australian weather conditions in order to preserve stored grain quality and minimize insect activity in commercial silos.

Developing and Validating a Fumigant Loss Model for Bulk Stored Grain to Predict Phosphine Concentrations with Fumigant Leakage and Sorption

An existing finite element model was expanded to simulate fumigant movement and loss by incorporating equations to predict phosphine leakage and sorption. This model was validated with data from an experimental fumigation conducted using a sealed Australian silo under U.S. weather conditions. The key results are:

- The verification demonstrates that the model effectively predicted the trend of phosphine concentrations, and accurately predicted the overall Ct-product of the fumigation. Based on a 24h phosphine release model the predicted Ct-product differed from the experimental value by 0.9%. A 30h release model predicted a Ct-product that differed by 4.3% from the experimental value.
- The fumigation model is most accurate during the times of highest phosphine concentration. However, the model under predicts phosphine concentrations during the first 12h of fumigation and over predicts phosphine concentrations beyond the first six days of fumigation.
- While silo average Ct-products were within 5%, the simulation was not able to accurately reproduce differences observed between the north, east, south, and west sides of the grain mass.
- Predicted Ct-products from areas in the silo not monitored during the experimental fumigation such as near the surface of the grain mass demonstrate the possibility that a

fumigation that is ruled successful on average Ct-product might fail to control insects in these specific areas.

Sensitivity Analysis of a Fumigant Movement and Loss Model for Bulk Stored Grain to Predict Effects of Environmental Conditions and Operational Variables on Fumigation Efficacy

The validated M-L-P 3D ecosystem model was successfully applied to investigate the sensitivity of fumigation efficacy as a function of ambient temperatures, relative humidity, and wind speed, recirculation rate, type of fumigant, and degree of silo seal. The key results are:

- Improving degree of seal in a poorly sealed silo has less impact on improving fumigant concentrations than reducing leakage rate in an already moderately well sealed silo.

Reducing leakage rate to 50% and 75% increased fumigant concentrations by 111% and 36% compared to -21% and -34% for 125% and 150% leakage rate changes, respectively.

- Increasing fumigant recirculation rates resulted in decreased overall Ct-products.

However, Ct-products did not increase proportionally in the most vulnerable areas of the silo (i.e., where the silo wall meets the headspace). The optimum recirculation rate was found around 37.5% of the original recirculation rate. By the end of the simulation, average phosphine concentrations changed by 118%, 41%, -28%, and -47% for the 50%, 75%, 125%, and 150% recirculation rates investigated, respectively.

- Sulfuryl-fluoride concentrations (in kg/m^3) were slightly lower than phosphine concentrations under the same conditions. Sulfuryl-fluoride sorbed less and moved more slowly due to its greater molecular weight. By the end of the simulation, sulfuryl-fluoride concentrations were predicted to be 6.1% lower compared to phosphine concentrations.
- Increasing temperature and wind speed decreased phosphine concentrations, with temperature changes having a more significant impact overall than wind speed changes. However, given the larger variability of wind effects and the greater impact of increasing wind speeds relative to temperature, high wind weather events such as thunderstorms have the potential for significant impact on phosphine concentrations. Changes in relative humidity had no effect in the closed loop fumigation system.
- Larger silos with smaller surface area to volume ratios dampened the impact of changing weather conditions on phosphine concentrations. This is an important consideration for farmers especially in Australia where thermosiphon fumigation of smaller hopper silos with larger surface to volume ratios is common

Modeling Post-Fumigation Desorption of Phosphine in Bulk Stored Grain

An experimental fumigation trial that included monitoring fumigant venting and holding grain was conducted in Lake Grace, Australia. The M-L-P 3D ecosystem model was modified to include two estimates for phosphine fumigant desorption. Both approaches were validated using the experimental data. Simulations were conducted to test minimum times of post-fumigation

grain venting to reach phosphine desorption levels below 0.3 ppm that are considered safe for handling grain. The key results are:

- The sealed silo showed phosphine concentration increases during two consecutive periods after venting, resulting in 28 ppm and 29 ppm increases, respectively.
- Simulations were able to reproduce overall desorption trends, but consistently over predicted initial desorption values and under predicted desorption values after the second period of venting.
- Two equations estimating fumigant desorption were tested, with an average of -55.5% error for Case 1 (reversed sorption equations) and 86.3% error for Case 2 (equations from Darby, 2008).
- The assumption that desorption rate was the same as sorption rate proved to be inaccurate. The simulation analysis indicated desorption rate was 10x as large as the sorption rate.
- Simulations with Case 1 equation indicated that a 3h or 7h venting periods were not sufficient in either the U.S. or Australian context. Further investigation under the Australian context showed that 8h, 10h, 12h, and 18h venting times were insufficient but a 24h venting time would have been sufficient to reduce phosphine concentrations below 0.3 ppm for the safe handling of grain post-fumigation.
- Simulations with the Case 2 equation indicate that the 3h or 7h venting periods were not sufficient in the Australian context, but the 7h venting period would have been sufficient in the U.S. context. Further investigation under the Australian context showed that 8h, venting times were insufficient but 10h, 12h, 18h, and 24h venting times would have

been sufficient to reduce phosphine concentrations below 0.3 ppm for the safe handling of grain post-fumigation.

- Given the incomplete and somewhat contradictory literature and grain handling standards in the U.S. and Australia, there is a need for additional research into fumigant desorption and venting of post-fumigation grain to achieve levels safe for grain handling, especially when considering higher gas concentrations, longer exposure times, and better sealed silos to overcome phosphine resistance in stored product insects.

Chapter 9 - Future Work

Based on the findings of this dissertation research, the following recommendations are made for future research:

- Modify forced convection in the model to be an additive instead of set property in order to improve handling of small velocity factors such as diffusion.
- Include equations for insect movement to allow for more accurate insect model with the ability to consider reinfestation.
- Include in the insect equation a term for percentage insect death as a result of phosphine exposure on an hourly basis in order to create a grain storage model capable of analyzing the entire storage period together with aeration and fumigation.
- Conduct fumigant desorption experiments capable of determining a base desorption equation as a function of concentration applied, time of application, and time of desorption.

Chapter 10 - Bibliography

Abe, T., and Basunia, M. A. (1996). Simulation of temperature and moisture changes during storage of rough rice in cylindrical bins owing to weather variability. *Journal of Agricultural Engineering Research*, (65), 223-233.

Akdogan, H., and Casada, M. E. (2006). Climatic humidity effects on controlled summer aeration in the hard red winter wheat belt. *Transactions of the American Society of Agricultural and Biological Engineers*, 49(4), 1077-1087.

Armitage, D. M., and Stables, L. M. (1984). Effects of aeration on established insect infestations in bins of wheat. *Protection Ecology*, 6(1), 63-73.

Arthur, F. H., and Casada, M. E. (2005). Feasibility of summer aeration to control insects in stored wheat. *Transactions of the American Society of Agricultural and Biological Engineers*, 21(6), 1027-1038.

Arthur, F. H. and Flinn, P. W. (2000). Aeration management for stored hard red winter wheat: Simulated impact on rusty grain beetle (coleoptera: Cucujidae) populations. *Journal of Economic Entomology*, 93(4), 1364-1372.

Banks, H. J. (1986). Sorption and desorption of fumigants on grains: Mathematical descriptions. *Australian Centre for International Agricultural Research international seminar*. Manila, Philippines. 179-193.

Banks, H. J. (1990). Behaviour of gases in grain storages. *In Fumigation and Controlled Atmosphere Storage of Grain*, 96-107.

Banks, H. J., and Annis, P. C. (1984). Importance of processes of natural ventilation to fumigation and controlled atmosphere storage. *Controlled Atmosphere and Fumigation in Grain Storages*, Perth, Australia. 299.

Banks, H. J. and Annis, P. C. (1984). On criteria for success of phosphine fumigations based on observation of gas distribution patterns. *Controlled Atmosphere and Fumigation in Grain Storages Proceedings of an International Symposium*. Perth, Australia. 327-341.

Berck, B. (1968). Sorption of phosphine by cereal products. *Journal of Agriculture and Food Chemistry*, 16(3), 419-425.

Beukema, K. J., Bruin, S., and Schenk, J. (1983). Three dimensional natural convection in a confined porous medium with internal heat generation. *International Journal of Heat and Mass Transfer*, 26(3), 453.

- Bibby, I. P., and Conyers, S. T. (1998). Numerical simulations of gas exchange in leaky grain silos, using measured boundary conditions. *Journal of Stored Products Research*, 34(4), 217-229.
- Bielorai, R., and Alumot, E. (1975). Temperature effect on fumigant desorption from cereal grain. *Journal of Agricultural and Food Chemistry*, 23(3), 426-429.
- Bond, E. J. (1989). Manual of fumigation for insect control. *Food and Agriculture Organization Plant Production and Protection Paper 54*, London, Ontario, Canada: Food and Agriculture Organization of the United Nations.
- Brooker, D. B. (1969). Computing air pressure and velocity distribution when air flows through a porous medium and nonlinear velocity-pressure relationship exist. *Transactions of the American Society of Agricultural and Biological Engineers*, 12(1), 118-120.
- Brunauer, S., Emmett, P. H., and Teller, E. (1938). Adsorption of gases in multimolecular layers. *Journal of the American Chemical Society*, 60(2), 309-319.
- Burges, H. D., and Burrell, N. J. (1964). Cooling bulk grain in the British climate to control storage insects and to improve keeping quality. *Journal of the Science of Food and Agriculture*, 15, 32-50.

- Calderon, M., and Barkai-Golan, R. (1999). In Calderon M. (Ed.), *Food preservation by modified atmospheres*. Boca Raton: CRC Press.
- Casada, M. E. and Alghannam, A. (1999). Aerating over-dry grain in the northwest. *Transactions of the American Society of Agricultural and Biological Engineers*, 42(6), 1777-1784.
- Casada, M. E. and Noyes, R. T. (2000). Future bulk grain bin design needs related to sealing for optimum pest management – a researcher’s view. *Proceedings for the Controlled Atmosphere and Fumigation Conference*, Fresno, California.
- Chayaprasert, W., Maier, D. E., and Subramanyam, B. (2010). A simplified and improved modeling approach for the structural fumigation process using computational fluid dynamics. *10th International Working Conference on Stored Product Protection*, Lisbon, Portugal.
- Chayaprasert, W., Maier, D. E., Subramanyam, B. and Hartzler, M. (2012). Gas leakage and distribution characteristics of methyl bromide and sulfuryl fluoride during fumigations in a pilot flour mill. *Journal of Stored Products Research*, 50(0), 1-7.
- Chayaprasert, W., Nukham, K., and Sukcharoen, A. (2015). Evaluation of the superposition method for predicting gas leakage rates during fumigations in empty model silos. *Journal of Stored Products Research*, 64, 13-20.

Chourasia, M. K., and Goswami, T. K. (2007). Three dimensional modeling on airflow, heat and mass transfer in partially impermeable enclosure containing agricultural produce during natural convective cooling. *Energy Conversion and Management*, 48(7), 2136-2149.

Collins, P. (2009). *Strategy to manage resistance to phosphine in the Australian grain industry*. National Working Party on Grain Protection. Cooperative Research Centre for National Plant Biosecurity.

Converse, H. H., Graves, A. H., and Chung, D. S. (1969). Transient heat transfer within wheat stored in cylindrical bin. *Transactions of the American Society of Agricultural and Biological Engineers*, 16(1), 129-133.

Cook, S. (2016). Evaluation of sealed storage silos for grain fumigation. (Unpublished Master of Science). Kansas State University.

Cryer, S. A. (2008). Predicted gas loss of sulfuryl fluoride and methyl bromide during structural fumigation. *Journal of Stored Products Research*, 44(1), 1-10.

Cryer, S. A., and Barnekow, D. E. (2006). Estimating outside air concentrations surrounding fumigated grain mills. *Biosystems Engineering*, 94(4), 557-572.

Cuperus, G. W., Prickett, C. K., Bloome, P. D. and Pitts, J. T. (1986). Insect populations in aerated and unaerated stored wheat in Oklahoma. *Journal of the Kansas Entomological Society*, 59(4), 620-627.

Daglish, G. J., and Pavic, H. (2008). Effect of phosphine dose on sorption in wheat. *Pest Management Science*, 64(5), 513-518.

Darby, J. (1999). *Aeration field trials for control and model testing*. (No. CSE150). Commonwealth Scientific and Industrial Research Organization. Entomology Stored Grain Research Laboratory.

Darby, J. (2008). A kinetic model of fumigant sorption by grain using batch experimental data. *Pest Management Science*, 64(5), 519-526.

Darby, J. (2011). *Technology to overcome inadequate fumigations and resistance selection*. (No. CRC50059). Black Mountain, ACT, Australia: Cooperative Research Centre for National Plant Biosecurity.

Desmarchelier, J. M. (1988). The relationship between seed wet-bulb and the intrinsic rate of increase of eight species of stored product coleoptera. *Journal of Stored Products Research*, 24(2), 107-113.

Driscoll, R., Longstaff, B. C., and Beckett, S. (2000). Prediction of insect populations in grain storage. *Journal of Stored Products Research*, 36, 131-151.

Dumas, T. (1980). Phosphine sorption and desorption by stored wheat and corn. *Journal of Agricultural and Food Chemistry*, 28(2), 337–339.

FAO, 2014. *Stemming post-harvest waste crucial to African food security*. Food Agriculture Organization. United Nations.

FAO, WFP and IFAD. 2012. *The State of Food Insecurity in the World 2012. Economic growth is necessary but not sufficient to accelerate reduction of hunger and malnutrition*. Rome, FAO.

Fields, P. (2006). Alternatives to chemical control of stored-product insects in temperate regions. *Proceedings of the 9th International Working Conference on Stored-Product Protection*, Sao Paulo, Brazil. 653-662.

Flinn, P. W., and Hagstrum, D. W. (1998). Distribution of *Cryptolestes ferrugineus* (coleoptera: Cucujidae) in response to temperature gradients in stored wheat. *Journal of Stored Products Research*, 34(2–3), 107-112.

Fluent Inc. (1996). *Gambit software*. Lebanon, New Hampshire.

Fong, H. R., Johnson, J., and Schneider, F. (2008). *An overview of phosphine-generating pesticides used in California in 2005*. (No. HS-1863). Sacramento, California: California Environmental Protection Agency.

Fraser, B. M., and Muir, W. E. (1981). Airflow requirements predicted for drying grains with ambient air and solar heated air in Canada. *Transactions of the American Society of Agricultural and Biological Engineers*, 24(1), 208-210.

Gurusinghe, P. (2014). *Fumigants: Phosphine and phosphine-generating compounds risk characterization document*. California Environmental Protection Agency.

Hagstrum, D. W., and Subramanyam, B. (2006). *Fundamentals of stored-products entomology*. St. Paul, MN: AACC International.

Harner, J. P., and Hagstrum, D. W. (1990). Utilizing high airflow rates for aerating wheat. *Applied Engineering in Agriculture*, 6(3), 315-321.

Hwaidi, M., Collins, P. J., Sissons, M., Pavic, H., and Nayak, M. K. (2015). Sorption and desorption of sulfur dioxide by wheat, flour and semolina. *Journal of Stored Products Research*, 62, 65-73.

Isa, M. Z., Fulford, G. R., and Kelson, N. A. (2011). Simulation of phosphine in vertical grain storage: A preliminary numerical study. *Australian Mathematical Society*, (52), 759-772.

Isa, Z. M., Farrel, T. W., Fullford, G. R., and Kelson, N. A. (2016). Mathematical modelling and numerical simulation of phosphine flow during grain fumigation in leaky cylindrical silos. *Journal of Stored Products Research*, 67, 28-40.

Jia, C. C., Sun, D. W., and Cao, C. (2000). Computer simulation of temperature changes in a wheat storage bin. *Journal of Stored Products Research*, 37, 165-167.

Jian, F., Jayas, D. F., White, N. D. G., and Alagusundaram, K. (2005). A three-dimensional, asymmetric, transient model to predict grain temperatures in grain storage bins. *Transactions of the American Society of Agricultural and Biological Engineers*, 48(1), 263-271.

Kaur, R., Ebert, P. R., Walter, G. H., Swain, A. J. and Schlipalius, D. I. (2013). Do phosphine resistance genes influence movement and dispersal under starvation? *Journal of Economic Entomology*, 106(5), 2259-2266.

Kaur, R., Daniels, E. V., Nayak, M. K., Ebert, P. R. and Schlipalius, D. I. (2013). Determining changes in the distribution and abundance of a *rhyzopertha dominica* phosphine resistance allele in farm grain storages using a DNA marker. *Pest Management Science*, 69(6), 685-688.

Konemann, C. E., Opit, G. P., Shakya, K. and Bajracharya, N. S. (2014). Phosphine resistance in rusty grain beetles, *Cryptolestes Ferrugineus* (stephens), (coleoptera: Laemophloeidae) from stored wheat in Oklahoma. *Integrated Protection of Stored Products*, 98, 363-366.

Langmuir, I. (1918). The adsorption of gases on plane surfaces of glass, mica and platinum. *Journal of American Chemical Society*, 40(9), 1361-1403.

Lawrence, J. (2010). *Three dimensional transient heat, mass, momentum and species transfer stored grain ecosystem model using the finite element method* (Ph.D.) Purdue University, West Lafayette, Indiana.

Lawrence, J. and Maier, D. E. (2011). Aeration strategy simulations for wheat storage in the subtropical region of north India. *Transactions of the American Society of Agricultural and Biological Engineers*, 54(4), 1395-1405.

Lawrence, J. and Maier, D. E. (2011). Development and validation of a model to predict air temperatures and humidities in the headspace of partially filled stored grain silos. *Transactions of the American Society of Agricultural and Biological Engineers*, 54(5), 1809-1817.

- Lawrence, J. and Maier, D. E. (2011). Three-dimensional airflow distribution in a maize silo with peaked, levelled and cored grain mass configurations. *Biosystems Engineering*, 110(3), 321-329.
- Magan, N., and Lacey, J. (1988). Ecological determinants of mould growth in stored grain. *International Journal of Food Microbiology*, 7(3), 245-256.
- Maier, D. E. (1992). *The chilled aeration and storage of cereal grains. (volumes I and II)* (Ph.D.). Available from ProQuest Dissertations & Theses Global. (303984107).
- Mann, D., Jayas, D. S., Muir, W. E. and White, N. D. G. (1999). Predicting the gas tightness of grain storage structures. *Canadian Agricultural Engineering*, 41(4), 259-265.
- Montross, M. D., Maier, D. E. and Haghghi, K. (2002). Development of a finite-element stored grain ecosystem model. *Transactions of the American Society of Agricultural and Biological Engineers*, 45(5), 1455-1464.
- Montross, M. D. (1999). *Finite element modeling of stored grain ecosystems and alternative pest control techniques* (Ph.D.). Available from ProQuest Dissertations and Theses Global. (276290016).

Morales Quiros, A. (2017). *Evaluation of Ambient and Grain Chilling Strategies to Maintain the Quality of Stored-Grain in Tropical Climates and During Summer in Temperate Climates*. (Unpublished Master of Science). Kansas State University.

Mulhearn, P. J., Banks, H. J., Finnigan, J. J. and Annis, P. C. (1976). Wind forces and the influence on gas loss from grain storage structures. *Journal of Stored Products Research*, 12(3), 129-142.

Navarro, S. (1998). Pressure tests for gaseous applications in sealed storages: Theory and practice. *7th International Working Conference on Stored Product Protection*, Beijing China. 385-390.

Noyes, R. T., and Phillips, T. W. (2007). A model for selecting tablet vs pellet dosages in storages with closed loop fumigation (clf) systems. *Proceedings of the International Conference on Controlled Atmosphere and Fumigation in Stored Products*, Gold Coast, Australia. 393-401.

Noyes, R. T., Phillips, T. W., Cuperus, G. W., and Bonjour, E. L. (1998). Advances in recirculation fumigation technology in the U.S.A. *Proceedings of the 7th International Working Conference on Stored-Product Protection*, Beijing, China. 454-461.

Occupational Safety and Health Administration. (1988). *Phosphine in Workplace Atmospheres* (Standard No. 180). Retrieved from

<https://www.osha.gov/dts/sltc/methods/inorganic/id180/id180.html>

Opit, G. P., Phillips, T. W., Aikins, M. J. and Hasan, M. M. (2012). Phosphine resistance in *tribolium castaneum* and *rhyzopertha dominica* from stored wheat in Oklahoma.

Entomological Society of America, 105(4), 1107-1114.

Queensland Department of Agriculture and Fisheries. (2010). Fumigation to control insects in stored grain. Retrieved from [https://www.daf.qld.gov.au/plants/field-crops-and-](https://www.daf.qld.gov.au/plants/field-crops-and-pastures/broadacre-field-crops/grain-storage/fumigation)

[pastures/broadacre-field-crops/grain-storage/fumigation](https://www.daf.qld.gov.au/plants/field-crops-and-pastures/broadacre-field-crops/grain-storage/fumigation)

Rauscher, H., Mayer, G. E. and Sullivan, J. B. (1972). Sorption and recovery of phosphine.

Journal of Agricultural and Food Chemistry, 20(1), 331–333.

Reddy, P. V., Yellappa, R., Begum, K., Leelaja, B. C. and Rajendran, S. (2007). The relation between phosphine sorption and terminal gas concentrations in successful fumigation of food commodities.

Pest Management Science, 63(1), 96-103.

Reed, C. C., and Pan, H. (2000). Loss of phosphine from unsealed bins of wheat at six combinations of grain temperature and moisture content. *Journal of Stored Products*

Research, 36(3), 263-279.

- Ripp, B. E. (1984). Leak detection in sealed grain storages. *Cooperative Bulk Handling Limited*, 5, 293-297.
- Rocha, and Oliveira, K. S. (2013). Three dimensional modeling and simulation of heat and mass transfer process in porous media: An application for maize stored in a flat bin. *Drying Technology*, 31(10), 1099-1106.
- Sato, K., and Suwanai, M. (1974). Adsorption of hydrogen phosphide to cereal products. *Japanese Society of Applied Entomology and Zoology*, 9(4), 127-132.
- Sing, K. (1982). Reporting Physisorption Data for Gas/Solid Systems with Special Reference to the Determination of Surface Area and Porosity. *Pure Applied Chemistry*, 54, 2201.
- Singh, A. K., and Thorpe, G. R. (1993). A solution procedure for three-dimensional free convective flow in peaked bulks of grain. *Journal of Stored Products Research*, 29(3), 221-235.
- Sinicio, R., and Muir, W. E. (1998). Aeration strategies for preventing spoilage of wheat stored in tropical and subtropical climates. *Transactions of the American Society of Agricultural and Biological Engineers*, 14(5), 517-527.
- Sriranjini, V., and Rajendran, S. (2008). Sorption of sulfur dioxide by food commodities. *Pest Management Science*, 64(8), 873-879.

- Sudakin, D. L. (2005). Occupational exposure to aluminium phosphide and phosphine gas? A suspected case report and review of the literature. *Human and Experimental Toxicology*, 24(1), 27-33.
- Sutherland, J. W. (1968). Grain Aeration in Australia. *Preserving grain quality by aeration and in-store drying: Proceedings of an international seminar*, Kuala Lumpur, Malaysia. 206-218.
- Sun, Y.P. (1946). An analysis of some important factors affecting the results of fumigation on insects. St. Paul, Minnesota Agricultural Experiment Station. Technical Bulletin No. 177.
- Thorpe, G. R. (1997). Modelling ecosystems in ventilated conical bottomed farm grain silos. *Ecological Modeling*, 94(2)
- Throne, J. E. (1994). Life history of immature maize weevils (*coleoptera Curculionidae*) on corn stored at constant temperatures and relative humidities in the laboratory. *Journal of Economic Entomology*, 23(6), 1459-1471.
- Weller, G. L., and Pratt, S. J. (2003). Measuring phosphine: How sensors work. *Proceedings of the Australian Postharvest Technical Conferences*, Canberra, Australia. 183.

Wilson, S. G., and Desmarchelier, J. M. (1994). Aeration according to seed wet-bulb temperature. *Journal of Stored Products Research*, 30(1), 45-60.

WorldBank, NRI, FAO, 2011. *Missing food: The case of postharvest grain losses in Sub-Saharan Africa* (No. 60371-AFR), Other.

Xianchang, T. (1994). Evolution of phosphine from aluminium phosphide formulations at various temperatures and humidities. *Proceedings of the 6th International Working Conference on Stored-product Protection*, 17-23 April 1994, Canberra, Australia. CAB International, Wallingford, UK, pp. 201-203.

Chapter 11 - Chapter 4 Appendices

Appendix 4.1:

The expression for the effect of temperature is of the form ae^{bT} . From Darby (2011), $ae^{b(35)} = 5*ae^{b(15)}$. Therefore, $e^{b(35)} = 5*e^{b(15)}$, $35b = \ln(5)+15b$, $35b = 1.609 + 15b$, $20b = 1.609$, $b = 0.0805$. We also know from Banks and Annis, 1984, that the expression ae^{bt} equals one at 25°C. Therefore, $1 = ae^{0.0805*25}$. $1 = ae^{2.0125}$, $1 = 7.482a$, $a = 0.13365$. So the expression for the dependence on Temperature is

$$0.13365e^{0.0805T} \quad \text{Eq A4.1.1}$$

Appendix 4.2:

The expression for the effect of moisture is of the form ae^{bM} . From Reed and Pan (2008), $ae^{b(13.5)} = 1.8*ae^{b(11)}$. Therefore, $e^{b(13.5)} = 1.8*e^{b(11)}$, $13.5b = \ln(1.8)+11b$, $13.5b = 0.588 + 11b$, $2.5b = 0.588$, $b = 0.235$. We also know from Banks and Annis, 1984, that the expression ae^{bt} equals one at 11.5%. Therefore, $1 = ae^{0.235*11.5}$. $1 = ae^{2.7025}$, $1 = 14.92a$, $a = 0.067$. So the expression for the dependence on Moisture Content is

$$0.067e^{0.235M} \quad \text{Eq A4.2.1}$$

Appendix 4.3:

The equation for the effect of wind speed is of the form $C = dC_1ae^{bW}$. D is the scalar estimate from Banks and Annis (1984), and is the estimate of $0.108/\text{day} * 1\text{day}/24\text{h} = 0.0045$. From Cryer (2008), $ae^{b(4)} = 4*ae^{b(1)}$. Therefore, $e^{b(4)} = 4*e^{b(1)}$, $4b = \ln(4)+b$, $3b = 1.386$, $b = 0.4621$. We also know from Banks and Annis, 1984, that the expression ae^{bt} equals one at 6.4

m/s. Therefore, $1 = ae^{0.4621*6.4}$. $1 = ae^{2.957}$, $1 = 19.24a$, $a = 0.05195$. So the equation for the wind speed effect is:

$$C = 0.0002233e^{0.4621Ws} \quad \text{Eq A4.3.1}$$

Appendix 4.4:

The equations for the effect of chimney temperature effect is of the form $C = dCi ae^{bT}$. D is the scalar estimate from Banks and Annis (1984), and is the estimate of $0.019/\text{day} * 1\text{day}/24\text{h} = 0.000792$. From Reed and Pan (2008), $ae^{b(30)} = 4 * ae^{b(20)}$. Therefore, $e^{b(30)} = 4 * e^{b(20)}$, $30b = \ln(4) + 20b$, $10b = 1.386$, $b = 0.1386$. We also know from Banks and Annis, 1984, that the expression ae^{bt} equals one at 25°C . Therefore, $1 = ae^{0.1386*25}$. $1 = ae^{3.465}$, $1 = 31.976a$, $a = 0.03127$. So the equation for the temperature chimney effect is:

$$C = Ci * 0.0000248 e^{0.1386Tc} \quad \text{Eq A4.4.1}$$

The equations for the effect of temperature variation effect is of the form $C = dCi ae^{0.1386T}$. The b value was assumed to be the same as the previous temperature value, as no literature on its impact was found. D is the scalar estimate from Banks and Annis (1984), and is the estimate of $0.025/\text{day} * 1\text{day}/24\text{h} = 0.00104$. Therefore, the temperature variation effect is:

$$C = Ci * 0.0000326e^{0.1386Td} \quad \text{Eq A4.4.2}$$

Appendix 4.5

The original intention was to use results provided from several Australian collaborators, most notably the Plant Biosecurity Cooperative Research Consortium (PBCRC) for use in validating the model, as these results specifically target Australian fumigations.

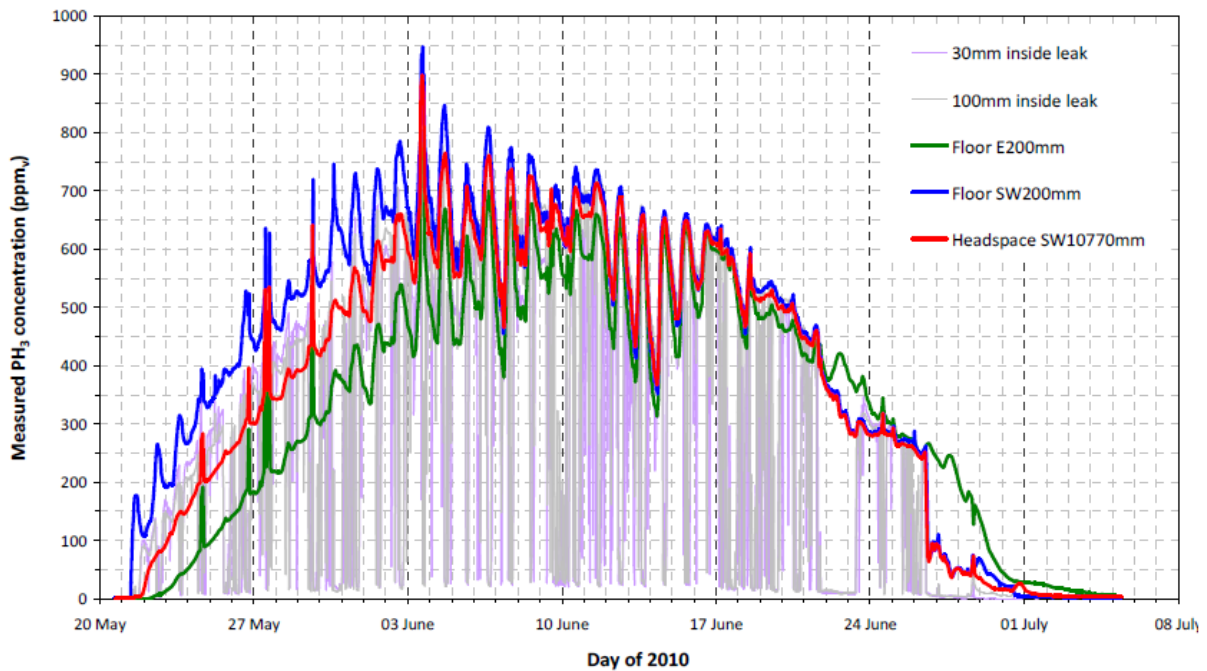


Figure 11:1 Phosphine concentrations (ppm) in silo fumigation data provided by the Plant Biosecurity Cooperative Research Center (Darby 2011)

Figure 11.1 shows the data that was provided by the PBCRC for use in validating the model, it originates from a study by Darby in 2011. It demonstrates a phosphine fumigation whose profile resembles a parabolic arc. This data set did not include many variables necessary for use in verification of the model, including recirculation information, pressure half loss time, and complete data for all points shown. Therefore, this data set could not be used in performing the model verification, but it does provide an example of the trend of a specific fumigation.

The general trends exhibited by a fumigation depends on several factors including size of silo, recirculation and mixing, rate of evolution of phosphine, and leakages. It takes a considerable amount of time for the phosphine to build up concentration in the silo to the maximum concentration, and then phosphine decay follows a similar curve. In this fumigation, a

relatively high amount of time required for the phosphine to attain gas form seems long with respect to estimations on evolution times of phosphine (Xianchang, 1994). Concentrations are similar throughout the silo, although it takes a long time for the phosphine concentrations to approach maximum value. In addition, there is a point leak mentioned in the data set, and the values near this location vary wildly throughout the fumigation. This data set did not contain any information on recirculation rates used. It may be that the parabolic shape is due to a combination of factors such as the specific leak, and a potentially slow creation rate of gaseous phosphine. The parabolic shape of the curve also seems to fit poorly with the equations of phosphine leakage adapted from the literature (Banks and Annis, 1984), in that the loss of phosphine was described as relative to the amount. Under those equations, phosphine is lost more quickly at high concentrations, and the amount of loss decreases as the phosphine leaks out over time. This is inconsistent with the curve presented in this data, as it seems to indicate slow initial loss that increases as the concentration decreases. The phosphine values are also variable with multiple situations involving a drop and then recovery in the concentrations of phosphine, both related to a leaking area of the silo and in other areas as well. As such, this data is poorly behaved with respect to expected fumigation parameters and is inconsistent with the results of the phosphine fumigation model.

In Figure 11.2, fumigation data from another Australian Fumigation is provided that shows a different trend. The concentrations at each of the locations along the wall in the silo are similar, which suggests an effective mixing of fumigant. The maximum concentration of phosphine is attained early on in the fumigation, which is consistent with normal estimations of phosphine evolution times (Xianchang, 1994). The concentrations then decay over time at a rate that decreases in relation to decreasing quantities of phosphine. This trend follows with the

expected result from the literature phosphine loss equations (Banks and Annis, 1984). The overall trend matches well with the trend seen in the overall average phosphine graph produced by modeled phosphine simulation, as seen in verification results of figure 11.2.

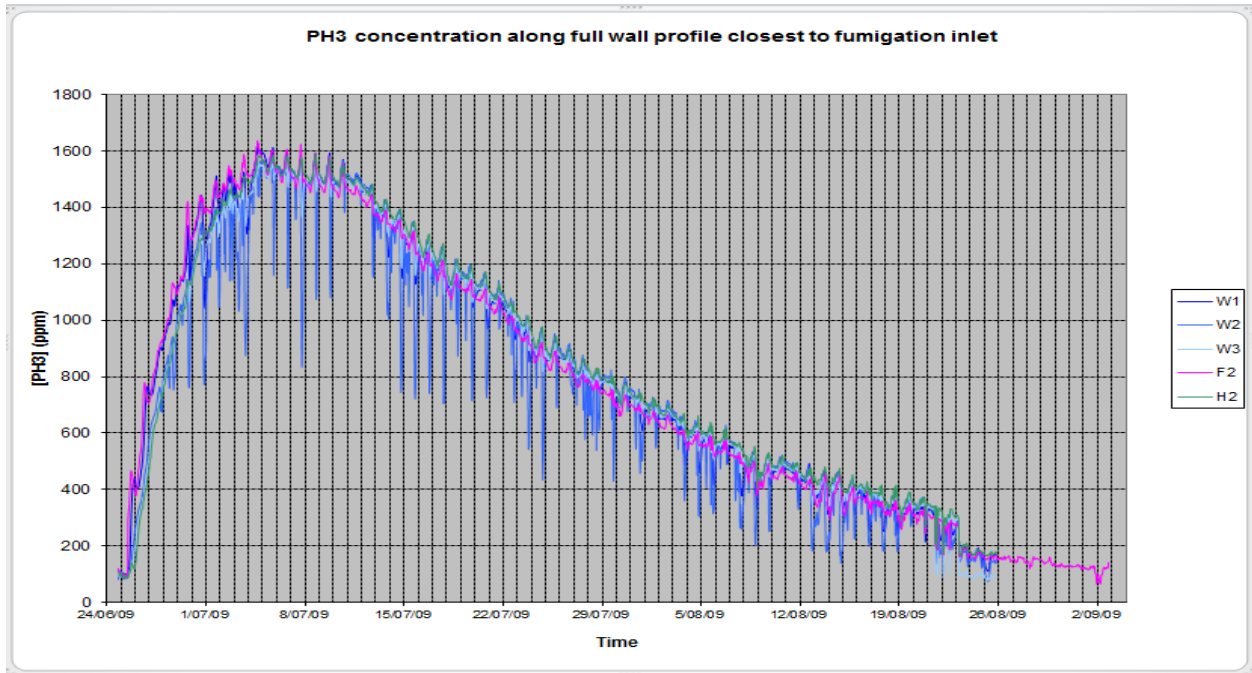


Figure 11:2 Phosphine concentrations (ppm) in silo fumigation data provided by Department of Agriculture and Fisheries, Queensland (DAF)

One feature observed in the results obtained from the Queensland Department of Agriculture and Fisheries that is not present in the simulated average results is the temporary decrease in phosphine concentration that are measured at night, but then recover in the day. One explanation for this effect has been described as silo breathing by Darby (2011) who says ‘Silo breathing refers to the expansion and contraction of the internal air in the silo due to solar heating and night time heat losses.’ The report goes on to calculate losses from silo breathing using mass balance and the ideal gas equation. However, while this may appear to be associated with a loss of phosphine in the trial conducted by Darby (2011) the data provided by DAF

suggests that there is no permanent loss, as there is a recovery of the phosphine concentration in the daytime. Another explanation for this is that the night time drop in phosphine concentrations may not actually be occurring, but rather is an artifact of the measuring devices used. Weller and Pratt (2003) state that despite the fact most sensors compensate for temperature difference, sensors may read high at temperatures above 25°C and low at temperatures below 25°C, with the effect in the range of 0.5-1.0% per degree Celsius. This effect could be the cause of the drops in phosphine content reported during cooler night time hours. Additionally, increased night time relative humidity may cause lower readings due to water condensation reducing the gas diffusion in the sensor (Weller and Pratt, 2003). These combined effects could be large enough for a typical night time temperature drop to account for much of the night time drop in phosphine concentration observed in figure 11.2.

Appendix 4.6:

Table 11:1 Comparison between average experimental and predicted phosphine concentration (ppm) considering only data from the same locations and times used in Cook (2016) between Aug 31 and September 9, 2015, with a 24h fumigant release.

Date	Hours of fumigation	Experimental	Simulated	% Difference	Total Difference
8/31/15 12:01 PM	0	35.9	16.5	54.0	19.4
8/31/15 1:30 PM	1.5	74.6	88.3	-18.5	-13.8
8/31/15 2:55	3	124.4	130.6	-5.0	-6.2

PM					
8/31/15 4:15	4.25	163.5	172.7	-5.6	-9.2
PM					
8/31/15 5:30	5.5	190.7	196.8	-3.2	-6.1
PM					
8/31/15 6:30	6.5	202.4	218.3	-7.8	-15.9
PM					
8/31/15 7:30	7.5	217.1	239.8	-10.4	-22.6
PM					
8/31/15 9:00	9	213.8	282.0	-31.9	-68.2
PM					
8/31/15 9:50	9.75	216.3	302.9	-40.0	-86.6
PM					
8/31/15	11	232.6	322.7	-38.7	-90.1
11:10 PM					
9/1/15 7:45	19.75	363.0	433.9	-19.5	-70.9
AM					
9/1/15 8:10	20	337.9	433.9	-28.4	-96.0
AM					
9/1/15 11:20	23.25	318.6	442.0	-38.7	-123.4
AM					
9/1/15 1:25	25.5	376.2	436.6	-16.0	-60.4
PM					

9/1/15 2:40	26.75	399.5	422.5	-5.8	-23.0
PM					
9/1/15 4:00	28	415.4	414.7	0.2	0.7
PM					
9/1/15 5:00	29	424.3	410.5	3.2	13.8
PM					
9/1/15 6:40	30.5	434.5	402.1	7.5	32.4
PM					
9/1/15 8:50	32.75	425.5	393.6	7.5	31.9
PM					
9/1/15 10:30	34.5	415.1	389.3	6.2	25.8
PM					
9/2/15 12:10	36.25	410.6	380.8	7.3	29.8
AM					
9/2/15 7:50	43.75	388.9	347.3	10.7	41.6
AM					
9/2/15 9:30	45.5	372.2	341.5	8.2	30.7
AM					
9/2/15 10:35	46.5	367.0	330.8	9.9	36.2
AM					
9/2/15 3:00	51	373.8	308.2	17.6	65.6
PM					
9/2/15 5:00	53	360.6	299.1	17.1	61.5

PM					
9/2/15 7:25	55.5	350.1	293.4	16.2	56.6
PM					
9/2/15 9:45	57.75	331.9	285.4	14.0	46.5
PM					
9/3/15 1:10	61.25	314.7	277.5	11.8	37.2
AM					
9/3/15 9:25	69.5	282.9	254.0	10.2	28.9
AM					
9/3/15 10:45	70.75	279.5	245.3	12.2	34.2
AM					
9/3/15 12:20	72.25	279.0	241.0	13.6	37.9
PM					
9/3/15 1:20	73.25	271.9	236.8	12.9	35.1
PM					
9/3/15 2:20	74.25	265.2	232.7	12.3	32.5
PM					
9/3/15 3:20	75.25	260.3	228.5	12.2	31.8
PM					
9/4/15 2:00	98	178.4	172.8	3.1	5.6
PM					
9/6/15 3:20	147.25	70.5	90.7	-28.7	-20.2
PM					

9/9/15 12:10	216.25	26.6	46.0	-72.9	-19.4
PM					

1

Appendix 4.7:

Table 11:2 Comparison between average experimental and predicted phosphine concentration (ppm) considering only data from the same locations and times used in Cook (2016) between Aug 31 and September 9, 2015, with a 30h fumigant release.

	Hours of fumigation	Experimental	Simulated	% Difference	Total Difference
8/31/15 12:01 PM	0	35.9	3.3	90.8	32.6
8/31/15 1:30 PM	1	74.6	24.7	66.8	49.8
8/31/15 2:55 PM	3	124.4	39.8	68.0	84.5
8/31/15 4:15 PM	4	163.5	56.6	65.4	106.9
8/31/15 5:30 PM	5	190.7	76.8	59.8	114.0
8/31/15 6:30 PM	6	202.4	88.6	56.2	113.8
8/31/15 7:30	7	217.1	102.0	53.0	115.2

PM					
8/31/15 9:00	9	213.8	116.9	45.3	96.8
PM					
8/31/15 9:50	10	216.3	133.2	38.4	83.1
PM					
8/31/15	11	232.6	150.3	35.4	82.3
11:10 PM					
9/1/15 7:45	20	363.0	317.5	12.5	45.5
AM					
9/1/15 8:10	20	337.9	317.5	6.0	20.4
AM					
9/1/15 11:20	23	318.6	379.0	-19.0	-60.4
AM					
9/1/15 1:25	25	376.2	405.3	-7.7	-29.1
PM					
9/1/15 2:40	27	399.5	426.6	-6.8	-27.1
PM					
9/1/15 4:00	28	415.4	433.2	-4.3	-17.8
PM					
9/1/15 5:00	29	424.3	435.8	-2.7	-11.5
PM					
9/1/15 6:40	31	434.5	435.2	-0.2	-0.7
PM					

9/1/15 8:50	33	425.5	430.4	-1.1	-4.8
PM					
9/1/15 10:30	34	415.1	427.3	-2.9	-12.1
PM					
9/2/15 12:10	36	410.6	424.1	-3.3	-13.6
AM					
9/2/15 7:50	44	388.9	388.7	0.0	0.2
AM					
9/2/15 9:30	45	372.2	372.5	-0.1	-0.3
AM					
9/2/15 10:35	47	367.0	365.9	0.3	1.1
AM					
9/2/15 3:00	51	373.8	343.6	8.1	30.2
PM					
9/2/15 5:00	53	360.6	334.5	7.2	26.1
PM					
9/2/15 7:25	55	350.1	328.3	6.2	21.8
PM					
9/2/15 9:45	58	331.9	319.0	3.9	12.9
PM					
9/3/15 1:10	61	314.7	309.6	1.6	5.1
AM					
9/3/15 9:25	69	282.9	283.4	-0.2	-0.6

AM					
9/3/15 10:45	71	279.5	274.1	1.9	5.4
AM					
9/3/15 12:20	72	279.0	269.1	3.5	9.8
PM					
9/3/15 1:20	73	271.9	264.5	2.7	7.4
PM					
9/3/15 2:20	74	265.2	259.8	2.0	5.4
PM					
9/3/15 3:20	75	260.3	254.9	2.1	5.4
PM					
9/4/15 2:00	98	178.4	193.1	-8.2	-14.7
PM					
9/6/15 3:20	147	70.5	101.6	-44.2	-31.1
PM					
9/9/15 12:10	216	26.6	51.3	-92.9	-24.7
PM					